TECHNISCHE UNIVERSITÄT MÜNCHEN

Lehrstuhl für Kommunikationsnetze

Joint PHY-MAC Cross-Layer Design in Wireless Ad Hoc Networks

Ulrike B. Korger

Vollständiger Abdruck der von der Fakultät für Elektrotechnik und Informationstechnik der Technischen Universität München zur Erlangung des akademischen Grades eines

Doktor-Ingenieurs (Dr.-Ing.)

genehmigten Dissertation.

Vorsitzender:		Univ.-Prof. Dr.-Ing. Dr. h.c. Alexander W. Koch
Prüfer der Dissertation:	1.	Univ.-Prof. Dr.-Ing. Jörg Eberspächer
	2.	Univ.-Prof. Dr.-Ing. Gerhard Bauch, Universität der Bundeswehr München

Die Dissertation wurde am 14.09.2011 bei der Technischen Universität München eingereicht und durch die Fakultät für Elektrotechnik und Informationstechnik am 07.12.2011 angenommen.

Preface

This thesis summarizes the results of my research activities at the Institute of Communication Networks at the TUM.
First of all, I want to thank Prof. Eberspächer that he gave me the opportunity to continue my first scientific steps at his institute and that he supported me throughout my thesis.
I would like to thank Prof. Bauch, whom I got to know from my cooperation with DOCOMO Euro-Labs, for serving as a second examiner. Many of the ideas presented in this thesis were developed as a collaboration project with DOCOMO Euro-Labs. My special thanks goes there to Dr. Katsutoshi Kusume and Dr. Jörg Widmer for many technical discussions.
I also want to mention all my colleagues that provided a warm and pleasant atmosphere at the LKN. My particular thank for many fruitful technical discussions as well as for reviewing the thesis draft goes to my colleague Jan Ellenbeck. Without the continues support and the excellent ideas from Dr. Christian Hartmann this thesis would not have been possible in this form! Thanks also to Dr. Robert Nagel and Oliver Hanka that helped me with their implementation expertise.
I also would like to mention my graduate students. Vasil Kumanov, Yingrui Chen, and Manuel Wocheslander contributed with their works to this thesis. Last but not least I want to thank my family. They always encouraged me on my way!

Munich, September 2011 Ulrike Korger

Contents

1. Introduction

In wireless networks, multiple nodes communicate over a wireless channel. Depending on the underlying architecture, the networks can be categorized differently. Two types of networks that vary strongly in their architectures are the classical cellular system and the ad hoc network.
In one cell of a cellular system, the user terminals do not communicate directly, but via a central entity, the *base station*. The base station performs multiple decisions centrally, e. g, it controls the access to the medium and decides on resource allocation.
In ad hoc networks, no central entity like a base station exists. All communication decisions have to be performed fully distributed. Two nodes wishing to communicate either do so directly, or by routing the packets over multiple intermediate nodes.
The access to the medium has to be controlled fully distributed, resulting in *contention based* medium access. In contention based medium access, all nodes that have data to send contend for the channel. If two nodes transmit their data simultaneously, the packets cause mutual interference at the unintended receivers. Dense ad hoc networks typically suffer from this Multiple Access Interference (MAI). The magnitude of interference depends on the attenuation that the interfering signal undergoes on its way from the interfering transmitter to the unintended receiver.
A well-known approach to battle MAI is to block all transmissions in the *communication range* of a sender and a receiver for the duration of the transmission. This is shown in Fig. 1.1. The communication range reflects the area around a node where another node can decode a packet from this node successfully. The area covered by the communication range is simplified reflected by a circle. In practical networks due to shadowing and fading effects it has an irregular shape.
Blocking all other transmissions in communication range diminishes the MAI strongly. It

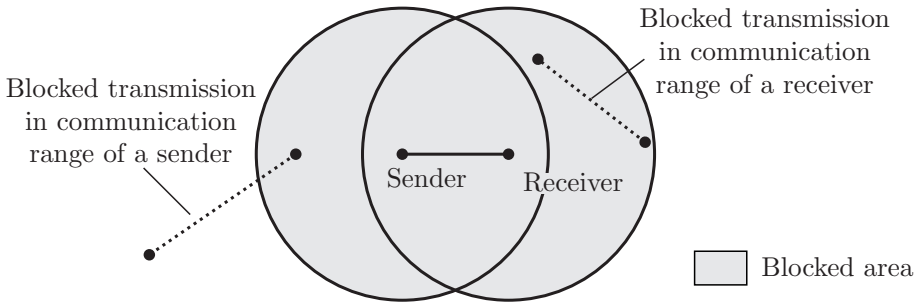

Figure 1.1.: Blocked transmissions in communication range of a sender or a receiver.

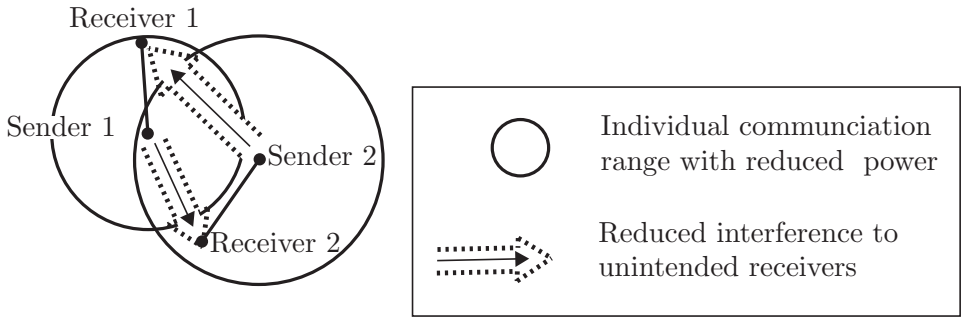

Figure 1.2.: Power control as physical layer technology to suppress MAI on the transmitter side.

obviously, however, limits the *spatial reuse*, i. e., the number of simultaneous transmissions in a network. Also, if multiple nodes outside the communication range of a receiver transmit simultaneously and the interferences sum up at a receiver, blocking transmissions in communication range is still not sufficient.

When targeting a denser spatial reuse, more sophisticated means for dealing with interference on the Physical layer (PHY) are required. Some of the advanced physical layer technologies suggested in literature to prevent MAI are *power control*, *multiuser detection*, and *multiple antenna signal processing*. As shown in Fig. 1.2, power control avoids MAI on the transmitter side, by individually reducing the transmit power to an extent that is still suitable to serve the associated partner. Thereby, also the interference at unintended receivers is reduced. In contrast to power control that suppresses interference at the transmitters, MultiUser Detection (MUD) is a physical layer technology that allows receivers to handle multiple simultaneously arriving signals. By decoding not only their wanted signals, but also unintended interfering signals, the influence of these signals is subtracted from the wanted signal. The number of simultaneously decodable signals equals the number of *detection branches*. With increasing number of detection branches, also the computational complexity of the multiuser detection receiver increases.

Multiple antenna, or Multiple Input Multiple Output (MIMO) signal processing summarizes a variety of different methods that require that transmitters and receivers are equipped with multiple antennas. Two commonly applied methods are *beamforming* and *spatial multiplexing*. While the methods differ significantly in their way to obtain MIMO gains, they both aim at exploiting the additional degrees of freedom offered by the multiple antennas.

An overview of the underlying physical layer technologies that we consider throughout the work as basis for cross-layer designs is shown in Fig. 1.3.

While the application of power control, multiuser detection, and MIMO signal processing is basically well understood in cellular environments, it still constitutes a challenge to apply these three technologies efficiently in ad hoc networks where no infrastructure is available. Therefore, distributed protocols are required that interact closely with the advanced physical

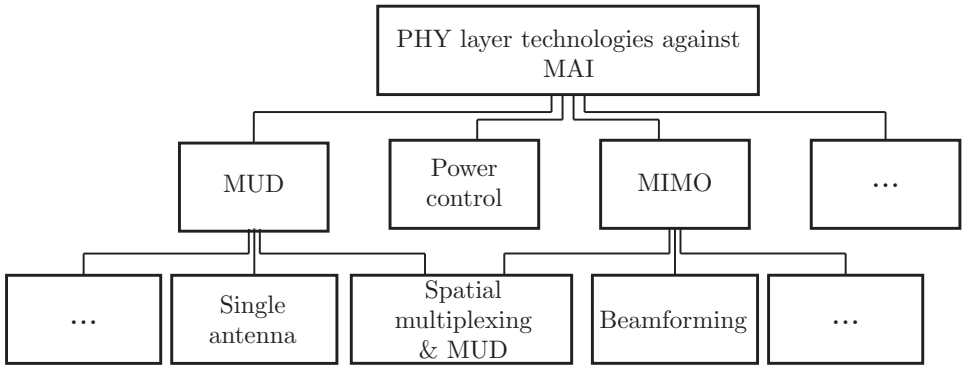

Figure 1.3.: Overview of physical layer technologies that are applied in cross-layer designs and are considered in this work.

layer technology. Hence, it is not sufficient to solely consider the physical layer. One rather has to look at joint cross-layer designs in which the Medium Access Control (MAC) protocol is specifically designed to support the respective physical layer technique. Throughout the work, we classify the joint PHY-MAC cross-layer designs depending on their underlying physical layer technology into a class for multiuser detection, a class for power control, and a class for MIMO signal processing as physical layer strategy. Note that, as shown in Fig. 1.3 for the example of *Spatial Multiplexing & MUD*, there is no sharp separation between the underlying physical layer technologies. Thus, some approaches belong to multiple classes.
We introduce the topic in the following chapter by summarizing basic principles of ad hoc networking. We further clarify the classification of joint PHY-MAC cross-layer designs in the global cross-layer design context.
In the main part of this thesis, the three cross-layer design classes are investigated. For the MIMO signal processing class, the cross-layer designs are further separated into designs with beamforming as signal processing method and designs that apply spatial multiplexing combined with MUD, see Fig. 1.3. Thereby, the following contributions to the field of interest are achieved:

- **Evaluation of existing solutions:**
  - For each of the three classes, the challenges arising by the underlying physical layer technology are thoroughly investigated. Existing cross-layer designs that fall into the class are in-depth reviewed regarding their ability to meet these challenges as well as with respect to their practical applicability.
  - A detailed simulative comparison of cross-layer designs that base on *power control* as physical layer strategy with cross-layer designs that require *multiuser detection* as physical layer strategy is performed. The simulations compare the performance of two reference schemes, one for each class of cross-layer designs. The reference schemes were chosen as the best representative schemes from their respective class

by a detailed literature review. To the best of our knowledge, this comparison is the first detailed simulative performance evaluation of both categories of cross-layer designs.

- **Development and evaluation of new solutions:** For *MIMO signal processing* as physical layer technology two new cross-layer design solutions are developed. While one applies the multiple antennas by means of beamforming, the other combines spatial multiplexing and MUD. The new cross-layer designs continue the work of existing solutions in this class, but overcome known shortcomings of these approaches. By evaluating the performance of both cross-layer designs, principal aspects of the different MIMO signal processing methods if applied in cross-layer designs are identified. Also, design criteria for appropriate MAC protocol solutions are developed.

- **Consideration of heterogeneously equipped nodes:** Existing cross-layer designs of all three classes are mostly developed for networks where the nodes are equally equipped. In future systems it can, however, be expected that nodes even if they apply the same physical layer technology, vary in their individual equipment. In multiple antenna systems, for example, nodes with different numbers of multiple antennas might alternate with single antenna nodes; in systems with multiuser detection as physical layer technology, the number of multiuser detection branches and thus the number of separable signals might vary. This variations in the physical layer equipment require in-depth considerations for appropriate cross-layer solutions. We consider *heterogeneously equipped nodes* throughout the work.

The first part of this work deals with cross-layer designs that consider power control as physical layer strategy and cross-layer designs that apply multiuser detection on the physical layer. It is structured as follows.
In Chapter 3, we compare cross-layer designs that are based on power control with cross-layer designs that apply multiuser detection. We explain the principle functionality of each physical layer technique and point out requirements and known shortcomings. We further present a summary of existing solutions for each class of cross-layer designs. These summarized approaches are investigated regarding their ability to meet the expounded requirements and to overcome the known shortcomings. From the existing solutions the most favorable candidate is chosen as the representative of the respective class.
We define appropriate measures to evaluate these two reference schemes not only regarding the aggregate throughput, but also regarding their offered Quality of Service (QoS). To achieve a simulative comparison that is as meaningful as possible, different simulation assumptions of both candidates are adopted to achieve equal simulation conditions.
Results with respect to variable measures that allow for a performance evaluation are presented for both cross-layer designs and the IEEE 802.11 protocol. All effects that lead to the respective results are thoroughly explained.
Both reference schemes are *time-slot-synchronous* cross-layer designs (cf. Sec. 2.3.2). In Chapter 4 an adaptive contention resolution algorithm for these time-slot-synchronous cross-layer designs is presented. The *Overload Adaptive Contention Resolution (OACR)*

algorithm specifically addresses fairness issues if heterogeneously equipped nodes exist in the network and the system runs on *overload*. Overload describes that the contention in the scenario is so severe that nodes are blocked multiple times consecutively and start dropping packets from their queues. In these scenarios the question arises if fairness in the sense that each node obtains a similar performance, named *classical fairness* in this work, is still meaningful; the classical fairness definition leads to a minority of weakly equipped nodes blocking all spatial reuse for a majority of better equipped nodes if heterogeneously equipped nodes exist. This results from the goal of classical fairness to obtain a common average aggregate throughput that is similar for all nodes, regardless of their equipment.
We newly define fairness as a trade-off between, on the one hand, allowing better equipped node to exploit their advanced equipment especially in overload situations, and, on the other hand, avoid a complete starving of weakly equipped nodes. To measure the achievements of the OACR algorithm, we define an appropriate fairness measure, since classical fairness indicators like the Jain's fairness index [JCH84] are not meaningful for this new fairness definition.
We show by simulations that the newly developed OACR algorithm improves the overall system throughput in overload situations. Still, weakly equipped nodes are not completely starved. The degree of unfairness compared with fairness in the classical sense can be influenced by varying a simulation parameter.
The second part of the thesis deals with cross-layer designs that apply *multiple antenna signal processing* as physical layer strategy. It is structured as follows.
In Chapter 5 we present background information about fundamental MIMO antenna techniques. The information does not aim at a more or less complete summary of existing techniques, but is meant as an introduction to those techniques that we reference during the remainder of the work.
In addition we describe essential characteristics that influence MIMO channel modeling. These characteristics reflect effects that occur in mobile wireless environments. Besides a short summary of the theoretical background for each of the characteristics, we describe its practical implementation in our channel model. This channel model is applied for all simulations in Chapter 6, Chapter 7, and Chapter 8.
In Chapter 6 we address those cross-layer designs out of the class of MIMO signal processing cross-layer designs that apply beamforming as signal processing method. At the beginning of the chapter, we identify key challenges that arise for directional transmission in wireless ad hoc networks. Continuing the work of two existing cross-layer designs, we present a new beamforming based MAC protocol. The protocol integrates the advantages of both schemes while avoiding their known disadvantages and overcomes the elaborated challenges. The performance of the new *CIE-MAC* protocol is investigated for heterogeneously equipped nodes in terms of aggregate throughput. Further, a Gaussian distributed channel estimation error is modeled and its influence on the system performance, as well as on the control message exchange, is investigated. To this end, the statistics of certain control messages are evaluated.
Chapter 7 deals with those cross-layer designs out of the class of MIMO signal processing cross-layer designs that apply spatial multiplexing as signal processing method. By a review

of existing cross-layer designs we identified major requirements for the development of a new cross-layer design. These are fulfilled by the newly presented *Fully Distributed Spatial Multiplexing (FDSM)-MAC* protocol. It continues principle ideas of the MUD-MAC protocol, but supports multiple streams on the receiver, as well as on the transmitter side. The design further takes the specific requirements of heterogeneously equipped nodes into account.
In Chapter 8 we compare the CIE-MAC protocol with the FDSM-MAC protocol. The comparison allows for some principal insights into the advantages and disadvantages of the specific MIMO signal processing methods. Also, some aspects of appropriate MAC protocol design are summarized.
Finally, Chapter 9 summarizes our contributions and gives an outlook about potential future research questions of the respective chapters. Appendix A shows some additional simulation results to Chapter 7. Appendix B lists symbols, mathematical notation, and abbreviations used in this work.
Parts of the material of this thesis have already been published before, as indicated in the accordant chapters.

2. Ad Hoc Networks and Cross-Layer Design: Basic Principles

This chapter introduces the principles of both, ad hoc networking and cross-layer design. We further specify the focus of this thesis within the common cross-layer design framework.

2.1. Ad Hoc Networks Principles

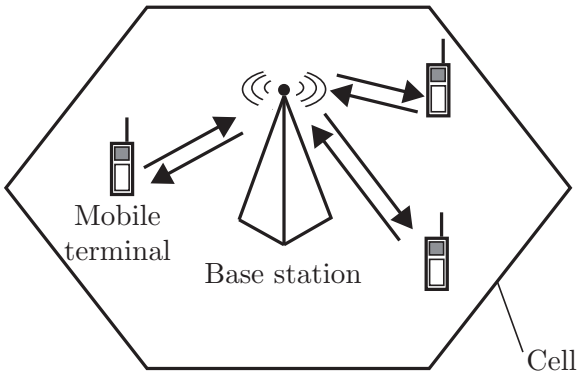

Figure 2.1.: One cell of a cellular network.

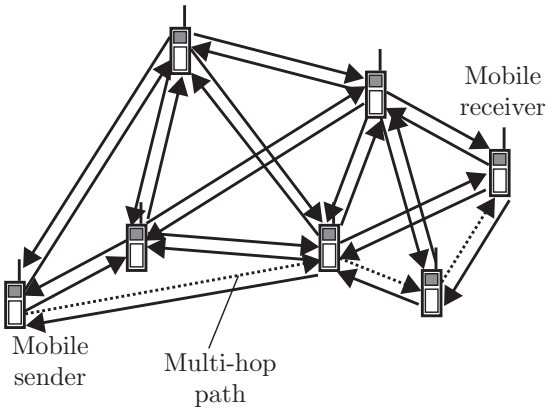

Figure 2.2.: Ad hoc network.

Today's wireless *cellular* systems, namely the Global System for Communication (GSM) and the Universal Mobile Telecommunication System (UMTS) provide access for mobile terminals to a wired backbone network by predefined access points, the *base stations*. An exemplary scenario is depicted in Fig. 2.1. The base stations are deployed throughout the area of interest so that a certain coverage is achieved and service can be facilitated reliably. Each station functions as a central entity, serving and scheduling the multiple *mobile terminals*. With the exception of *relay nodes*, which are basically introduced into a direct communication link for improving reception quality, all communication is performed directly from the base station to the mobile terminal and vice versa. Mobile terminals do not communicate with each other directly, but via the base station.

Ad hoc networks form in contrast to cellular systems spontaneously from a collection of wireless, maybe mobile nodes, and without any predefined infrastructure, see Fig. 2.2. Lacking any kind of a central entity, nodes have to perform all decisions regarding, e. g., networking or medium access control in a self-organizing, fully distributed way. All information about

other nodes in the network that is necessary at a node to perform decisions is obtained by an appropriate control message exchange. Since the communication range of each node is limited, nodes in ad hoc networks are likely to communicate not directly, but with the help of intermediate nodes. This *multi-hop* communication is shown in Fig. 2.2.

2.2. Ad Hoc Network - Modeling Assumptions

The application area of ad hoc networks is wide, ranging from battle-field applications, car-to-car-communication, and disaster relief scenarios to, e. g., indoor-office applications. As strong as the application area varies, as strong vary also the assumptions with respect to node mobility, node equipment, node density, and node distribution.

In this work, we analyze the performance of ad hoc networking by means of simulations. In the following we summarize models and parameters that we applied during the simulations with respect to the underlying ad hoc network. We set the models to be as general as possible, avoiding unnecessary details, but also grasp all essential effects.

2.2.1. Scenario and Node Distribution

This work investigates pure ad hoc networks without any infrastructure and no hierarchical organization of the nodes. The nodes are randomly and uniformly distributed among a two-dimensional square area. Inhomogeneous node distributions as well as specific topologies like, e. g., line topologies or star topologies are not considered in this work. All nodes are active, i. e., they generate packets and potentially transmit during simulation time.

2.2.2. Mobility and Traffic Modeling

Mobility Modeling

Mobility modeling is required to investigate the influence of, e. g., handovers or link changes on the system performance. The modeling of such influences is, however, out of scope of this work. Thus, in the first part of the work, i. e., Chapter 3 and Chapter 4, mobility of the nodes is not taken into account.

In the second part of the work, i. e., Chapters 6–8, cross-layer designs that apply MIMO signal processing methods are simulated. In these chapters, we are besides others, interested in the influence of fast fading on the system performance. Fast fading changes on the order of milliseconds, or even lower. Thus, the distance covered by a mobile node in between two temporal realizations that resolve these fading effects can be neglected. But a nodes' mobility influences the fast fading by changing certain characteristics of the underlying channel model. Thus, we consider pedestrian speeds for all nodes in the channel model. The influence of mobility on the channel modeling is further described in Chapter 5.

Traffic Modeling

We model best effort traffic with a fixed packet size that is the same for all nodes. These packets are generated with negative exponential distributed inter arrival times, leading to Poisson distributed packet arrivals. The traffic load at a node is varied by varying the mean inter arrival time of the packets. All nodes operate a transmission queue that works in a First In First Out (FIFO) manner.

2.2.3. Channel Modeling

In the first part of the work, i. e., Chapter 3 and Chapter 4, fading is not considered in the channel model. A line-of-sight channel is assumed, and all nodes are equipped with one omnidirectional antenna. We model the path loss attenuation A_{PL} between a transmitter and a receiver by a modified free-space path loss model as follows

$$A_{\mathrm{PL}} = \left(\frac{\lambda}{4\pi d_{\mathrm{TX,RX}}}\right)^2 \left(\frac{d_0}{d_{\mathrm{TX,RX}}}\right)^{\alpha-2}, \tag{2.1}$$

where λ is the carrier wavelength, $d_{\mathrm{TX,RX}}$ is the distance between a transmitter (TX) and a receiver (RX), d_0 is a reference distance that is set to $d_0 = 1\,\mathrm{m}$, and α is the path loss coefficient. To account for influences like reflection, diffraction, or scattering, it is set to $\alpha = 3.0$ [Rap02] throughout the work.
The receive power P_{r} at the receiver can thus be calculated as

$$P_{\mathrm{r}} = P_{\mathrm{t}} G_{\mathrm{t}} G_{\mathrm{r}} A_{\mathrm{PL}}, \tag{2.2}$$

where P_{t} is the transmit power that is set to $P_{\mathrm{t}} = 0.1\,\mathrm{Watt}$ for all nodes, and G_{t} and G_{r} are the omnidirectional antenna gains at the transmitter and the receiver. They are set to $G_{\mathrm{t}} = G_{\mathrm{r}} = 1.0$ and thus do not influence the receive power.
In the second part of the work, i. e., Chapters 6–8, the nodes are equipped with multiple antennas. We account for fast fading effects in our MIMO channel model. Details on the MIMO channel model can be found in Sec. 5.2.

2.2.4. Communication Range and Routing

We do not consider routing issues in this work. Thus, throughout the work we focus on single link transmission. At the beginning of a simulation, each node randomly chooses on other node as a sink. These destinations are fixed for the whole simulation time of 12 s. For all simulations in the first part of this work, i. e., Chapter 3 and Chapter 4, a nodes' sink is chosen from all nodes that are in static communication range of this node.
A node is in static communication range of another node if it receives packets from this node with a receive power P_{r} that exceeds the minimum *communication sensitivity*. This communication sensitivity is set to $-81\,\mathrm{dBm}$ for all simulations. Similar, a sensing sensitivity of $-91\,\mathrm{dBm}$ is assumed for all simulations. If the receive power is lower than this value, a node does not even sense the signals of another node.

For the second part of this work, i. e., Chapters 6–8 an additional *fading margin* is considered that accounts for fading losses that reduce the receive signal power additionally. A nodes' sink is chosen out of all nodes in the vicinity that achieve the *communication sensitivity* after additionally subtracting a fading margin of 10 dB from the transmit power.

2.3. Medium Access in Ad Hoc Networks

The particular properties of ad hoc networks pose major challenges with respect to, e. g., routing protocols, medium access control, and resource allocation. Within the context of this thesis, we concentrate on the design of specific MAC protocol solutions that support different PHY strategies. We give a first top-level classification of medium access control in the following. A more detailed state-of-the-art report on appropriate PHY-MAC cross-layer designs is given later on in the corresponding Chapters 3, 6, and 7.
Since no central entity exits, MAC decisions have to be performed fully distributed, resulting in a contention based medium access. Contention based medium access suffers from MAI. The amount of MAI at the active receivers has to be controlled by appropriate MAC protocol solutions. For each new transmission request, a MAC protocol has to decide if the transmission can start or has to be blocked in order to protect ongoing transmissions. Different ways to block transmissions exist. Either the transmissions are blocked internally by the transmitting node itself that requires to follow certain rules established by the MAC protocol. In case it would violate such a rule, it is not allowed to access the medium. Or the blocking can be performed externally, by another node objecting to the transmission request. In any of the cases, information on, e. g., transmission durations of active transmissions or of nodes involved in ongoing transmissions has to be available for each node. Also, the intended communication partner of a potential transmitter needs to be informed about the planned transmission and might reply to agree to the transmission before the actual data transmission starts. Unintended nodes might have the opportunities to object to the announced transmission. Thus, preceding the actual data transmission, a control message exchange takes place that enables such information exchange.
To decode a control message and thus to obtain the information contained in the message, a node needs to be in the communication range of the node transmitting the control message. To inform neighboring nodes that a transmission has started without including additional information, the sensing range is sufficient.
A significant distinction criterion for a principle classification of MAC protocol designs is the synchronization between the nodes during the control and data message exchange as well as the temporal arrangement of control and data packets. By these criteria, we classify the protocols into *MAC-layer-asynchronous* and *time-slot-synchronous* protocol designs.

2.3.1. MAC-Layer-Asynchronous Protocol Design - IEEE 802.11

Protocols that we classify as *MAC-layer-asynchronous* protocol designs require no temporal synchronization of the nodes to the beginning of the MAC control message exchange. A potential transmitter announces the start of a new transmission by a control message (CTRL)

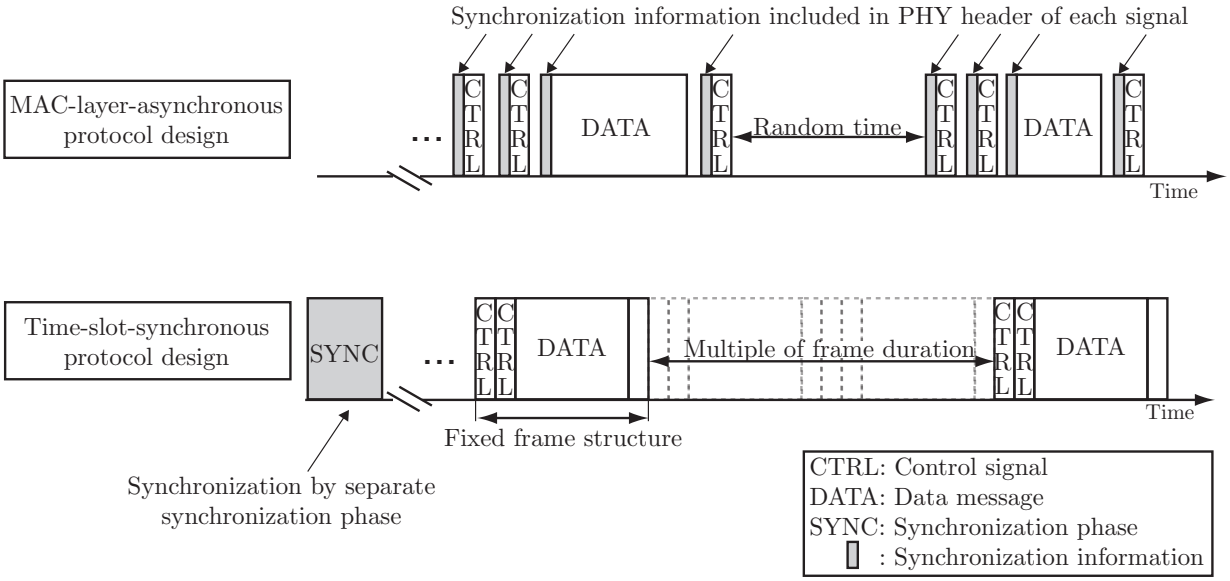

Figure 2.3.: MAC-layer-asynchronous and time-slot-synchronous protocol design.

at a random point in time, as shown by the upper row of Fig. 2.3. Since the nodes are not synchronized, in the physical header preceding the information part of the control message synchronization information to decode the control message is included. Nodes in the communication range of the potential transmitter use this information to synchronize to the control message and decode the control information.

In the example in Fig. 2.3 another control message is subsequently transmitted, e. g., as a reply by the intended receiver. The period between the first and the second control message is random and depends on the transmission delay from the potential sender to the replying node. By the synchronization information preceding the second control message, the potential transmitter and other nodes that overhear the message can synchronize to the control message and decode the message.

The intended receiver similarly synchronizes to the begin of the actual data transmission (DATA). The duration of the data transmission is of variable length. In the example of Fig. 2.3 after the data transmission, an additional control message is sent to complete the transmission. After a random period, another transmission starts with a new control message exchange.

The most prominent example for a MAC-layer-asynchronous protocol design in ad hoc networks is the IEEE 802.11 protocol [WLA97] including a Carrier Sense Multiple Access Collision Avoidance (CSMA-CA) mechanism. In its simplest form, a potential transmitter senses the medium. In case it cannot sense the signal of another transmitter, it waits for a random interval and starts transmitting data afterwards. Without optional mechanisms, the CSMA-CA algorithm suffers from the *hidden node problem*. This problem is explained by

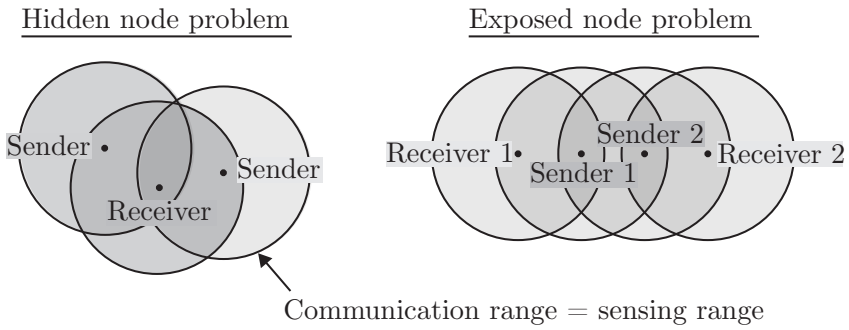

Figure 2.4.: Hidden node and exposed node problem.

means of Fig. 2.4. For simplicity, sensing and communication range are assumed to be the same and are marked as circles around the nodes in Fig. 2.4.
The hidden node problem describes that two senders are out of mutual sensing range, but have at least one node as joint neighbor. In case one of the senders transmit to this node, and the other sender starts transmitting simultaneously to this or another node, the packets collide at the node. To overcome the hidden node problem, a Distributed Coordination Function (DCF) with an optional Request To Send (RTS) Clear To Send (CTS) exchange was introduced.
A node willing to transmit first senses the medium to determine if another node is transmitting. If it senses the medium free, it transmits an RTS message. The RTS contains, besides others, the accurate transmission duration of the planned transmission. All nodes that overhear the RTS include the information into their Network Allocation Vector (NAV) and defer from accessing the medium for the duration of the transmission. In case the potential partner can decode the RTS message, it replies with a CTS message. The CTS, among other things, contains the duration of the data transmission as well. By the CTS, hidden nodes that are in the communication range of the potential receiver, but not of the transmitter get informed of the transmission and abstain from transmitting on their own for the duration of the transmission. After a successful data transmission, the receiver acknowledges the reception with an Acknowledgement (ACK) message.
While the RTS/CTS exchange solves the hidden node problem, the *exposed node problem*, shown in the right part of Fig. 2.4, remains unsolved. Both transmitters are in mutual sensing range. The associated receiver of each transmitter is, however, not interfered by the other transmitter. In this case carrier sensing blocks one of the two transmitters unnecessarily. A solution to this problem could be that nodes that overhear an RTS message, but not the replying CTS message are allowed to transmit.

2.3.2. Time-Slot-Synchronous Protocol Design

In contrast to MAC-layer-asynchronous protocol designs, *time-slot-synchronous* protocol designs assume a certain time slotted *frame structure* that is repeated consecutively over time (cf. lower row of Fig. 2.3). Nodes are *time-slot-synchronous*, i. e., synchronized so that

they can identify the beginning and end of time slots in this frame structure. Time slot synchronization is less strict and thus easier to obtain than bit level synchronization. The way it is achieved is out of scope of this thesis. Different solutions exist in literature that propose methods to achieve synchronization in ad hoc networks fully distributed, e. g., within a separate synchronization phase [SV04, ZL07] as shown by Fig. 2.3, or by piggy-backing synchronization information within the data message exchange [TAB10].
The frame structure itself consists of a control message slot, followed by a slot for data information, and, depending on the protocol design, complemented by an additional control slot. The slots are separated by small inter frame spacings to account for small variations in the synchronization. The duration of all slots is fixed, i. e., the data duration for this protocols is determined and does not have to be included in the control messages. Additional synchronization information in the PHY header preceding each slot is not required.
In contrast to MAC-layer-asynchronous protocol designs where nodes start at random points in time, in time-slot-synchronous protocol designs the contention starts solely at the beginning of a frame in a predefined slot. Thus, pauses in the channel usage last always for multiple of the frame duration.

2.4. Cross-Layer Design Principles

The term *cross-layer* refers to all approaches that complement, combine, or optimize over multiple *layers*. To understand the principles of cross-layer design, we first present in Sec. 2.4.1 the Open Systems Interconnection (OSI) reference model [ITU94] that introduced layers to regularize communication. Cross-layer design in principle violates this strict layered structure. We explain the motivation for cross-layer designs in Sec. 2.4.2. A general classification of cross-layer designs is shown in Sec. 2.4.3. With reference to this classification we clarify the focus of this work.

2.4.1. OSI Reference Model

The International Organization for Standardization (ISO) standardized the *OSI reference model* [ITU94]. The basic objective of the model is to regulate the interaction between interconnected systems. While the internal organization and functioning of each individual *Open System* is not regularized by the model, the external behavior of the open system has to follow the OSI architecture.
As shown by Fig. 2.5, the model subdivides all tasks that are necessary to run a communication system into seven layers. The grouping into the layers is performed depending on similar functionalities. Detailed information about the functionalities of each layer can be found in [ITU94]. Each layer provides *services* to the next higher layer. By defining the services but not the way these services are provided, independence of the layers is guaranteed. The services of one layer are provided by one or more *entities* over a *service access point* to the entities of the next higher layer. Entities of two open systems that operate on the same layer are *peer entities*. *Protocols* enable the interaction of peer entities.

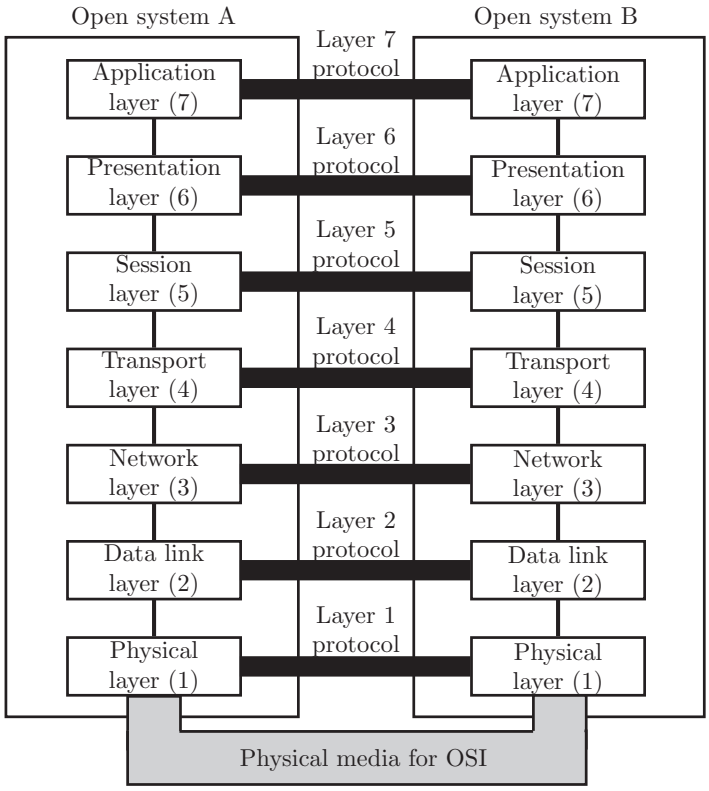

Figure 2.5.: Two open systems with layering according to the OSI reference model.

[Zim80] lists thirteen points that justify the seven layer structure. According to [Zim80], the goals of the layers are, besides others, to:

1. create a boundary at a point where the services description is small and the **interactions across the boundary is minimized,**

2. enable changes of functions or protocols within a layer **without affecting the other layers**, and

3. create for each layer interfaces with its **upper and lower layer only**.

2.4.2. Motivation for Cross-Layer Design

The OSI model is widely accepted and the goals of the layering are clear and reasonable. The question arises what motivates to violate this well defined structure by, e. g., interacting across the boundaries of a layer, or designing layers so that changes on functions or protocols of one layer force another layer to change as well?
The answer lies in the fundamental different properties of wireless and wired communication. The OSI model was originally developed for wired communication. Wireless communication, however, has different characteristics compared to wired communication. In [Big05], four major points describing these different characteristics are elaborated, namely:

1. **Link connectivity:** A link in a wireless ad hoc network differs significantly from a link in a wired network. In a wired network, a link between two nodes exists only if a wire connects both nodes.

   In wireless ad hoc networks, a node can communicate theoretically with all other nodes in the network with a rate that depends on the Signal to Interference and Noise Ratio (SINR) of this link. The SINR of a link and thus the supportable data rate varies strongly in space and time. It is further influenced by the magnitude of the MAI that varies as well.

2. **Power control:** Related to the link connectivity, in wireless networks the quality of each link and thus the supportable data rate can be improved by increasing the transmit power. Also, the number of one-hop neighbors and thus the whole topology of the network depends on the transmit power level.

3. **Medium access control:** Both, wired as well as wireless media apply MAC protocols. But inherent in the broadcast nature of the wireless medium, specific problems, namely the before mentioned hidden node and exposed node problem exist. QoS parameters like delay or throughput of a network thus depend on the ability of the MAC protocol to overcome these problems.

4. **Mobility:** In wireless networks, nodes can be mobile. This node mobility affects multiple layers. As an example, the topology of a network is influenced by the mobility of nodes and thus influences also routing decisions. Simultaneously, node mobility

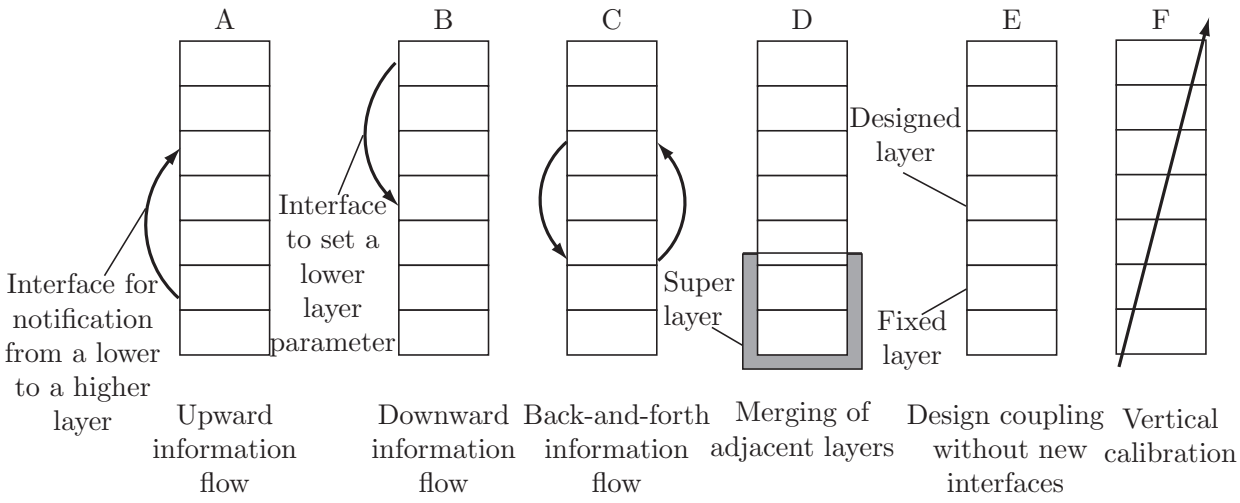

Figure 2.6.: Different kinds of cross-layer design proposals [SM05].

influences also the link layer, since the mobility determines how fast the link quality varies.

While layering according to the OSI model simplifies the network design, it suffers from inflexibility. The strongly increased variability in wireless networks regarding link connectivity, power control, medium access control, and mobility requires a more flexible structure. Since characteristics like the mobility influence multiple layers simultaneously, a coordination and adaptation between the layers that reacts on rapid changes of the wireless network is required. Interaction across the boundaries of a layer can help to coordinate adjacent layers. But from the different characteristics of wireless communications also new interdependencies between non adjacent layers exist that require new interfaces between these non adjacent layers.

2.4.3. Cross-Layer Design Classification

Obviously, various possibilities of how to realize cross-layer designs exist. In order to clarify the focus of this thesis we summarize a cross-layer design classification taken from [SM05]. Other taxonomies can be found in, e. g., [FGA08, CPN08]. The authors of [SM05] classify cross-layer designs by the way the original OSI reference model is violated. They distinguish six kinds of cross-layer designs that are depicted in Fig. 2.6. Examples A-C reflect models where completely new interfaces are created. This can be the case if information is passed from a lower to a higher layer (A), like in [CISN05]. There a *bottom-up* approach supports video transmissions over wireless channels by passing information about equivalence classes of operating points from the physical layer to the upper layers. We present the opposite of a bottom-up approach, namely a *top-down* approach in [KGGH08b]. There, for each *user service class* that describes individual QoS requirements on the application layer, an appropriate SINR requirement is passed down to the physical layer. The PHY layer achieves

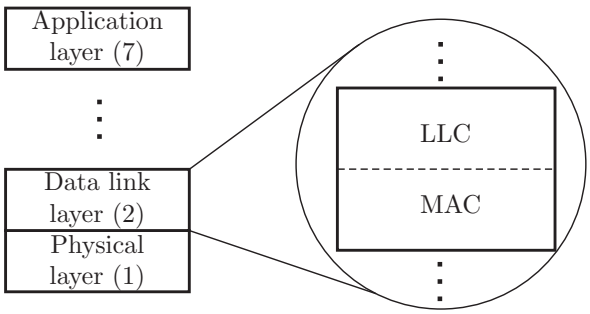

Figure 2.7.: LLC and MAC sub-layers of the data link layer.

the requirement by an advanced spatial processing technique [KGGH08a]. New interfaces are built by handing down information from an upper to a lower layer, corresponding to class B in Fig. 2.6. Class C represents all approaches, where new interfaces are created by two-way information flows between two layers.
In contrast to the classes A-C, where new interfaces are created, class D merges adjacent layers. The resulting *super layer* unites the services of two or more merged layers. No new interfaces are created. A joint PHY-MAC cross-layer design that, e. g., suppresses multiple access interference, approaches such a super layer. before explaining class E, we summarize class F. Class F does a *vertical calibration* of all layers. It either sets parameters on all layers statically at design time depending on a certain metric; or it adjusts the parameters dynamically at runtime as a reaction to variations in the channel or network conditions.
Class E does not create any new interfaces, nor does it alter the predefined structure of the OSI reference model by merging layers. The behavior of a certain layer is fixed instead, and another layer adapts its functionality to the behavior of the fixed layer. An example for this class of cross-layer designs is the MUD-MAC protocol [KVM+09]. This protocol is developed to increase the spatial reuse by an appropriate MAC protocol design if the underlying physical layer is capable of MUD.
The MAC layer is besides the Logical Link Control (LLC) layer defined as one in two sub-layers of the data link layer of the OSI reference model, as depicted in Fig. 2.7. It determines the access strategy in order to avoid MAI if multiple participants try to access a shared medium simultaneously.
Similar to the MUD-MAC protocol that represents class E of the cross-layer design classification, we focus in this work on a joint design of a specific (fixed) physical layer and a functional adapted, appropriate MAC protocol solution. The physical layer technologies that we investigate as fixed physical layer strategies are the ones in Fig. 1.3.
In the work, we will use the term protocol and cross-layer design synonymously to refer to specific MAC protocol solutions that demand a certain fixed physical layer technology.

3. Power Control Based Versus Multiuser Detection Based Cross-Layer Design

Power control, which has been applied successfully to cellular networks, has received considerable attention in the field of ad hoc networks as well. It has been combined with specific MAC protocols in order to apply it in distributed ad hoc networks for MAI suppression by many authors, e. g., [MK05, HL07, TG06].
A different physical layer technique, which also has received considerable attention in literature, is multiuser detection applied on the receiver side [Ver98]. A MultiUser Detection (MUD) receiver detects interfering streams in order to subtract their interference contribution from the received signal, thus canceling MAI. MUD has also been investigated by several authors in the context of ad hoc networks by combining it with appropriate MAC protocols, e. g., [ECS+07, CLZ06, KVM+09].
We are interested in the capability of both, power control based and MUD based cross-layer solutions. Both classes of cross-layer designs aim at increasing the spatial reuse by avoiding MAI; but the two physical layer techniques differ fundamentally in the way they treat MAI as well as in their required interaction with the MAC protocol. Although the performance of both techniques is well understood as far as the physical layer is concerned, an in-depth simulative comparison between power control based and MUD based cross-layer designs is not yet available.
A detailed review and discussion of available cross-layer designs for power control and MUD is given in Sec. 3.1 and Sec. 3.2. We are further concerned with the QoS achieved by the different cross-layer design classes. Thus, we thoroughly investigate two representative cross-layer designs, one for each class. More precisely, we compare the Progressive BackOff Algorithm (PBOA) [TG06], which is a good representative for power control based cross-layer design, with the MUD-MAC cross-layer design, which was presented in [KVM+09]. Both protocols are time-slot-synchronous approaches as explained in Sec. 2.3.2. They are functionally designed to support the respective physical layer technology. We assess and compare the QoS of both schemes by means of extensive system simulations regarding data throughput as well as delay and fairness aspects in Sec. 3.3. Finally Sec. 3.4 summarizes this chapter.
Parts of the results presented in this chapter have earlier been published in [KHKW10b, KHKW10a, KHKW11].

3.1. Power Control Based Cross-Layer Design

Power control has been employed successfully in cellular networks. But applying it in the specific environment of ad hoc networks is not a straight forward option. In Sec. 3.1.1 the principle functionality and the specific challenges of power control in ad hoc networks compared with cellular networks are explained. Sec. 3.1.2 gives a detailed overview of power

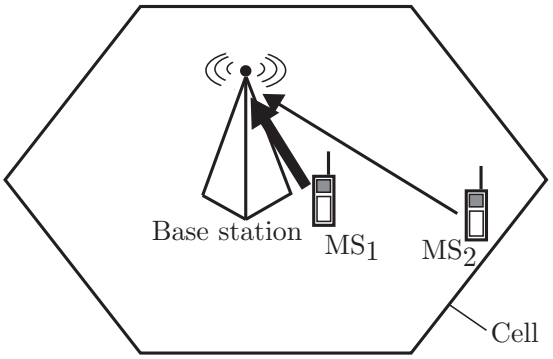

Figure 3.1.: Exemplary uplink scenario in a UMTS network.

control based cross-layer designs that suppress MAI. The power control based cross-layer design that is chosen as representative approach, namely PBOA, is summarized in Sec. 3.1.2.

3.1.1. Principle Functionality of Power Control

Fig. 3.1 shows an exemplary scenario for power control in the uplink of a UMTS network. UMTS applies Code Division Multiple Access (CDMA) to separate users, i. e., mobile station one (MS_1) and mobile station two (MS_2) spread their data with ideally orthogonal codes. If the spreading sequences applied offered perfect cross-correlation properties and the base station operated ideally, both messages could be received without mutual interference [SW02].

Practical CDMA systems are, however, interference limited. This leads to severe performance degradations by the *near-far problem* if the senders have strongly varying distances to the receiver as in Fig. 3.1. There, since MS_1 is close to the base station while MS_2 is far away, the MAI caused by MS_1 to the transmission from MS_2 might very likely disrupt the reception of data from MS_2 at the base station.
Thus, in UMTS systems the base station as central entity controls the mobile stations' transmit power levels in the uplink by *transmit power commands* via a control channel (*closed loop power control*) [SW02]. This is possible since the base station can measure the receive Signal to Interference Ratio (SIR) and compare it with a target SIR for every transmission.
In contrast to a cell of a cellular network in ad hoc networks no central control unit similar to a base station exists (cf. Sec. 2.1). Thus, information on the magnitude of interference induced by a transmitter at multiple unintended receivers has to be obtained fully distributed. Also, the power adaptation process has to be operated without any central coordination. Moreover, since multiple transmissions take place simultaneously, a solution with power control might be inaccessible. Certain *blocking situations* might occur that require that some transmitters have to abstain from transmitting.
An exemplary situation for power control is depicted in Fig. 3.2. Three transmission pairs

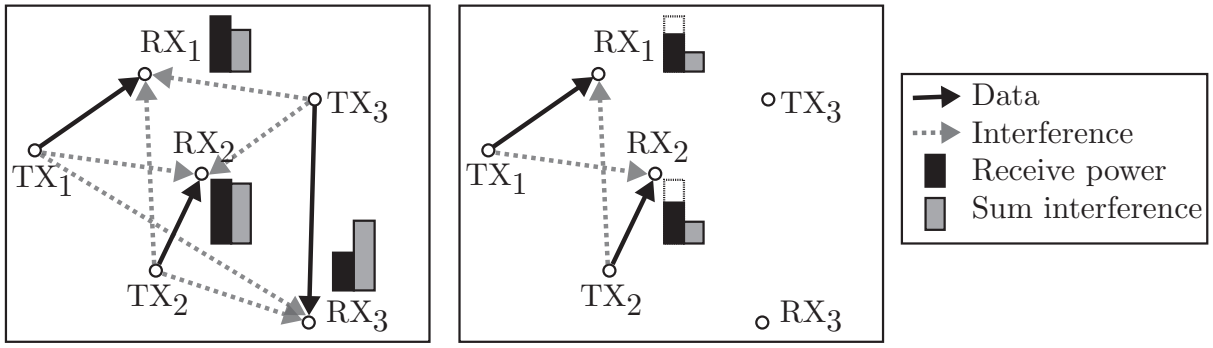

Figure 3.2.: Power control adaptation in a wireless ad hoc network.

plan to access the wireless medium simultaneously. Next to each receiver, two bars reflect the receiver power of the *wanted* transmission, i. e., from the associated partner, colored in black, and the sum of unintended and thus *unwanted* interferences, colored in grey. At the initial phase of the power adaptation process (left picture of Fig. 3.2), all three transmitters (TX_1, TX_2, TX_3) try to serve their associated partners (RX_1, RX_2, RX_3) simultaneously. Without power adaptation the interference for all receivers is rather high. Specifically, for RX_3 the interference power is even higher than the receive signal power, since the associated partner TX_3 is further away than the interfering transmitter TX_2. On the other hand, TX_3 also causes strong interference to RX_2. This leads to a blocking situation that cannot be resolved by power control, since in order to avoid interference to RX_2, TX_3 had to reduce its transmit power (the same for TX_2 w.r.t. RX_3), but then the receive signal power at the associated partner would also shrink. Thus, one of the transmitters has to abstain from transmitting.
A possible outcome of the power adaptation process is shown in the right part of Fig. 3.2. TX_3 abstains from transmitting, thus facilitating the successful transmission from TX_2 to RX_2. Additionally, TX_1 and TX_2 power down to an individual minimum power level that is required to serve their associated partners. Thereby the interference in the system is further reduced.
From this example, four essential requirements of power control based cross-layer design in ad hoc networks can be observed. An appropriate MAC protocol solution has to:

1. identify and resolve blocking situations,

2. provide for each transmitter information on the minimum required receiver power level of its associated partner,

3. make information about the magnitude of unintended interferences at others than the intended receiver available at a transmitter, and

4. handle the mutual interference in the network that is influenced by each individual decision fully distributed.

The second and third point are critical, since the information required depends in both cases on the actual channel quality between the transmitter and the receiver(s). Since the channel quality is time-varying, the information is only valid as long as the channel remains almost constant.

3.1.2. Related Work

In the following, we present a state-of-the-art report on power control based cross-layer designs in wireless ad hoc networks. We focus exclusively on those cross-layer designs that perform power control with the goal of suppressing MAI. Cross-layer designs that primarily aim at energy savings or topology control are not taken into account.
In [EE04] results based on a combination of centrally performed scheduling and fully distributed power control are presented. The scheduling is performed prior to each data transmission phase and determines a subset of senders that can transmit simultaneously. It overcomes blocking situations as the one described in Fig. 3.2. Once a valid subset is selected, an iterative power control algorithm that is an extension of a power control algorithm applied in cellular systems is operated.
Although the approach shows the results for optimal scheduling policies and points out resulting performance gaps if simpler scheduling algorithms are applied, it is not directly applicable in wireless ad hoc networks. There, in principle no central entity (like a central scheduler) exists. This holds also for the COMmon POWer (COMPOW) algorithm [KK05]. The approach aims at one common power level for all transmitters in the network that is the lowest one to still keep the network connected. By additional information included in the routing message exchange, a *power control agent* centrally decides the magnitude of this common power level. Besides the above-mentioned impracticality of a central entity, obtaining interference information with the help of routing packets is not realistic due to a prohibitive overhead if the underlying channel is non-static.
This overhead also limits all approaches that exchange information, e. g., tables, between different participants. These exchange information to inform nodes about power information between neighbors [HL07, NLJ05], to obtain routing information for multiple different power levels [KK05], to get interference tolerance levels of the neighborhood [LKL03], or to learn information about link gains between two neighboring nodes (*indirect links*) [MK04]. The mentioned approaches are thus restricted to static channels. The authors of [BCP00] explicitly formulated the property of a static channel as a constraint. For the proposed Distributed Power Control algorithm with Active Link Protection (DPC/ALP) the authors restrict the application field to quasi-static channels where the time scale of mobility is much larger than the one of power adaptation.
Other approaches split the available bandwidth into two frequency bands, one for a data channel and one for a separate control channel. The channels are assumed to experience similar channel conditions, i. e., they lie in the coherence bandwidth of the channel (cf. Sec. 5.2). The separate control channel is either used by active receivers to inform transmitters in their

vicinity of the additional amount of interference they can tolerate [MBH01]; or to transmit all control messages separately in order to avoid collisions between control and data packets [MK03]. It does not assure automatically though that control messages from different nodes do not collide. Furthermore, if data and control messages are transmitted at the same time, a node is either required to own two transceivers, as assumed in [MK04, MBH01, MK03], in order to receive and transmit simultaneously; or it is deaf to all incoming messages on the control channel while it is transmitting data, leading to packet losses due to missed control messages. But transmitting data and control messages in a time-division manner to avoid two transceivers, as argued by the authors of [NP06], makes the application of a separate control channel unnecessary.

As discussed so far, most approaches rely on impractical or costly assumptions such as a central entity, additional hardware, or time invariant channels. Only a few proposals [MK05, TG06, LGF09], which we discuss in the following, are designed without such strict assumptions.

In [MK05] the MAC-layer-asynchronous POWMAC protocol is proposed. This protocol uses an *access window phase* to agree on a set of transmissions that can proceed simultaneously. During this phase, each potential receiver announces the transmission power to be used by the communication partner, and, with respect to this wanted receive power, a *common maximum interference level*. This is the amount of interference that it can tolerate from a single newly starting transmission. Each transmitter that starts transmitting afterwards must assure that it does not violate any of the interference tolerance levels included in preceding messages. By this strategy, a certain receive SINR at each receiver is attained. After the access window phase multiple data transmissions can take place simultaneously.

Based on the POWMAC protocol, the Adaptive Transmission Power controlled MAC (ATPMAC) protocol [LGF09] was developed. The authors of [LGF09] avoid reserving time for the access window phase by transmitting control messages in parallel to data transmissions.

The major drawback of both schemes [MK05, LGF09] is the assumption of one common maximum interference level that is the same for all interfering nodes. This level is more or less the overall tolerable interference power at a receiver divided by the number of interferers in its vicinity. But defining one common average interference level is highly inefficient, since the interference varies strongly with the distance (or channel) between the interferer and the interfered node. A distant transmitter is allowed to cause more interference than it actually requires due to the common interference level and thus does not exhaust its interference budget; a nearby node might fail to hold the common interference limit and thus abstain from transmitting. If it was allowed to use the additional budget from the far away node, both transmissions could take place in parallel without violating the overall tolerable interference at the receiver.

Due to the shortcomings of the algorithms presented above [MK05, LGF09], the Progressive BackOff Algorithm (PBOA) [TG06] is chosen as the most reasonable reference scheme. We will present it in the following.

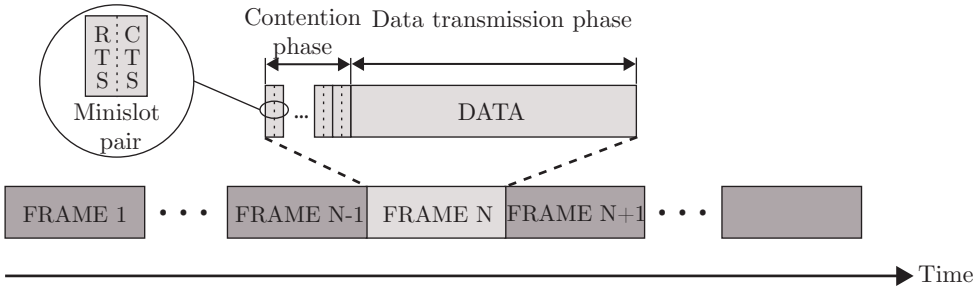

Figure 3.3.: General frame structure of the PBOA algorithm.

The PBOA Algorithm

The PBOA protocol is a time-slot-synchronous protocol design (cf. Sec. 2.3.2) and assumes a certain time slotted *frame* structure that is depicted in Fig. 3.3. The duration of the frame is chosen such that the channel is at least constant for the duration of one frame. A frame is further subdivided in a *contention phase* and a *data transmission phase*. During the contention phase, a subset of all potential transmissions is decided fully distributed to transmit simultaneously during the data transmission phase. Also the transmit power for each transmission is decided during the contention phase. During the data transmission phase, this subset of the transmissions takes place with the decided transmit powers.

The contention phase is build up by several *minislot pairs*. Each minislot pair consists of an RTS and a CTS message. At the beginning of the contention phase all potential transmitters transmit their RTS messages simultaneously with maximum power. Fig. 3.4 illustrates this (First minislot pair, RTS slot). TX_1 to TX_4 represent transmitters simultaneously transmitting during the contention phase. RX_1 to RX_4 represent their intended receivers.

If the intended receiver can decode the RTS, it replies with a CTS also with maximum power. Depending on its receive SINR and its actual SINR requirement, it includes a factor into the CTS that tells its associated partner how much to power down in the next RTS minislot of the contention phase. In the first minislot pair, TX_1, TX_2, and TX_3 are not successful. Only RX_4 can decode the RTS and replies with a CTS. (First minislot pair, CTS slot).

If a transmitter does not receive a CTS during one minislot, it will contend again during the consecutive minislot pair with a *win probability* p_{win}, or it will go to backoff and turn into a potential receiving node until the end of the frame with the probability of $1 - p_{\text{win}}$. By reducing transmission powers and the number of potential transmitters (backoff) progressively, other transmitters are given more chance to reach their intended receivers.

In the RTS slot of the second minislot pair, the successful transmitter TX_4 transmits an RTS message, but, according to the information from the received CTS message, with reduced transmit power. While TX_2 lost according to $1 - p_{\text{win}}$ and went into backoff, TX_1 and TX_3 contend again for channel access. Notice, however, that TX_3 chooses a different receiver, namely the second receiver in its single transmission queue. This is proposed by the authors of PBOA since by changing the intended receiver, a weakly interfered receiver might be

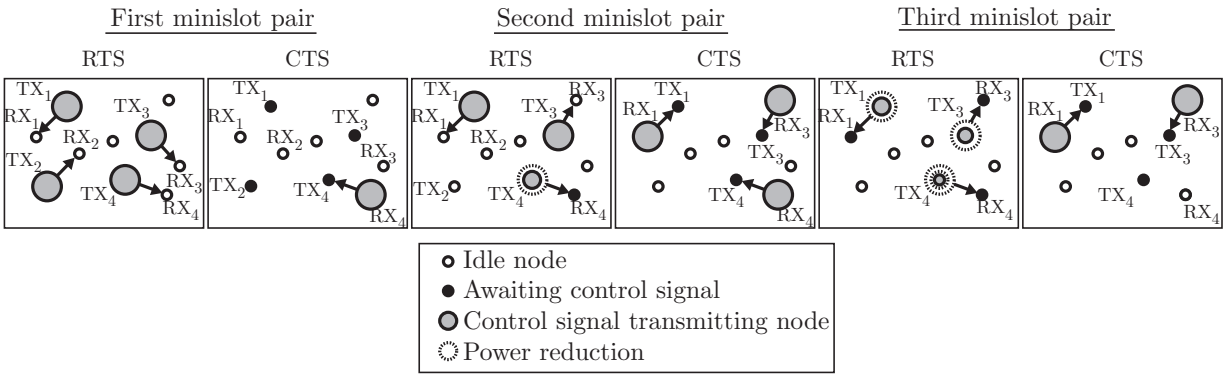

Figure 3.4.: Power adaptation and backoff during the contention phase of the PBOA protocol.

addressed. This increases the probability that RTS messages reach the intended receivers. In the CTS slot of the second minislot pair, RX_1 replies with a CTS message. It was able to decode the RTS this time, since by TX_2 backing off the interference was decreased. Also, the newly chosen receiver RX_3 replies with a CTS, since it was less interfered than the other intended receiver of TX_3 and thus was able to decode the RTS message. RX_4 replies as well and includes a factor to further reduce the transmission power at TX_4.
This successive power reduction goes on in consecutive minislots, unless a minimum for the acceptable transmission power at a receiver is reached. Afterwards, the receiver abstains from transmitting further CTS messages, as shown in the CTS slot of the third minislot pair for RX_4. TX_4 proceeds transmitting RTS messages with the minimum transmission power until the contention phase ends. This enables other receivers to still estimate the interference expected during data transmission correctly.
After the contention phase all successful transmitters send their data to their intended receivers with the individual transmit power levels that were decided during the contention phase. The authors of [TG06] argue that an additional acknowledgement is not required since the channel is constant for the duration of the frame and thus the transmission is expected to be successful.

3.2. Multiuser Detection Based Cross-Layer Design

In contrast to power control that suppresses MAI on the transmitter side, the principle of multiuser detection is to deal with interference at the receiver. To explain the motivation for MUD we go back to the UMTS uplink scenario depicted in Fig. 3.1.
As we already stated in Sec. 3.1.1, a certain cross-correlation exists between MS_1 and MS_2. This cross-correlation is treated as interference in the conventional demodulation process that applies a bank of matched filters, one for each spreading sequence.
The base station, however, actually knows certain properties about the interfering stream, e. g., the applied spreading sequence. This knowledge can be exploited to improve the

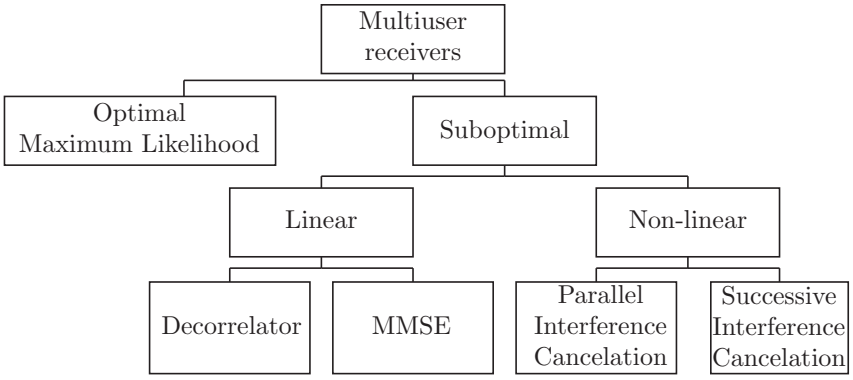

Figure 3.5.: Classification of multiuser detection receivers [CM05].

performance of the conventional receiver.

3.2.1. Principle Functionality of Multiuser Detection

There are different methods to use a certain knowledge of the interfering streams in literature. All approaches have in common that the receiver detects all streams, the wanted stream as well as all interfering streams. The latter are detected in order to subtract their interference contribution from the received signal. A classification of multiuser detection receivers from [CM05] is shown in Fig. 3.5. The optimum maximum-likelihood receiver is too complex to be applied in reality ($O(2^K)$ for K users [And05]), where $O()$ denotes the computational complexity. Different suboptimum linear and non-linear receivers exist that tend to approach the performance of the optimum receiver. The schemes differ significantly in their computational complexity, their prerequisites for the detection process, and their performance gap to the optimum maximum-likelihood receiver. We will summarize them shortly in the following. For details of the different multiuser detection schemes we refer to [Ver98, DHHZ95, LR97, And05, KBK02].
The class of linear multiuser detectors applies a linear transformation to the matched filter outputs. In case the different streams are separated by orthogonal spreading sequences, with a decorrelator receiver the resulting MAI can be eliminated completely by an inversion of the code cross-correlation matrix. As an advantage, it does not require knowledge of the receive amplitudes (Channel State Information (CSI)) at the receiver. Another advantage is that it eliminates the MAI completely, hence it is near-far resistant. As a disadvantage, it is likely to enhance the background noise.
The Minimum Mean Square Error (MMSE) detector considers noise as well and minimizes the mean square error by adding a noise term to the code cross-correlation matrix. This noise term contains information on the receive amplitudes of all impinging signals. While it overcomes the noise enhancement and outperforms the decorrelator receiver in noisy environments, it requires CSI at the receiver. If the background noise approaches zero, the MMSE receiver becomes the decorrelator receiver. Although the linear receivers are less

complex than the optimum receiver, they still require a complexity of ($O(K^3)$), related to the inversion of the code cross-correlation matrix of size $K \times K$.
Instead of performing the optimization over the whole set of users simultaneously, non-linear approaches use decisions on the bits of previously decoded interfering users to demodulate the bit of interest. Similar to the MMSE detector, they require CSI on the receiver side.
If the bit estimates of previously decoded users are applied to subtract the influence of these users from the received sum signal, the multiuser detection method is called Successive Interference Cancelation (SIC). As an advantage, the SIC detector is among the least complex multiuser detectors. Without additional methods, it is very sensitive to decision errors in previous stages though. The implementation complexity and the detection delay of the SIC detector grow linearly with K. To overcome the latter, also Parallel Interference Cancelation (PIC) detectors exist. While they reduce the detection delay significantly, they have a higher complexity than SIC.
Multiuser detection can also be applied without separating the different signals by codes if the receivers are equipped with multiple antennas. In this case, the differences in attenuation and phase shift that the different signals experience on their way to the receiver can be exploited to separate the signals. The detection process then is a combination of space-matched filtering and, e. g., successive interference cancelation. A well-known example is the Vertical-Bell Laboratories Layered Space-Time (V-BLAST) receiver presented in [WFGA98].
In [Vil09] six requirements (**R1** – **R6**) for a MAC protocol design that supports multiuser detection with successive interference cancelation in ad hoc networks are identified:

- time synchronization on frame level (**R1**),
- knowledge of signatures in use (**R2**),
- channel estimation with respect to all signal sources (**R3**),
- knowledge of the start time and duration of packets (**R4**),
- receiver-individual avoidance of interference exceeding the number of multiuser detection branches (**R5**), and
- protection of weak receivers having only single-user detectors (**R6**).

R2 holds only if the different streams are separated by codes. In case of multiple antennas at a receiver, the additional usage of codes is possible, but not a requirement. To exploit the multiple antennas, knowledge of the channels to all signal sources is required though (**R3**). In case of a single antenna multiuser detector receiver, the requirement of channel state information depends on the underlying multiuser detection class. **R1**, **R4**, **R5**, and **R6** are substantial for all multiuser detection based cross-layer designs in ad hoc networks. All schemes that we summarize in the following are time-slot-synchronous (**R1**) and assume a certain time slotted frame structure. Thus, requirement **R4** is met.
To achieve **R3**, it has to be considered that channel estimation is performed by transmitting known pilot symbols from each signal source before the actual multiuser detection phase

starts. At the receiver, the attenuation and phase shift that the symbols experienced on their way to the receiver is estimated.
In case only one source transmits a pilot symbol at a time, the channel estimation process can be performed reliably at the receiver. Notice, however, that channel estimation may not be performed reliably if multiple senders transmit the pilots simultaneously. The signals of all transmitters then superimpose, unless the pilots are somehow made orthogonal, i. e., by individual orthogonal codes.
If a medium access control protocol design transmits all control messages that precede a data transmission simultaneously, the channel estimation has to be performed separately, i. e., by a separate proactive channel estimation phase that is periodically repeated.
Estimating the channel to all neighbors periodically in a proactive manner in a *periodical channel estimation phase* introduces a non negligible overhead that might easily get prohibitive in high node density scenarios. Moreover, the majority of channel estimations is preventible in case only the channels to the active transmitters are estimated.

3.2.2. Related Work

[CLZ06, CLZ08] address cross-layer designs with multiple antennas at the transmitters and at the receivers. As physical layer strategy, spatial multiplexing (for further explanation cf. Sec. 5.1.2) on the transmitter side and a V-BLAST type multiuser detector [WFGA98] on the receiver side is applied. The approaches adapt the IEEE 802.11 CSMA-CA scheme in the sense that nodes are time-slot-synchronous and the RTS/CTS messages are transmitted simultaneously. The control messages are not exchanged to avoid collisions but rather to agree on multiple parallel transmissions.
Note that the decoding of multiple simultaneous control messages requires all nodes to be capable of multiuser detection. Nodes with only a single detector branch are excluded from channel access (**R6**) automatically. Moreover, providing the channel information required at the receivers by including pilots into the control message exchange is not an option (**R3**). As a solution, a separate periodical channel estimation phase is required, as also proposed by the authors of [LTZ08]. This phase suffers from the before mentioned disadvantages.
The authors of [ZDGK09] present a MAC protocol design that combines CDMA with a linear MMSE receiver. They decide on the number of suitable transmissions by means of a distributed scheduling algorithm, thus solving **R5**. During the information exchange that leads to the distributed scheduling, multiple nodes transmit RTS messages simultaneously. Since in the proposed protocol each node has an individual code assigned, channel estimates that are required for the MMMSE receiver are possible by these RTS messages (**R3**). Also, nodes equipped with a single branch can overhear control messages (**R6**). But, for a higher number of nodes, assigning each node an individual spreading code increases both, the bandwidth requirement as well as the computational complexity of the MMSE detector strongly. The former increases since the code length and thus the bandwidth requirement increases with the number of separable codes and nodes, respectively; the latter increases since the MMSE detector requires an inversion of the code cross-correlation matrix that increases with an increasing number of codes and an increasing code length.

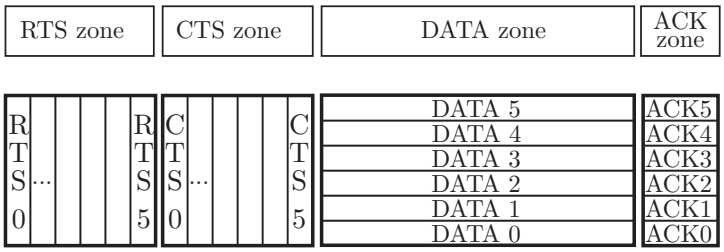

Figure 3.6.: Frame structure of the *Interference Division Multiple Access* protocol.

The authors of [CW10] propose a cross-layer design based on MUD combined with multiple antennas at the senders and at the receivers. As a prerequisite set by the authors, the neighbor density is limited so that channel estimation is possible. Each node has one individual code out of a code list that is common and known to all nodes in the network. On these assumptions, the authors propose a distributed scheduling algorithm that exploits multiuser and spatial diversity gains by selecting nodes and antennas with good channel conditions.

In order to overcome limitations regarding the node density due to channel estimation requirements or limited spreading code length, and also to support nodes with only a single detector branch (**R6**), a possible solution is to avoid multiuser detection as a prerequisite during the control message phase. A step into this direction is performed by the authors of [ECS+07]. One frame of their *Interference Division Multiple Access* protocol consists of an RTS zone, a CTS zone, a DATA zone, and an ACK zone, see Fig. 3.6. Instead of a parallel transmission of multiple messages during the RTS and CTS zone, the authors subdivide these zones into multiple RTS and CTS slots, one slot per node. Thus, neighboring nodes can estimate the channel to all transmitting nodes (**R3**), since all RTS messages are transmitted in a Time Division Multiple Access (TDMA) manner. Also, subdividing the RTS and CTS zones into slots with only one node transmitting allows nodes with only a single detector branch to overhear this messages. But since the ACK messages are transmitted simultaneously in [ECS+07], the method nevertheless fails to achieve **R6**.

Full support also for nodes with a single detector branch is achieved by the *MUD-MAC* protocol [KVM+09]. The protocol assumes non-linear SIC multiuser detection combined with a spread spectrum multiple access scheme, e. g., CDMA or Interleave Division Multiple Access (IDMA), with moderate spreading signature length. Signatures are transmitter based, and a spreading signature is identified by a transmitters' IDentifier (ID). During all control message slots, multiuser detection is not required, since only one node transmits at a time. This allows also for channel estimation to all active transmitters in the network (**R3**). The protocol further manages to fulfill also the other requirements, and is thus chosen as reference scheme for multiuser detection based cross-layer designs. We summarize its functionality in the following.

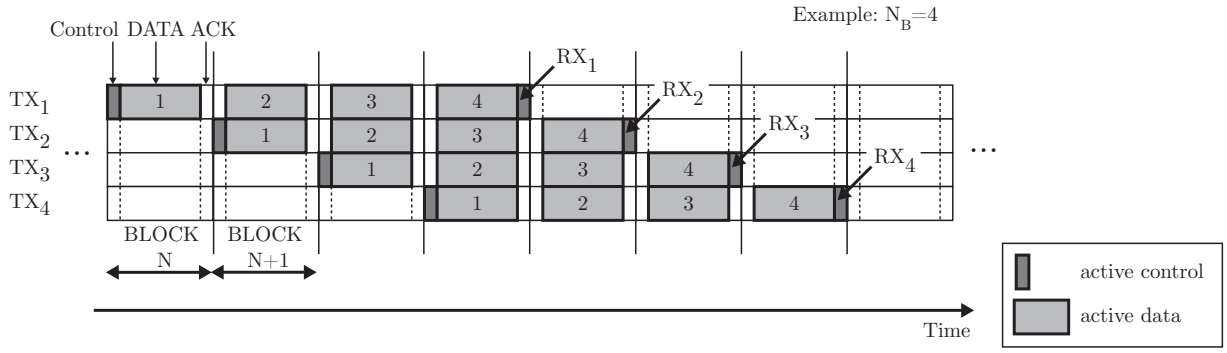

Figure 3.7.: Control message transmission and parallel data transmission over multiple consecutive blocks for the MUD-MAC protocol.

The MUD-MAC Protocol

Similar to PBOA, MUD-MAC requires a time-slotted frame structure. We refer to this frame structure as *block* in the following, since the data frame to be transmitted is not one-to-one contained in a *block*. Each data frame is subdivided into N_B fractions instead and transmitted in the data part of N_B consecutive blocks. This is explained by Fig. 3.7 for an example with $N_\mathrm{B} = 4$.
The motivation to subdivide a data frame into multiple blocks is to avoid multiuser detection as mandatory capability during the control message exchange (**R6**), but to support multiple parallel data transmissions during the data transmission phase, even in case the transmitter switches its associated partner every packet. This is likely to happen in ad hoc networks, since intermediate nodes pass the packets from multiple sources to multiple sinks.
Simplified, a block structure of the MUD-MAC protocol consists of a control message phase in the beginning (Control) where the channel access is regulated, a data phase (DATA), and a subsequent acknowledgement slot (ACK). We assume that transmitter TX_1 in Fig. 3.7 signals the start of its new transmission during the control message phase of block N. It starts transmitting the first of its N_B data blocks during the data slot of block N. During the control phase of the next block $(N + 1)$ another transmitter, TX_2, announces the begin of a new data transmission. In the following data phase both transmitters, TX_1 and TX_2, transmit data simultaneously. The number of senders simultaneously transmitting is increased from block to block, until TX_1 finished the transmission of all N_B blocks.
Only then acknowledges the associated receiver RX_1 the successful transmission of all N_B blocks. In the subsequent block, RX_2 acknowledges the successful reception of N_B blocks and so forth.
By this mechanism, referred to as *blockwise parallel transmission* in the remainder of the work, parallel transmissions of up to N_B data streams can be achieved. The size of the blocks is chosen so that the channel coherence time is larger than the time required for the transmission of all N_B blocks.
The amount of de facto simultaneously transmitted streams, however, depends on the

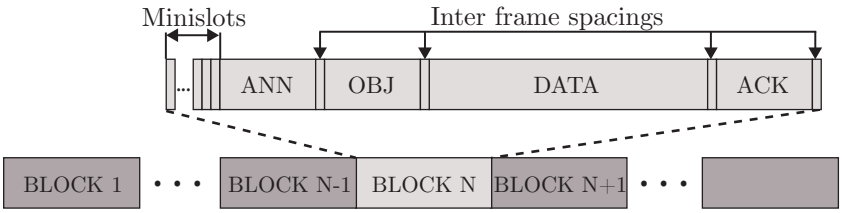

Figure 3.8.: One block of the MUD-MAC protocol.

outcome of the contention during the control phase. How this is performed is explained in the following.
The detailed block structure of MUD-MAC is depicted in Fig. 3.8. The control phase consists of two control messages, namely an Announcement (ANN) and an Objection (OBJ) message. Unlike PBOA, transmitters do not start their control messages simultaneously. Each transmitter randomly chooses one minislot instead and abstains from a planned transmission if it senses another transmitters' signal in an earlier slot. This contention resolution mostly avoids collisions during the ANN slot.
The successful transmitter announces its planned transmission and includes the ID of its associated partner and its own ID. The latter identifies the individual spreading signature of the potential transmitter.
By the ANN message, channel estimation can be performed at the associated receiver as well as at receivers that are already involved in ongoing transmissions. During the OBJ phase the intended receiver raises an OBJ if it is already involved in another ongoing data reception. Active receivers other than the intended receiver also have a *receiver objection capability*, i. e., the opportunity to object to the announced transmission. They object if they cannot handle the additional interference, e. g., if they have no more free MUD branches.
If no OBJ can be sensed, the transmitter starts transmitting the first of N_{B} blocks. If the transmission is successful, the receiver acknowledges the reception of multiple blocks at the end of the transmission once. Since transmissions start one after the other and last for N_{B} blocks, only one ACK per acknowledgement slot will be transmitted.
By the blockwise parallel transmission concept, multiple parallel data transmissions exploit the multiuser detection capabilities while during the control slots (ANN, OBJ, and ACK) no multiuser detection capabilities are required.

3.3. Comparison Between Power Control and Multiuser Detection Based Cross-Layer Design

After a detailed description of the reference schemes for power control based medium access control, namely PBOA, and multiuser detection based medium access control, MUD-MAC, we now present a simulative comparison between these protocols. Additionally, the performance obtained by the IEEE 802.11 protocol is shown. To achieve a comparison that is as meaningful

as possible, we adapt in Sec. 3.3.1 different simulation assumptions of the protocols to achieve equal simulation conditions. In Sec. 3.3.2 we define appropriate measures to evaluate the protocols not only regarding their throughput, but also regarding their QoS. Sec. 3.3.3 shows the corresponding simulation results.

3.3.1. Adaptation of Simulation Assumptions

The two reference schemes are both time-slot-synchronous protocols. Thus, in this respect they match very well. But other assumptions on the network, the MAC, and the physical layer have to be adapted to make the comparison meaningful and also to make both cross-layer designs comparable with the IEEE 802.11 protocol.

Network Layer

Each node in the network has a single transmission queue. During the contention phase of the PBOA protocol transmitters can switch to the next receiver awaiting the transmission of a packet in their queue (cf. Fig. 3.4, TX_3). MUD-MAC applies a pure First In First Out (FIFO) packet queueing. We apply FIFO as queueing strategy for all protocols.

MAC Layer

IEEE 802.11 and MUD-MAC assume a globally unique MAC address space for the nodes resulting in 6 Bytes per node ID; PBOA requires the IDs to be short, i. e., only locally unique, since a nodes' ID is contained in each of the RTS/CTS minislots. Thus, a global address space would result in a prohibitive overhead. It is also not commonly required to share a global unique address space in ad hoc networks since the number of active nodes is rather limited. Thus, a locally unique address space of 1 Byte, i. e., 256 addresses, is assumed for all schemes and the MAC overhead is adapted accordingly.
All control information included as overhead in the IEEE 802.11 MAC header [WLA97] for frame control and error correction purposes is also included for the two cross-layer designs. Information about the actual transmission duration is, however, neglected, since for time-slot-synchronous protocol designs the transmission duration is a constant.
The frame length is set to 8192 bits for all schemes. For the MUD-MAC cross-layer design this frame is split into $N_B = 4$ blocks, resulting in a data length of 2048 bits per block.

Physical Layer

The PHY header overhead as specified for IEEE 802.11 is included into both cross-layer designs as well. Only bits that are required for synchronization by the MAC-layer-asynchronous IEEE 802.11 protocol are not included as overhead for the time-slot-synchronous protocols. The corresponding bits per frame for IEEE 802.11 and PBOA, and per block for the MUD-MAC protocol are shown in Tab. 3.1. For PBOA, 15 minislots are included into the overhead.

Table 3.1.: Control and data bits.

	802.11 in bits	PBOA in bits	MUD-MAC in bits
Control message 1	RTS = 272	per minislot RTS = 96	ANN = 96
Control message 2	CTS = 272	per minislot CTS = 96	OBJ = 88
Control message 3	ACK = 272	-	ACK = 88
Data bits	8192	8192	2048
Control overhead per 8192 data bits	816	2880	1088

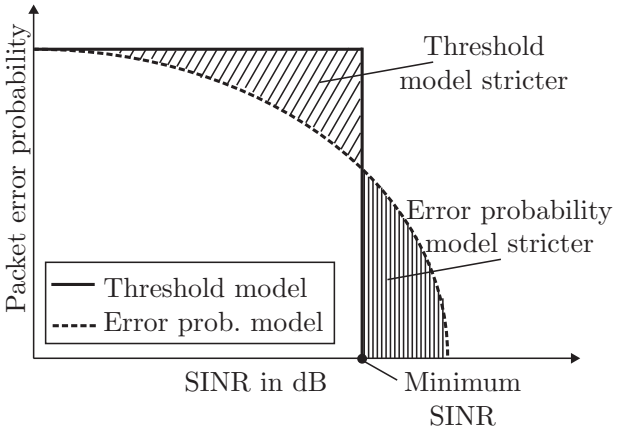

Figure 3.9.: Qualitative trend of packet error probability over SINR for the threshold model and the error probability model. The y-axis is logarithmic scale.

In order to model packet error probabilities the authors of the PBOA protocol use a *threshold model*. If the SINR of a packet is lower than a certain minimum SINR threshold, the packet is lost, if it is higher, the packet is received error free.
For the IEEE 802.11 and the MUD-MAC protocol, depending on the SINR, a Bit Error Rate (BER) is derived analytically according to the error probability of the additive white Gaussian noise channel [Pro89]. This BER results in a corresponding Packet Error Rate (PER). Packets are thus lost with a certain probability, depending on the actual SINR. We refer to this model as the *error probability model* in the following.
A qualitative PER trend is depicted in Fig. 3.9 for both models. Depending on the actual value for the minimum SINR threshold, the threshold model results in a stricter or less strict packet loss. A drawback of the threshold model is that it simplifies reality. Thus, all schemes apply the error probability model instead.
For the MUD-MAC protocol a moderate spreading signature length with a spreading gain of 11 is assumed, resulting in an 11-times increase of bandwidth compared to the single transmission band. In the IEEE 802.11 protocol, the same spreading gain of 11 is applied to control out-of-band interferers. PBOA does not require additional bandwidth except the single transmission band.
In order to balance the bandwidth requirements for all schemes, we assume that PBOA also performs some kind of spread spectrum communication scheme and include a spreading gain of 11 while estimating the interference levels at the receivers for PBOA. Receivers include this spreading gain as well while they estimate during the contention phase how much their associated partner can reduce the transmission power.

Energy Efficiency

Since PBOA avoids interference by reducing transmit power levels individually, besides an increased spatial reuse, also the energy efficiency can be improved. We do not consider improvements regarding energy efficiency throughout the work, since the MUD-MAC protocol is not designed to improve the energy efficiency.

3.3.2. Quality of Service Measures

Commonly used measures to describe the QoS of a system are, e. g., throughput, delay, and packet error probability, and sometimes also delay jitter and fairness. Since the error probability model of the physical layer (cf. Sec. 3.3.1) implicitly reflects the influence of the packet error probability on the overall performance, error probability is not evaluated separately. Furthermore, delay jitter is not taken into account.
In the following, we specify the measures that we consider in order to evaluate the throughput, delay, and fairness of the cross-layer designs and IEEE 802.11.

Throughput

An important measure for the system performance is the aggregate system throughput Th. To evaluate it, in a first step, the aggregate throughput of one simulation run r, Th_r, is

calculated as

$$Th_r = \frac{\sum_{k=1}^{K} N_{k,r} N_\mathrm{P}}{T_\mathrm{sim}}, \tag{3.1}$$

where K is the number of nodes in the network, $N_{k,r}$ is the number of successfully transmitted packets of node k in run r with a packet size of N_P bits, and T_sim is the simulation time per run.
The result of Th_r depends strongly on the placement of the nodes in the scenario. Thus, N_R runs are performed while every time the nodes are newly randomly placed. We approximate the expected value $\mathbb{E}\{\}$ of the aggregate throughput by the mean value $\overline{Th}$ of the N_R runs:

$$\overline{Th} \approx \mathbb{E}\{Th\} = \lim_{N_\mathrm{R}\to\infty} \frac{1}{N_\mathrm{R}} \sum_{r=1}^{N_\mathrm{R}} Th_r. \tag{3.2}$$

The 95 % confidence interval is analyzed to check if the number of runs N_R is sufficient to approximate $\mathbb{E}\{Th\}$.

Delay

To investigate the delay behavior of the protocols, we evaluate per node an average delay of the packets successfully transmitted by this node. The measure depends, on the one hand, on the value for the *maximum per packet delay*. If the delay of a packet exceeds this limit, the packet is removed from the packet queue and lost. On the other hand, it depends on the way how the samples of the *per node mean packet delays* are averaged over the nodes.
According to [Jan03], besides traffic that has no delay restrictions, there exist real-time streaming services with very strict delay per packet requirements (150 ms–250 ms) and non-real-time services that are interactive. The latter require at least per packet delays that are lower than 2.0 s. But for, e. g., web browsing, which is a service contained in this group, a maximum per packet delay of 0.5 s would be desirable [Jan03]. As a compromise we restrict the maximum packet delay Δ_max per packet to 1.0 s.
To achieve a per node mean packet delay for each transmitting node, we build the mean packet delay of a nodes' successfully transmitted packets in one simulation run. Assuming a packet i transmitted by a node k has a packet delay $\Delta_{\mathrm{p}_{k,i}}$ after received successfully by the partner. The index r to express the dependency of the run r is omitted for $\Delta_{\mathrm{p}_{k,i}}$ for simplicity. We measure the per node mean packet delay $\overline{\Delta}_{\mathrm{p}_{k,r}}$ of node k while transmitting in run r as the sum of the individual packet delays $\Delta_{\mathrm{p}_{k,i}}$, divided by the quantity of successfully transmitted packets $N_{k,r}$

$$\overline{\Delta}_{\mathrm{p}_{k,r}} = \frac{\sum_{i=1}^{N_{k,r}} \Delta_{\mathrm{p}_{k,i}}}{N_{k,r}}. \tag{3.3}$$

To increase the number of samples of the per node mean packet delays, this is performed for N_R runs, resulting for K nodes in $N_\mathrm{R}K$ samples of the per node mean packet delays.
To average these samples, we build the median $\mu_{\frac{1}{2}}(\overline{\Delta}_{\mathrm{p}_{k,r}})$ from these samples. Unlike a mean, the median is insensitive to outliers. It is defined such that at most half of the samples

have a lower value than $\mu_{\frac{1}{2}}(\overline{\Delta}_{\mathrm{p}_{k,r}})$, and at most half of the samples have a higher value than $\mu_{\frac{1}{2}}(\overline{\Delta}_{\mathrm{p}_{k,r}})$. For unfair medium access, samples of single nodes that are frequently granted medium access can decrease the overall mean delay significantly. But the median will not be strongly influenced by these samples.

Fairness

We are interested in the per node fairness of the investigated cross-layer designs. We address the *classical fairness* understanding, namely, all nodes should be treated equally. This per node fairness is investigated by the standard deviation of the per node throughput Th_{pN}. The standard deviation reflects how much on average each measurement deviates from the mean. It can be stated that the lower the standard deviation is, the fairer in the classical sense is the access to the medium. To calculate the standard deviation of the per node throughput, $s_{Th_{\mathrm{pN}}}$, the throughput of node k and run r, $Th_{k,r}$, is calculated as

$$Th_{k,r} = \frac{N_{k,r} N_{\mathrm{P}}}{T_{\mathrm{sim}}}. \tag{3.4}$$

The standard deviation of the throughput per node, $s_{Th_{\mathrm{pN}}}$, is computed for $N_{\mathrm{R}}K$ samples as

$$s_{Th_{\mathrm{pN}}} = \sqrt{\frac{1}{N_{\mathrm{R}}K - 1} \sum_{k=1}^{K} \sum_{r=1}^{N_{\mathrm{R}}} (Th_{k,r} - \overline{Th}_{\mathrm{pN}})^2}, \tag{3.5}$$

where $\overline{Th}_{\mathrm{pN}}$ is the arithmetic mean of all samples:

$$\overline{Th}_{\mathrm{pN}} = \frac{1}{N_{\mathrm{R}}K} \sum_{k=1}^{K} \sum_{r=1}^{N_{\mathrm{R}}} Th_{k,r}.$$

Another measure for classical fair medium access is the *Jain's fairness index* F_J [JCH84]. This index is defined for K nodes as

$$F_J(w) = \frac{\left(\sum_{k=1}^{K} g_k(w) \right)^2}{K \sum_{k=1}^{K} g_k^2(w)} \qquad \text{with } 0 < F_J(w) \leq 1, \tag{3.6}$$

where w is a sliding window with a size of multiple packets, and $g_k(w)$ reflects the fraction of the overall medium access a node k obtained within this window. If the window is stepwise increased, it reflects the change from *short-term* to *long-term* fairness.
For perfectly fair channel access, all $g_k(w)$ equal $\frac{1}{K}$ and the Jain's fairness index is equal to 1. A scheme is fairer if its Jain's fairness index is closer to 1 and vice versa.

Table 3.2.: Simulation parameters.

Control signaling bit rate	1 Mbit/s
Data bit rate	2 Mbit/s
Packet size	8192 bit
Transmission power	100 mW
Decoding sensitivity	−81 dBm
Carrier sensing sensitivity	−91 dBm
Carrier frequency	2.4 GHz
Bandwidth	11 MHz
Path loss exponent	3.0
Simulation time	12.0 s
Number of runs	40

3.3.3. Simulation Results

After we defined in Sec. 3.3.2 the parameters to be investigated, we now present the corresponding simulation results that compare the QoS offered by PBOA and MUD-MAC. We additionally compare the two cross-layer designs with the IEEE 802.11 protocol.

Common simulation parameters are listed in Tab. 3.2. The number of minislots is a design parameter, as was also discussed in [TG06]. For the PBOA-MAC protocol it is furthermore strongly related to the win probability p_{win}. Thus, regarding the number of minislots we stick to the proposal of 15 minislots in [TG06] and adapt the win probability p_{win} instead. We use a win probability $p_{\text{win}} = 0.7$, since this value resulted in the best performance in our simulations.

For the MUD-MAC protocol we choose the number of minislots so that it balances losses due to an increased overhead in a medium traffic load scenario with packet losses due to control message collisions in a high traffic load scenario, resulting in 10 minislots. The number of minislots is not adapted depending on the traffic load in the scenario for either of the schemes.

Poisson packet arrivals are assumed so that the inter-arrival times of the packets are negative exponentially distributed. The channel is modeled with a modified free space path loss model, and line-of-sight is assumed, cf. Sec. 2.2.3. Fading influences are not considered in the channel model.

Based on the error probability model described in Sec. 3.3.1, we model the probability that a packet is corrupted according to the error probability of the additive white Gaussian noise channel [Pro89]. As modulation alphabet we assume Binary Phase Shift Keying (BPSK) for the control packets, and Quadrature Phase Shift Keying (QPSK) for the data transmissions. For a more detailed description of the channel model please refer to [KVM+09].

For the MUD-MAC protocol we simulate a MUD receiver with a maximum of four decoder branches. Furthermore, also a low complexity receiver with two decoder branches is simulated. We set the overall number of nodes to be simulated to 50. The nodes are uniformly distributed

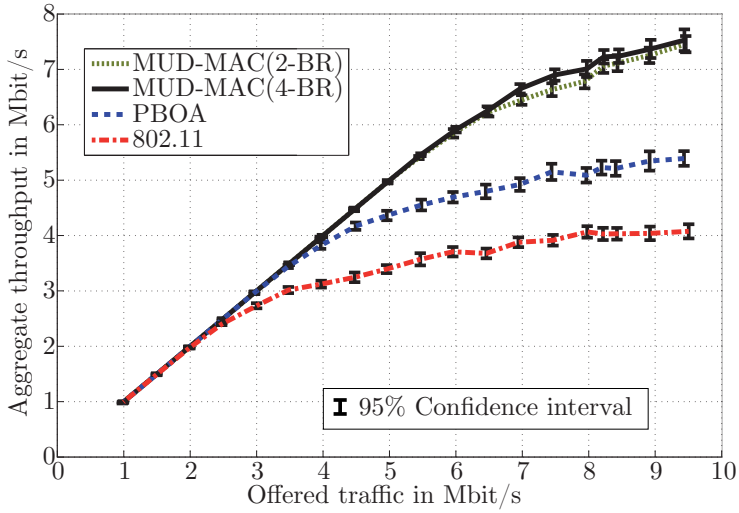

Figure 3.10.: Overall throughput versus offered traffic in a random node scenario with 50 nodes in a 500 m × 500 m area for the three schemes.

in the scenario. At the beginning of the simulation, each node selects randomly one other node out of the set of nodes within communication range as a sink, cf. Sec. 2.2.3. All nodes are active, i. e., they generate packets and potentially transmit during the simulation time. In the following, we refer to the expression *offered traffic* as the sum of packets generated at all nodes during simulation time.
To investigate the applicability of the schemes in different environments, we simulate two scenarios with strongly varying interference conditions:

1. Partly connected network: The investigated area is 500 m × 500 m. Not all nodes are in mutual communication range. Here, an appropriate MAC layer design is expected to achieve a noticeable spatial reuse.

2. Fully connected network: The network area is 50 m × 50 m. The interference is high, since each node is within the communication range of all other nodes. Here, the contention is expected to be too severe to result in an efficient spatial reuse from solely an appropriate MAC layer design. Cross-layer interaction between physical and MAC layer is required to overcome the severe interference.

3.3.4. Throughput Comparison

Fig. 3.10 shows the aggregate throughput plotted against the offered traffic for the partly connected network. Both cross-layer designs offer gains over the IEEE 802.11 protocol since they allow for spatial reuse; the RTS/CTS exchange of IEEE 802.11 blocks all transmissions except one within the mutual sensing range, cf. Sec. 2.3.1. The performance of MUD-MAC with two decoder branches is similar to the performance with four decoder branches, indicating

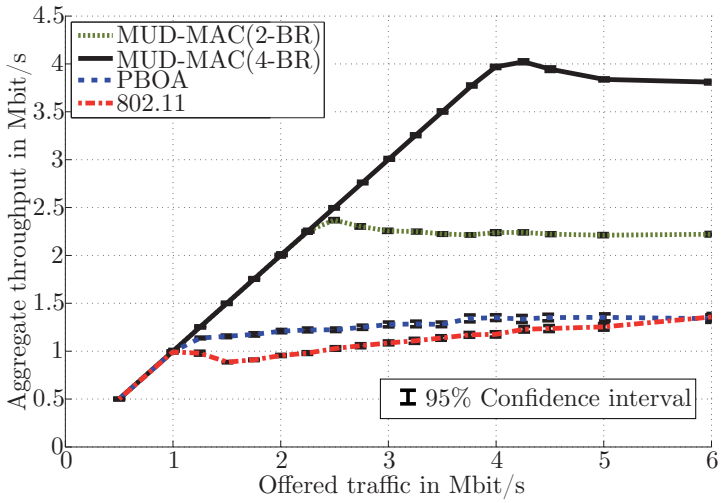

Figure 3.11.: Overall throughput versus offered traffic in a random node scenario with 50 nodes in a 50 m × 50 m area for the three schemes.

Table 3.3.: Throughput gains in percent compared with IEEE 802.11 at offered traffic of 9.50 Mbit/s (500 m) and 6.00 Mbit/s (50 m).

	Fig. 3.10 - 500 m in %	Fig. 3.11 - 50 m in %
PBOA	32.4	-2.2
MUD-MAC(2-BR)	83.3	63.2
MUD-MAC(4-BR)	84.7	180.1

that besides one branch to receive the wanted data, mostly one additional branch to cancel interference is sufficient.

The situation is different in the fully connected network (Fig. 3.11). Still MUD-MAC with four branches as well as two branches can outperform IEEE 802.11 remarkably. This time, the two additional branches at the detector can offer significant gains since the number of simultaneously interfering streams is high in the fully connected network. The power control based PBOA protocol can, in contrast to the trend of the curves in the partly connected network, never outperform IEEE 802.11 significantly.

An overview is given in Tab. 3.3 of the resulting additional throughput gains in percent for the cross-layer solutions compared with IEEE 802.11 at the maximum offered traffic of 9.50 Mbit/s in the 500 m × 500 m scenario and 6.00 Mbit/s in the 50 m × 50 m scenario.

We analyze the contention phase of PBOA, depicted in Fig. 3.12, for further explanation. In the lower row, either the RTS or the CTS message of the 1st, 4th, 7th, and 15th minislot pair of an exemplary contention phase in a 500 m × 500 m partly connected network are

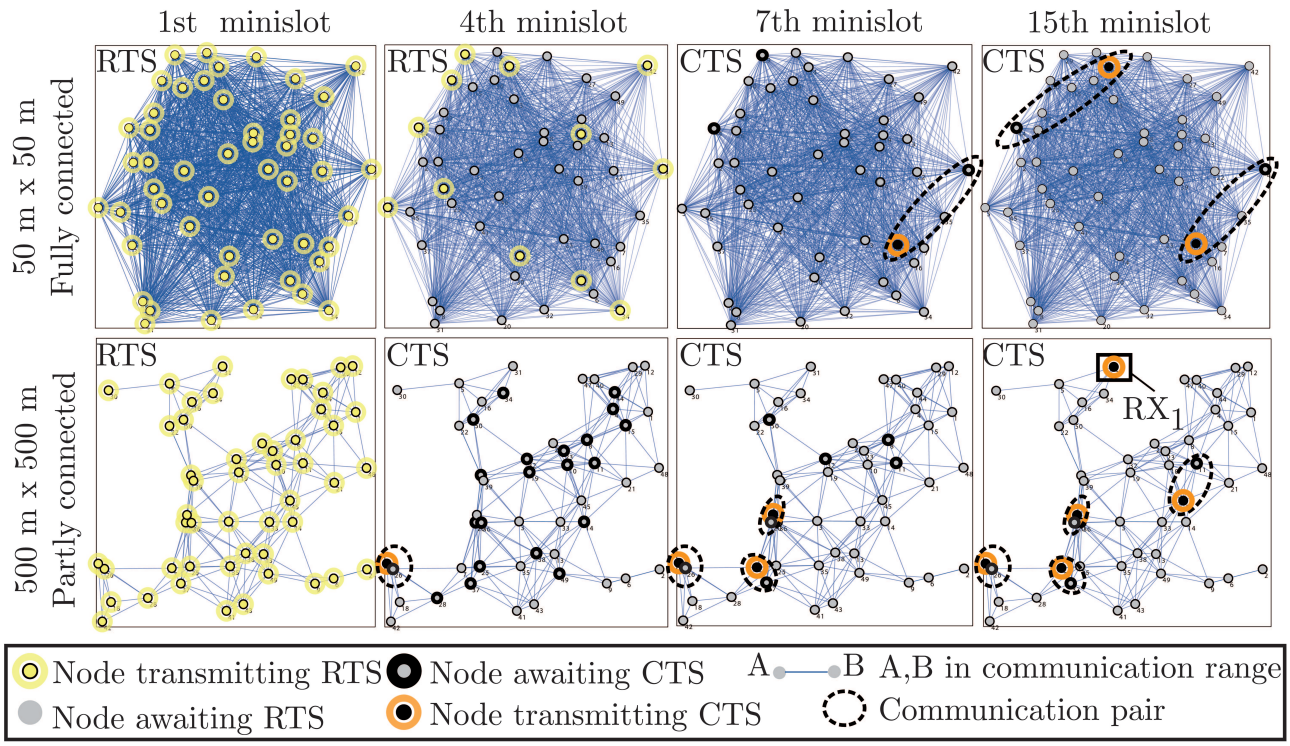

Figure 3.12.: Node states during the 1st, 4th, 7th, and 15th minislot of the contention phase of the PBOA protocol for the fully connected network (upper row) and the partly connected network (lower row).

depicted. During the RTS phase of the 1st minislot pair, all nodes transmit their RTS messages simultaneously. Blue connecting lines between the individual nodes indicate that these nodes are within mutual communication range ($\approx 108\,\mathrm{m}$). During the CTS slot of the 4th minislot pair one receiving node that is marked with an orange circle, was successful in decoding an RTS message and now replies with a CTS message. Still a noticeable number of nodes is awaiting CTS responses. The node replying has an advantage compared with other nodes in the scenario regarding the decoding of the RTS message since it is not in the middle of the scenario, where many nodes are within mutual communication range, but at a border. Also the majority of its neighbors already gave up transmitting RTS messages and its associated partner is very close.
Similar properties for receivers that were able to decode RTS messages can be observed during the CTS slot of the 7th minislot pair. There, the number of nodes replying with a CTS is increased to three. All successful receivers have in common that they are very close to their associated partners. Also no other active nodes can be found in their closer vicinity.
In the CTS slot of the 15th minislot pair the number of nodes replying with CTS messages is increased to five. Note that the number of simultaneous transmissions that will take place during the subsequent data phase is still four, since one node, named RX_1, marked with a rectangle, replies without an associated partner. This is the result of a previous CTS packet loss leading to the unsuccessful partner backing off.
In summary, most of the parallel transmissions for the power control based cross-layer design became solely possible since the concurrent transmissions in the communication vicinity backed off and the associated partners are close.
Besides a larger amount of parallel transmissions compared with PBOA, for MUD-MAC some transmissions take also place in close vicinity and partners do not have to be close, as depicted on the right hand side of Fig. 3.13. There an exemplary data transmission is depicted for MUD-MAC in the partly connected network. The contention resolution of the MUD-MAC protocol does not block all but one transmission within mutual communication range ($\approx 108\,\mathrm{m}$), which is mostly the case for the power control based cross-layer design. For the MUD-MAC protocol the physical and MAC layer interact instead and thus provide a higher spatial reuse, as was also shown in [KHKW10a].
These observations are approved if the contention phase of the $50\,\mathrm{m} \times 50\,\mathrm{m}$ fully connected network is further investigated. The upper row of Fig. 3.12 shows either an RTS or a CTS slot of the 1st, 4th, 7th, and 15th minislot pair of an exemplary contention phase in the fully connected network for the PBOA protocol. Similar to the $500\,\mathrm{m} \times 500\,\mathrm{m}$ scenario, during the RTS slot of the 1st minislot pair all potential senders transmit their RTS messages simultaneously. This time, the blue lines representing node pairs within communication range are very dense compared with the $500\,\mathrm{m} \times 500\,\mathrm{m}$ scenario, thus reflecting the strongly increased interference situation.
During the 4th minislot pair, in contrast to the $500\,\mathrm{m} \times 500\,\mathrm{m}$ scenario, not the CTS phase but the RTS phase is depicted since still not even a single CTS is started and hence in the event-driven simulation environment no visualization output is produced. By comparing the associated RTS phase with the situation in the 1st minislot, it can be observed that many nodes previously willing to transmit already backed off since they were not successful.

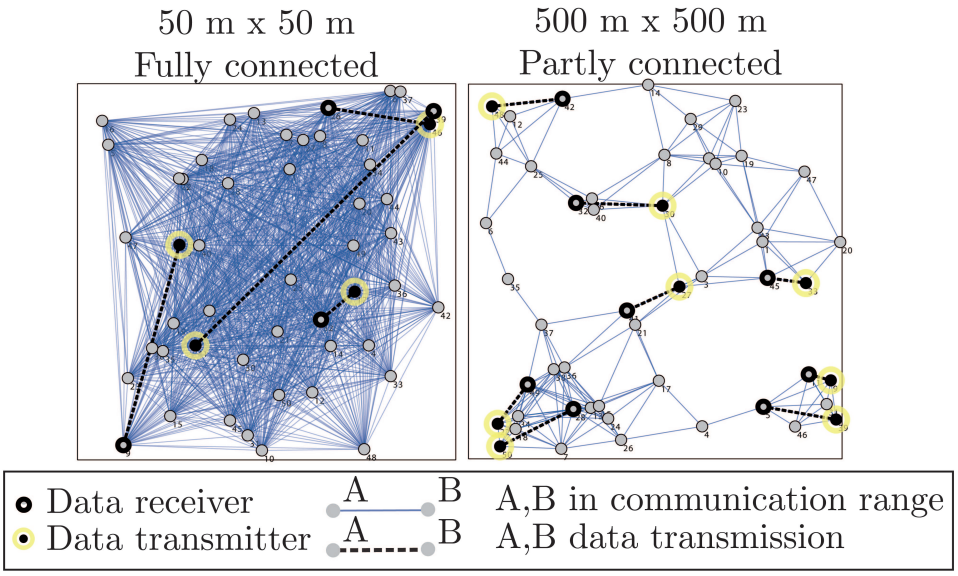

Figure 3.13.: Parallel data transmissions in the MUD-MAC protocol for the fully connected network (left) and the partly connected network (right).

During the CTS phase of the 7th minislot pair one node has managed to decode an RTS message and replies with a CTS to its partner. During the CTS slot of the 15th minislot pair two communication pairs remain. Note that they are so far apart that the mutual interference level is much lower than the receive signal level. Obviously, power control as physical layer technique cannot handle such a severe interference situation satisfactorily.

The multiuser detection based MUD-MAC protocol can in contrast to the PBOA protocol not only handle the interference situation, but it can even increase the spatial reuse in the high node density scenario by fully exploiting all four decoder branches. This is shown by comparing the left and the right hand side of Fig. 3.13. In the right part for the 500 m $\times$ 500 m scenario never more than two parallel transmissions are within communication range ($\approx$ 108 m) due to the medium node density, while in the 50 m $\times$ 50 m scenario (left part of Fig. 3.13) all four branches are exploited, leading to four parallel transmissions.

From these results it can be observed that power control based cross-layer designs can only be applied in medium density interference situations, whereas multiuser detection in interaction with an appropriate MAC layer is also applicable if the interference situation is severe. The achievable gain depends then on the number of decoder branches. Since the power control based PBOA protocol cannot be applied in so severe interference situations as the fully connected 50 m $\times$ 50 m scenario, we restrict all further simulations to the 500 m $\times$ 500 m partly connected network.

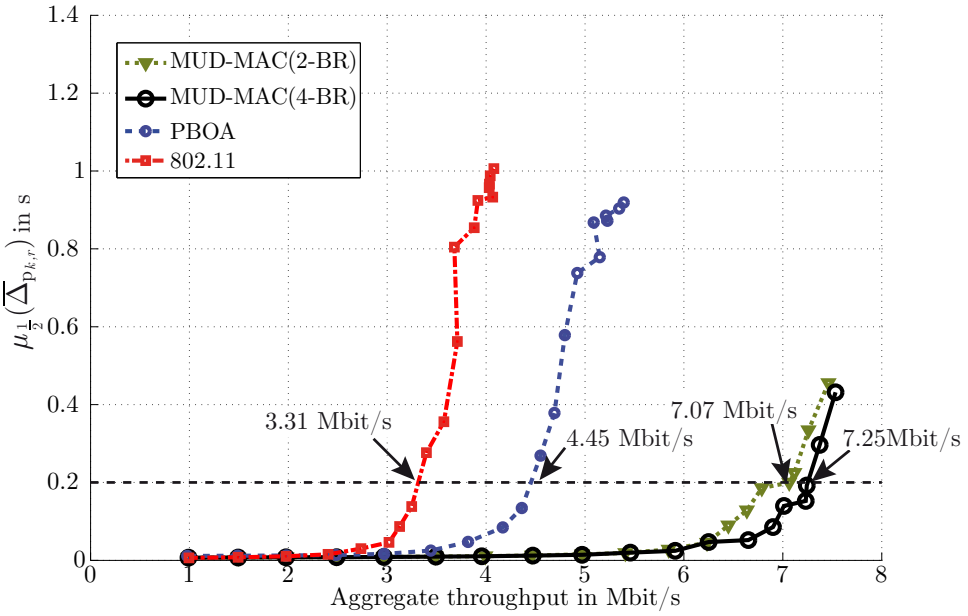

Figure 3.14.: Median of mean packet delay per node versus aggregate throughput for the IEEE 802.11, the MUD-MAC protocol, and the PBOA protocol with 50 nodes in a 500 m × 500 m random network.

3.3.5. Delay and Fairness in the Random Topology

MUD-MAC gains significantly in terms of aggregate throughput compared with PBOA. But investigating the service provided by a cross-layer design solely with respect to the aggregate throughput can still lead to unsatisfactory solutions; namely, a solution that only serves the best users will offer good results in matters of aggregate throughput. Most of the users will suffer unacceptable delays and are excluded from channel access though.

In Fig. 3.14, the median of the mean packet delays per node, $\mu_{\frac{1}{2}}(\overline{\Delta}_{\mathrm{p}_{k,r}})$, is plotted against the aggregate throughput obtained by the protocols. From the principal trend of the curves it can be observed that the achievements of MUD-MAC in aggregate throughput do not come at the cost of a strongly increased mean per packet delay for some of the nodes. MUD-MAC can rather gain with both, two and four branches, compared with the PBOA cross-layer design.

Further looking at real-time streaming services with very high delay requirements of 200 ms (150 ms–250 ms [Jan03]) marked with a dashed line in Fig. 3.14, the multiuser detection based cross-layer design offers 7.25 Mbit/s aggregate throughput with four branches, and 7.07 Mbit/s with two branches. The corresponding result for the power control based cross-layer solution with 4.45 Mbit/s is significantly lower.

To gain insight into the fairness of the cross-layer designs, the mean throughput per node and the corresponding standard deviation curves as defined in Eqn. 3.5 are plotted against

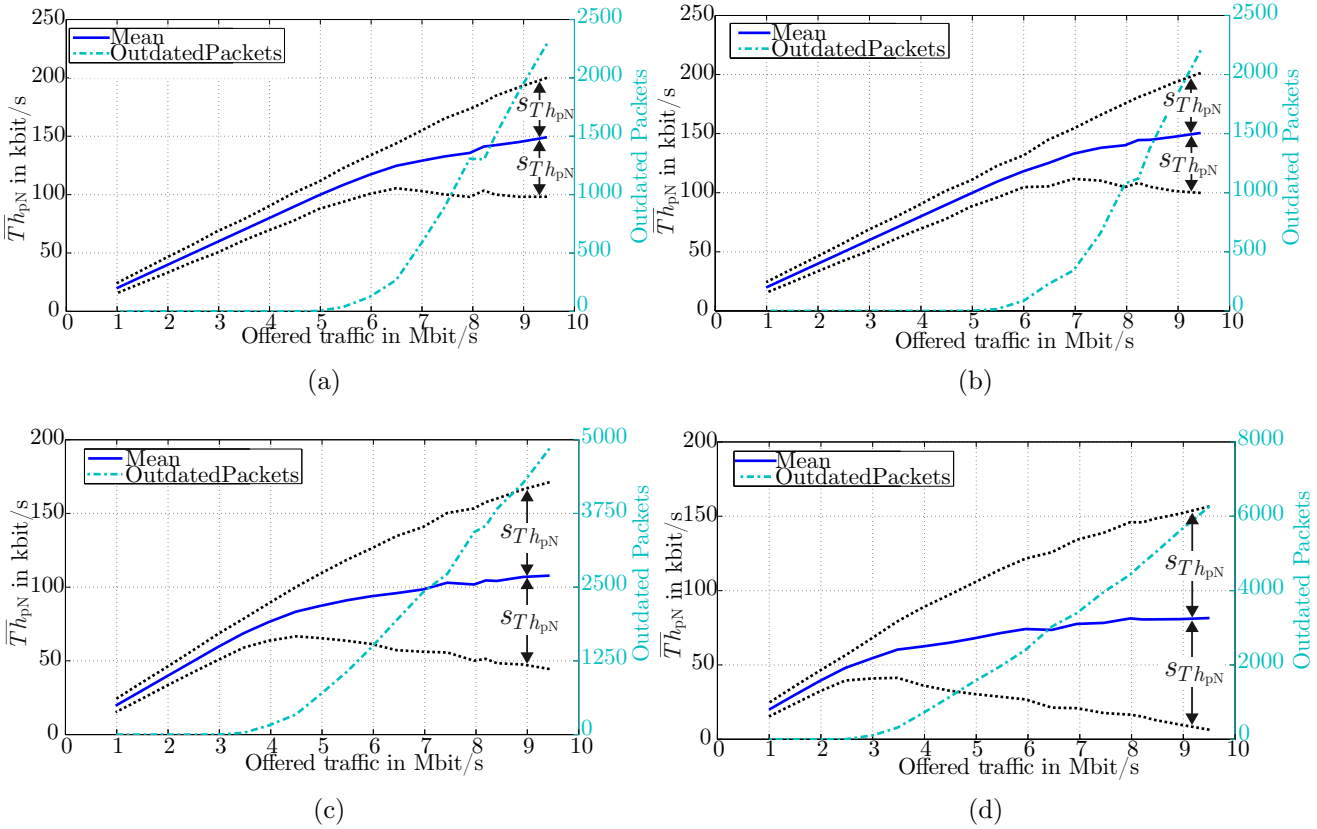

Figure 3.15.: Left axis: Mean of throughput per node $\overline{Th}_{pN}$ and corresponding standard deviation curves against offered traffic. Right axis: Number of outdated packets. (a) MUD-MAC with two branches; (b) MUD-MAC with four branches; (c) PBOA; and, (d) IEEE 802.11.

the offered traffic in Fig. 3.15, left axis. Additionally, the right axis shows the related trend of the outdated packets curve, i. e., how many packets have been dropped because they have exceeded $\Delta_{\max}$.

The standard deviation of the throughput per node starts increasing moderately at that time where the first nodes start dropping packets from their queues due to the restriction to an overall delay $\Delta_{\max}$ of 1.0 s. If the offered traffic approaches the *highest supported throughput* of a certain protocol, i. e., the aggregate throughput that corresponds to the maximal spatial reuse this protocol supports (cf. Fig. 3.10), the standard deviation increases strongly. This points out that operating a protocol close to or over its *highest supported throughput* leads to an increased unfairness in the system. Still, the standard deviation of the throughput per node is the lowest for the MUD-MAC protocol, further encouraging the conclusion that the improved aggregate throughput of this cross-layer design is not traded against fairness.

In Fig. 3.16 the corresponding trend of the Jain's fairness index (cf. Eqn. 3.6) is plotted for two offered traffic loads. For an offered traffic of 3.00 Mbit/s all schemes obtain similarly good fairness values, but for very high traffic loads (10.00 Mbit/s), the IEEE 802.11 protocol

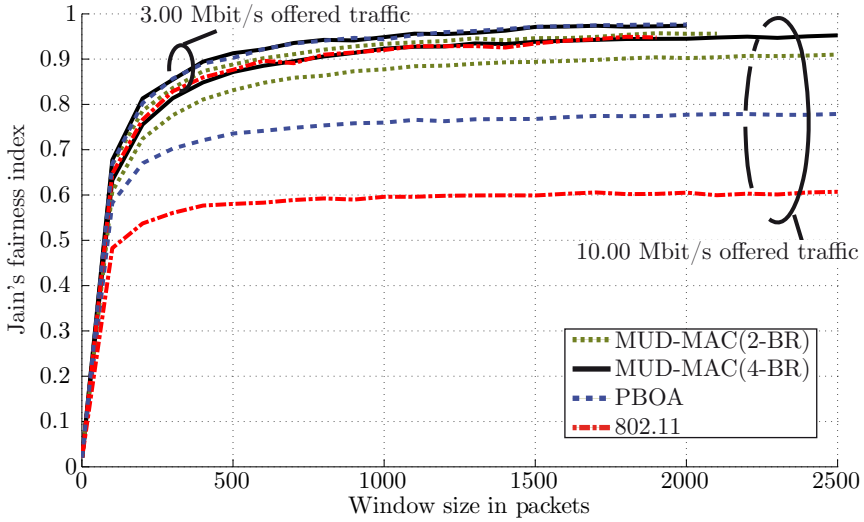

Figure 3.16.: Jain's fairness index for an offered traffic of 3.00 Mbit/s and 10.00 Mbit/s for the IEEE 802.11, the MUD-MAC and the PBOA protocol with 50 nodes in a 500 m × 500 m random network.

cannot even treat 60 % of the nodes fairly. PBOA is considerably fairer and handles 77 % of the nodes equally. But MUD-MAC with both, two and four branches, shows the best fairness trends and can achieve a fair behavior for more than 89 % (two branches) and 94 % (four branches) of the nodes.

3.4. Summary and Further Work

The goal of this chapter was a simulative comparison between two classes of cross-layer designs that are both applied in the specific environment of ad hoc networks and aim at an increased spatial reuse compared with IEEE 802.11. The first class contains all cross-layer designs that use power control as a physical layer strategy to suppress multiple access interference on the transmitter side. The second class of cross-layer schemes assumes multiuser detection on the physical layer. All algorithms within this class increase the spatial reuse by canceling interfering streams on the receiver side.
Our major contributions can be summarized as follows:

- **Review of power control based cross-layer designs:** We gave a detailed summary of methods based on power control as physical layer strategy. We showed the shortcomings and advantages of the algorithms proposed in literature in Sec. 3.1.

- **Review of MUD based cross-layer designs:** We summarized protocols proposed in literature that are based on MUD as physical layer technique in Sec. 3.2 and pointed out their benefits and drawbacks.

- **Choice of reference schemes:** For the simulative comparison we decided on the reference schemes by choosing in each case the most promising candidate out of the two classes. We considered for the choice the benefits and drawbacks identified during the reviews.
- **Definition of QoS parameters:** In order to investigate the QoS offered by the proposed cross-layer designs, we defined appropriate measures to evaluate the performance in aggregate system throughput, delay, and fairness in Sec. 3.3.2.
- **Detailed simulative comparison:** We presented detailed simulation results that compared the two reference schemes not only in terms of aggregate throughput, but also with respect to other QoS parameters that were defined in Sec. 3.3.2.

By these contributions, it was possible to state the following conclusions:

- **Conclusions regarding severe interference situations:** Power control based cross-layer design has strong limitations in networks with severe contention. While spatial reuse in so dense scenarios is generally limited by means of power control, the multiuser detection based cross-layer design can handle interference in the physical layer, achieving a good spatial reuse even in severe interference situations.
- **Conclusions regarding QoS:** The gains in throughput achieved by the multiuser detection based cross-layer design do not originate from an unfair behavior that supports only favorable nodes at the cost of others. This is ensured by an increased fairness as well as a better delay performance compared with the power control based cross-layer design.
- **Conclusions regarding complexity:** All above mentioned results also held for low complexity multiuser detectors with only two branches. It follows that even with reduced computational complexity, multiuser detection based cross-layer designs achieve the elaborated gains compared with power control based cross-layer designs.

The last point requires a more detailed investigation in further work. Up to this point, the schemes were solely compared by means of simulations, without taking the computational complexity of the underlying physical layer strategy into account.
Another possible point for future investigation is with respect to energy savings. Since the reference scheme for multiuser detection based cross-layer design does not support energy savings, it has to be adapted accordingly to allow for a meaningful comparison in this area. This could probably offer new insights into advantages of power control based cross-layer designs, since these methods inherently achieve gains in energy savings.

4. Overload Adaptive Contention Resolution

The Distributed Coordination Function (DCF) is a medium access control technique of IEEE 802.11 and it employs CSMA-CA with a binary exponential backoff algorithm. The DCF is designed to avoid simultaneous transmissions assuming a simple collision model in the physical layer.

It was soon recognized that the behavior of the DCF could be unfair in distributed environments (e. g., [XS01]) and several research efforts have been made to improve the fairness [DVB01, BDSZ94]. Unfortunately, those fairness schemes are designed based on the assumption of the physical layer as a simple collision model. Thus, they may not work well for medium access control protocols that apply more advanced signal processing techniques.

Given the recent advances in multiuser communications in the physical layer, a simple collision model is not suitable anymore. Heterogeneously equipped transmitters with, for instance, different number of antennas have different prerequisites to start a transmission in an interference dominated neighborhood successfully, e. g., in case of beamforming. On the receiver side, a certain amount of interference can be coped with by applying signal processing techniques in the physical layer, such as MIMO signal processing or, as for the MUD-MAC protocol, multiuser detection [TNV04, ZZA+06]. For heterogeneously equipped receivers, the tolerable interference level, however, depends on their individual equipment.

Heterogeneously equipped transmitters can be addressed by applying priority based conventional contention resolution algorithms like, e. g., [DVB01], and give different priorities depending on the transmitters' different equipment. But bringing heterogeneously equipped receivers with variable interference capabilities actively into the contention remains unconsidered then.

The authors of [SSIC04] present a specific MIMO based MAC protocol including a persistence based contention resolution algorithm that applies some ideas of [NKGB00] to the MIMO technique. Although they take *bottleneck nodes* into account and allow the receivers by the exchange of *winner lists* to somehow influence contention decisions, the actual contention resolution takes place only at the transmitters, not allowing receivers to influence this contention actively.

In general, this is quite important, since the amount of acceptable interference might differ for each receiver within the network, as for the MUD-MAC protocol if receivers have a varying number of multiuser detection branches. Thus, a receiver needs to be able to protect its ongoing reception against non tolerable interference and thus has to be capable of contending against a planned transmission.

On the other hand, if a weak receiver blocks all spatial reuse permanently in order to protect its own reception, this causes also a kind of unfairness in the system, since the better equipped nodes are then restrained from taking advantage of their excellent equipment. This gets severe if the system is in an *overload* situation, i. e., significantly more traffic is

generated than transmitted and thus a noticeable percentage of packets is dropped. In this case, better equipped nodes loose packets because they are blocked, although these losses could be diminished in case the weak receivers would abstain from objecting every time.
Investigating scenarios where nodes are heterogeneously equipped requires also a completely new point of view on the fairness definition. In traditional approaches, like, e. g., the Jain's fairness index as defined in Eqn. 3.6, a completely fair system is a system where each node accesses the channel exactly as often as all other nodes. We refer to this understanding of fairness as *classical fairness* in the following. As already stated, this automatically disadvantages better equipped nodes in scenarios where nodes are heterogeneously equipped. Fair contention resolution in such scenarios becomes a trade-off between, on the one hand, avoiding a permanent overwhelming of low level devices with interference, and, on the other hand, blocking of all spatial reuse by these low level devices. Restricting the latter one is especially important if the system runs on overload.
In this chapter, we address this problem and present a new algorithm for **time-slot-synchronous** protocol designs (cf. Sec. 2.3.2) that allows both parties, transmitters as well as receivers, to compete. The former contend for channel access while the latter compete in order to protect their actively ongoing receptions.
The Overload Adaptive Contention Resolution (OACR) algorithm balances spatial reuse and fairness in the system and improves the aggregate throughput in case an overload situation occurs. It is fully distributed and requires the exchange of only a single parameter between competing nodes. We introduce the OACR algorithm in Sec. 4.1. A measure how to investigate fairness in scenarios with heterogeneously equipped nodes is presented in Sec. 4.2. The practical application of the OACR algorithm to the MUD-MAC protocol is explained in Sec. 4.3. We show related simulation results in Sec. 4.4. Finally, Sec. 4.5 summarizes this chapter.
Parts of the results presented in this chapter have earlier been published in [KCH+10].

4.1. The OACR Algorithm for Heterogeneously Equipped Nodes

The proposed OACR algorithm aims at adjusting the channel access of all transmissions within communication range. We assume that a transmission consists of multiple consecutive packets exchanged between a transmitter and its intended receiver. The assignment of transmitter and receiver pairs is fixed during the investigated period of time.

4.1.1. Contention Window and Contention Cycle

Within this period, the *contention window* (CW), a transmitter TX_i obtains access to the medium n_{TX_i} times. Under the assumption of a completely fair channel access in the classical sense this value is the same for all nodes in the set of transmitters $\mathcal{T}$

$$n_{\mathrm{TX}_i} = N_{\mathrm{fair}} \quad \forall\, \mathrm{TX}_i \in \mathcal{T}.$$

The duration of the CW is a design parameter. For a relatively small CW, short-term fairness is measured whereas large values reflect long-term fair behavior. The minimum

duration of the CW is the *contention cycle* (CC). A contention cycle is the time required to transmit one packet of each transmission respectively, taking into account the different capabilities of the nodes and thus the limitations with respect to the achievable spatial reuse. We will explain its computation in Sec. 4.3.2 for an exemplary application of the OACR algorithm to the MUD-MAC protocol. The computation of the CC can either be performed locally at each node with local information overheard from neighboring nodes, since for a proper performance of the OACR algorithm, it is not mandatory for all nodes to work with the exact same CC value. Or the information required to estimate the achievable spatial reuse, like the individual number of MUD branches or the number of antennas at a node, can be globally distributed by additional information in routing packets. The latter is possible, since this information is not time critical. Global knowledge of the nodes' individual equipment is assumed for all simulations in Sec. 4.4.

We set the duration of a CW to the maximum tolerable packet delay $\Delta_{\max}$ of the system. The number of fair accesses N_{fair} for a transmitter can thus be calculated as follows

$$N_{\text{fair}} = \text{nint}\left(\frac{CW}{CC}\right) = \text{nint}\left(\frac{\Delta_{\max}}{CC}\right), \tag{4.1}$$

where $\text{nint}\,(a)$ is the nearest integer to a. For time-slot-synchronous protocols, the time is segmented into consecutive frames. We refer to the number of frames contained in a CW as N_{CW} in the following. The index of the frames is increased within a certain contention window from 1 to N_{CW}, and reset to 1 with the beginning of the next contention window.

4.1.2. Contention Level

In the OACR algorithm, the only information exchanged among different competitors is a *contention level*. During the contention phase of the i-th frame, each node k has a contention level $L_{k,i}$ that it compares with the level $L_{v,i}$ of a competitor node v. Node k is successful if its contention level is lower than the level of the competing node ($L_{k,i} < L_{v,i}$). In case that both competitors have the same contention level ($L_{k,i} = L_{v,i}$), the already receiving node wins, thus protecting existing transmissions. The overhead per control message is increased marginally, i. e., by 8 bit if 256 different level stages are assumed. Note that a node will start to compete either, if it is willing to transmit data or, if it wants to protect its ongoing reception.

After each contention, the contention level of both competitors is adaptively adjusted. This adaptation process is a function of these nodes' *contention history* and their *per packet accumulated delay*. The contention history accounts for a nodes' successes and defeats in the past. The per packet accumulated delay reflects how often a node was **consecutively** blocked. A node becomes more aggressive in the next contention if it was blocked consecutively for many contentions and/or its per packet accumulated delay is larger than the CC size. This behavior is attained by two parameters, namely the *utility index* UI and the *delay index* DI, which are described in the following.

4.1.3. Utility Index and Delay Index

The utility index represents successes in the contention history of a node, the delay index reflects losses during preceding contentions. The initial, the maximum, and the minimum values of the utility index (UI_{init}, UI_{max}, UI_{min}) and the delay index (DI_{init}, DI_{max} DI_{min}) are the same for all nodes. How they are derived is explained while explaining the functionality of the utility index and the delay index.

Utility Index: For time-slot-synchronous protocol designs, the time is split into consecutive frames. The UI depends on the number of successfully initiated transmission attempts and on the successfully protected received transmissions during previous frames. If node k is successful during the i-th frame, its utility index during frame i, $UI_{k,i}$, is decreased by one

$$UI_{k,i+1} = UI_{k,i} - 1,$$

where $UI_{k,i+1}$ is the utility index of node k at the beginning of frame $i+1$.

If $UI_{k,i}$ after subtraction reaches the minimum of the utility index UI_{min} that is set to zero ($UI_{\text{min}} = 0$), it would hold that $UI_{k,i+1} = 0$ at the beginning of the $i+1$-th frame. In this case, the contention level $L_{k,i+1}$ of node k is increased by one for the next frame at the end of the i-th frame

$$L_{k,i+1} = \begin{cases} L_{k,i} + 1 & \text{if } UI_{k,i+1} = 0, \\ L_{k,i} & \text{otherwise.} \end{cases} \tag{4.2}$$

With an increased contention level $L_{k,i+1}$, node k is more likely to loose in the next contentions, thus balancing its successes in preceding transmission attempts. The utility index is reset to its initial value. The initial value of the utility index (UI_{init}) equals its maximum value (UI_{max}). This maximum value is equal to $UI_{\text{max}} = N_{\text{fair}} + 1$, with N_{fair} the number of fair channel accesses within one CW, as derived by Eqn. 4.1. After each CW, $UI_{k,N_{\text{CW}}+1} = UI_{k,1}$ of node k is reset to its initial value UI_{max}. Thus, if node k obtains access to the channel within a CW exactly N_{fair} times and $UI_{k,N_{\text{CW}}}$ was therefore decreased by the magnitude of N_{fair}, $UI_{k,N_{\text{CW}}}$ is still greater than its minimum UI_{min} of zero and thus will not influence the contention in the next CW.

If node k obtained access to the medium more than N_{fair} times during the CW or it blocked other nodes repeatedly and thus possibly caused losses in spectral efficiency, the utility index will reach its lower bound and thus the related contention level will be increased, cf. Eqn. 4.2. Note that by penalizing a node for every successful outcome of a contention, a node that blocks multiple other nodes in order to protect its own transmission is also penalized multiple times, once for every node it blocks. Thus, losses in spatial reuse are taken into account here. Depending on the value for UI_{max}, weakly equipped nodes are more or less influenced by the OACR algorithm. Thus, in order to achieve different trade-offs between fairness and aggregate throughput, the maximum value of the utility index is varied by an additional factor δ

$$UI_{\text{max}} = \delta \cdot N_{\text{fair}} + 1, \tag{4.3}$$

where δ is a weighting constant.

In principle, by varying δ, different trade-offs between fairness and aggregate throughput can be achieved, i. e., the behavior of the algorithm can be scaled by adapting δ. We present related simulation results in Sec. 4.4.

Delay Index: The delay index DI records how many times one node's channel access is **consecutively** blocked. If node k is blocked during the i-th frame, its delay index is increased by 1

$$DI_{k,i+1} = DI_{k,i} + 1.$$

If node k is successful once during the i-th frame, $DI_{k,i+1}$ is reset to its initial value $DI_{\text{init}} = DI_{\text{min}} = 0$ again. DI_{max} depends on the CC and the underlying backoff strategy of the system. If $DI_{k,i}$ reaches DI_{max} at the end of the i-th frame, and it would therefore hold $DI_{k,i+1} = DI_{\text{max}}$ at the beginning of the $i+1$-th frame, it is reset to its initial value and the contention level $L_{k,i+1}$ is reduced by one

$$L_{k,i+1} = \begin{cases} L_{k,i} - 1 & \text{if } DI_{k,i+1} = DI_{\text{max}}, \\ L_{k,i} & \text{otherwise.} \end{cases} \tag{4.4}$$

For the Binary Exponential Backoff (BEB) backoff strategy applied in 802.11, which is also applied in MUD-MAC, the backoff duration is adjusted dynamically in order to react to possible congestion in the system. A backoff timer value is drawn randomly from a uniform integer distribution between [0, BWB], where BWB is the upper backoff window bound. Multiplying this backoff timer with a fixed time t_{slot} results in the backoff duration. The initial value for the backoff window bound BWB, namely BWB_{init}, is 32. In case the backoff timer expires, the station attempts to transmit. If the attempt is not successful, the BWB is doubled until a maximum is reached. Otherwise it is reset to its initial value.

To decide DI_{max}, we calculate the delay after consecutive lost contentions under the worst case assumption that the backoff timer always equals the BWB. If the sum of the backoff intervals is larger than the CC duration, the node was penalized during one CC. Thus, it should obtain access to the medium with a higher probability in the next round. DI_{max} can thus be bounded by

$$\sum_{s=1}^{DI_{\text{max}}} BWB_{\text{init}} 2^{(s-1)} t_{\text{slot}} \leq CC. \tag{4.5}$$

For backoff strategies other than BEB, DI_{max} has to be calculated accordingly.

A general overview of the relations between CC, CW, and related settings of the set of parameters can be found in Fig. 4.1.

Note that by setting the contention level not directly after each contention, but by a set of parameters, the influence of the outcome of a single contention is smoothed. Also, the time interval that the algorithm takes into account to influence the contention decision is larger than by setting the contention level directly. Thus, the algorithm does not aim at improving short-term fairness.

The behavior of the utility index and the delay index are chosen so that as long as the contention is moderate, the outcome of the contention is not much influenced by the algorithm. For example, the delay index requires that a node is **consecutively** blocked, i. e., if the

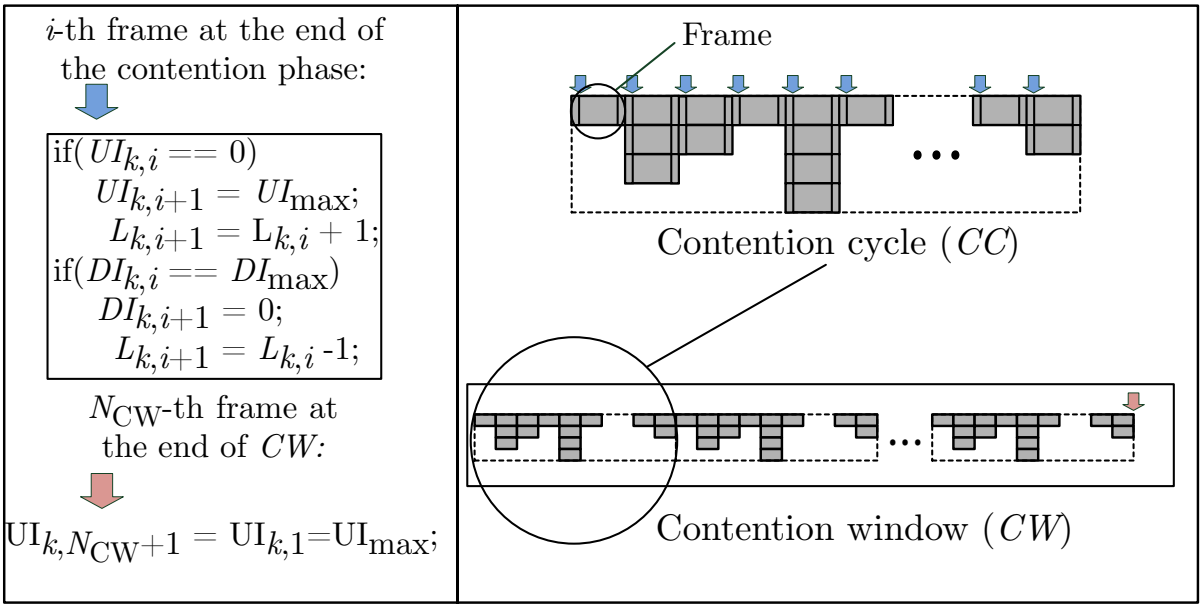

Figure 4.1.: Frame, contention cycle CC, contention window CW, and related settings for the set of parameters for the OACR algorithm.

contention is not severe, even if a node is blocked a couple of times, the delay index is reset to its initial value immediately if the node is successful once, thereby cleaning the influence of the preceding losses. Only in overload situations with very severe contention where the node is blocked permanently, the delay index reaches the maximum for a noticeable number of nodes and thus influences future contentions.
Also, the maximum of the utility index $UI_{\max}$ is set in that way that as long as the nodes do not require more frames within a contention window than can be on average offered per node by the system, the utility index is reset at the end of a contention window, thus not influencing further contentions. Only, if overload situations exist and nodes demand more frames than the system on average can offer, the utility index is diminished to zero for many nodes, thus actively influencing further contentions.

4.2. Fairness Measurement for Heterogeneously Equipped Nodes

As already stated, standard measures like the Jain's fairness index fail to reflect fairness as a trade-off between protecting weak users and still allowing excellently equipped users to exploit their equipment, since they aim at completely equal channel access. Thus, understanding fairness in the sense of a trade-off has to be investigated with other than such classical fairness measures.
To see the influence of the proposed OACR algorithm, we investigate the Cumulative Distribution Function (cdf) of the throughput per node. Qualitative trends of cdf curves

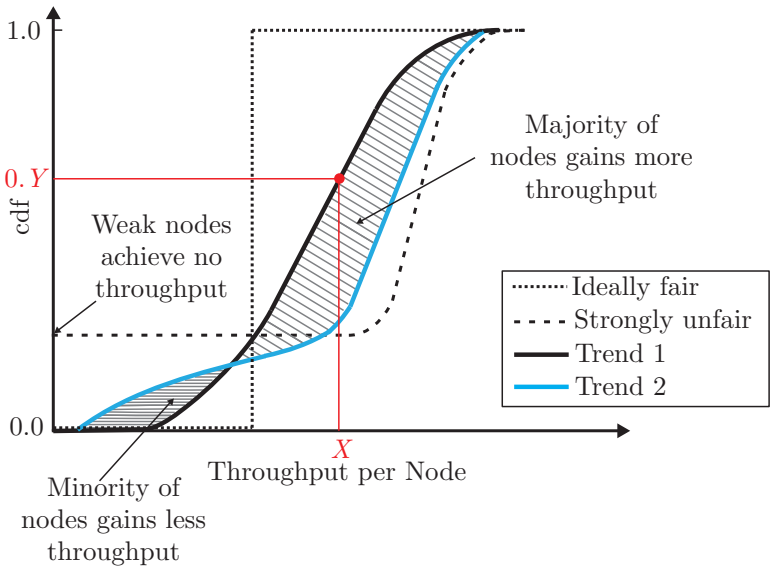

Figure 4.2.: Qualitative trends of cdf curves that reflect a different system behavior.

that reflect different system behaviors for a scenario with heterogeneously equipped nodes are shown in Fig. 4.2. The cdf of the throughput per node shows which amount of the nodes obtains up to a certain throughput value. Looking at the exemplary point marked with a red dot, $0.Y \cdot 100$ percent of the nodes achieve a throughput lower or equal to X. If the system is ideally fair in the classical sense, and influences of packet errors are neglected, each node obtains exactly the same throughput. Then, the trend of the cdf follows the trend of the dotted line, i. e., at a certain value for the throughput per node, the cdf jumps from zero to one.

If weak nodes are excluded completely from channel access, represented by the dashed line, the cdf already starts with an offset on the ordinate. These nodes achieve zero throughput, but the throughput of the other nodes can be improved. From the behavior of these two curves it can be concluded that the steeper the trend of a curve, the fairer a system is in the classical fair sense.

Curves of practical systems, represented by trend one and trend two in Fig. 4.2, normally show a behavior that lies in between the two extreme trends presented above. Trend 1 (black solid line) with an already significant steepness reflects a system that is considerably fair in the classical sense; trend 2 (light blue solid line) in comparion with trend 1 traded of some throughput from a minority of nodes to improve the throughput for the majority of nodes. This could, e. g., be the case if the minority of nodes is weakly equipped, thus blocking an improved spatial reuse in an overload situation. Note that no node is starved completely, i. e., the cdf shows zero offset on the ordinate for both trends, trend 1 as well as trend 2.

By investigating the cdf of the throughput per node in heterogeneously equipped scenarios for different simulation settings, the varying behavior of the curves in steepness and, e. g.,

offset on the ordinate or minimum per node throughput (offset on the abscissa) can be observed. What is a still acceptable trade-off between fairness and spatial reuse and which trend tends to be too unfair depends on the strategy of the network and is not subject of this work.

4.3. Application to the MUD-MAC Protocol

In the following, we apply the OACR algorithm to the MUD-MAC protocol.

4.3.1. Challenges of Heterogeneously Equipped Nodes

The MUD-MAC protocol is strictly receiver-oriented, i. e., a receiver can block any announced transmission if the additional interference would exceed its tolerable number of interfering streams.
In general this is advantageous, since in ad hoc networks it is difficult for potential transmitters to precisely estimate the interference they would cause to unintended receivers. But if heterogeneously equipped nodes exist, the interference tolerance levels vary individually for each node. The strictly receiver-oriented protocol might then suffer from a lower spatial reuse than possible, since weak receivers might block parallel transmissions continuously. The OACR algorithm is expected to increase the spatial reuse for MUD-MAC in overload situations by restricting the amount of receiver objections to an appropriate level.

4.3.2. Contention Cycle and Maximum Delay Index

In order to apply OACR to the MUD-MAC protocol, the duration of a contention cycle has to be calculated. The duration of the contention cycle depends on the spatial reuse and is thus a function of the number of multiuser detection branches offered by the receivers.
By starting with homogeneously equipped nodes, we derive a formula that depends on a common number of MUD branches N_{br} per node. We adapt this formula to receivers that are heterogeneously equipped later on.
Note that although we derive the formulas for the specific settings of the MUD-MAC protocol, applying it to other time-slot-synchronous protocols that have to deal with heterogeneously equipped nodes, like MIMO based MAC protocols, is straight forward.
The consecutive flow of blocks is depicted in Fig. 4.3 if all receivers are equipped with four decoder branches, and in Fig. 4.4 if receivers offer two decoder branches.
We assume that a packet is separated into $N_{\mathrm{B}} = 4$ consecutive blocks, allowing for a maximum spatial reuse of four, as explained in Sec. 3.2.2. For four decoder branches the arrangement of the packets is a uniform flow with a shift of one packet between the different data transmissions. For two branches the shift is not uniform anymore, as marked by the black arrow. The reason is that the number of decoder branches is lower than the spatial reuse possible by the segmentation of a data packet into $N_{\mathrm{B}} = 4$ blocks.
Under the assumption that the maximum number of branches ($N_{\mathrm{br}_{\mathrm{max}}}$) is not larger than the number of blocks per packet N_{B}, the contention cycle duration CC_{Hom} for homogeneously

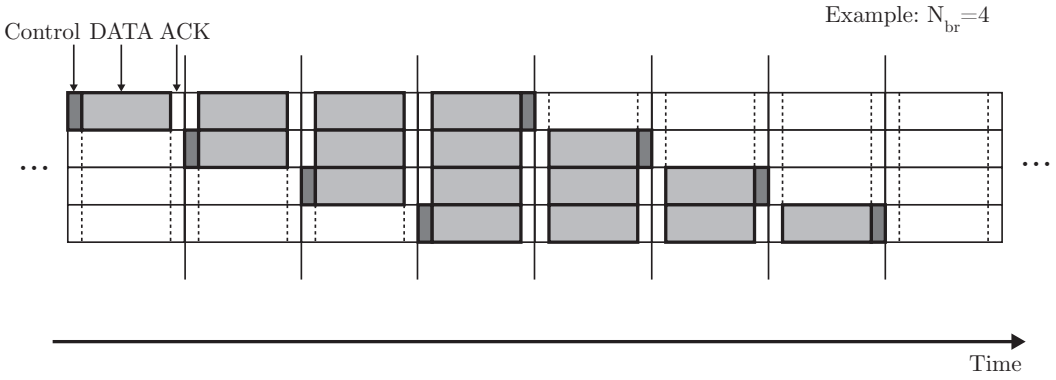

Figure 4.3.: Consecutive flow of blocks for the MUD-MAC protocol for a maximum spatial reuse of four and four multiuser decoder branches.

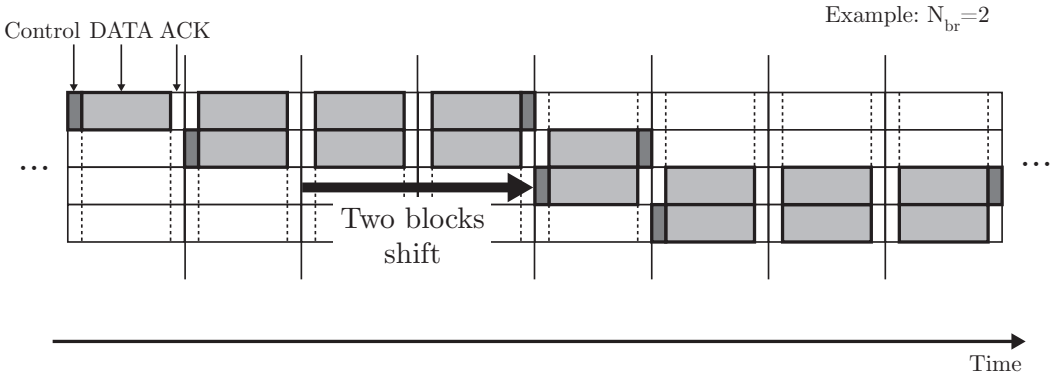

Figure 4.4.: Consecutive flow of blocks for the MUD-MAC protocol for a maximum spatial reuse of four and two multiuser decoder branches.

equipped nodes can be calculated as follows

$$CC_{\mathrm{Hom}} = \left[N_{\mathrm{B}} + \left\lfloor \frac{N_{\mathrm{T}} - 1}{N_{\mathrm{br}}} \right\rfloor N_{\mathrm{B}} + (N_{\mathrm{T}} - 1)\%N_{\mathrm{br}} \right] t_{\mathrm{BL}}. \tag{4.6}$$

Here N_{T} is the number of different transmission pairs, $N_{\mathrm{br}} \in \{1, \ldots, N_{\mathrm{br}_{\mathrm{max}}}\}$ the number of multiuser detection branches, % is the modulo operator, and t_{BL} is the duration of a MUD-MAC block. The three terms describe different segments of the blocks contained in one contention cycle, as shown by Fig. 4.5. They can be derived by inspection. For heterogeneously equipped nodes, the contention cycle CC_{Het} can be calculated as a sum of the duration of the contention cycle if all nodes are equipped with the maximum number of

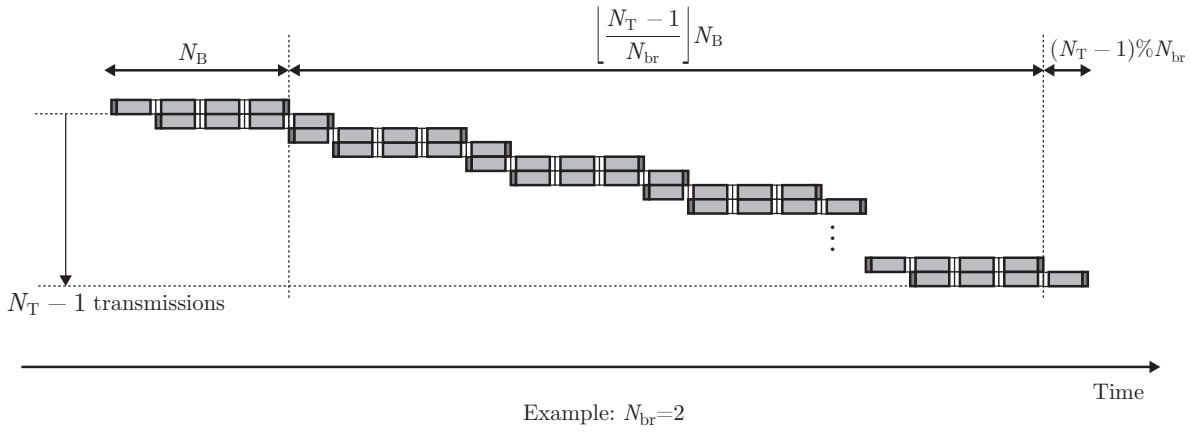

Figure 4.5.: Consecutive flow of blocks for the MUD-MAC protocol with two branches and related summation terms as taken from Eqn.4.6.

branches and an additional shift related to the unequal configuration

$$CC_{\text{Het}} = \left[CC_{\text{Hom}}(N_{\text{br}_{\max}}) + \sum_{N_{\text{br}_s}=1}^{N_{\text{br}_{\max}}-1} K_{N_{\text{br}_s}} 2(N_B - N_{\text{br}_s}) \right] t_{BL}. \tag{4.7}$$

$CC_{\text{Hom}}(N_{\text{br}_{\max}})$ is the contention cycle duration if all nodes are equipped with the maximum number of branches and $K_{N_{\text{br}_s}}$ represents the number of nodes with N_{br_s} branches, where $N_{\text{br}_s} \in \{1, \ldots, N_{\text{br}_{\max}} - 1\}$. The second summand can be calculated by inspection. Plugging the results of Eqn. 4.7 into the right hand side of Eqn. 4.5 leads to $DI_{\max}$.
Note that due to a beneficial ordering of the weakly equipped nodes it would theoretically be possible to reduce the number of frames required to serve all nodes compared to Eqn. 4.7. But since the access to the channel is random, and no central unit can, similar to a central scheduler, control the ordering, we assume the most unfavorable ordering of the nodes.

4.4. Simulation Results

We present simulation results for the MUD-MAC protocol with and without the OACR algorithm applied. The scenario under investigation is the 50 m × 50 m scenario with 50 nodes randomly and uniformly distributed, as described in Sec. 3.3.3. All system parameters are set as described in Tab. 3.2. All nodes are active, i. e., willing to transmit packets to a randomly chosen sink in their communication range.
To investigate the OACR algorithm in the context of scenarios with heterogeneously equipped nodes, we simulate a scenario where the majority of nodes, namely 35, is excellently equipped with four multiuser detection branches, but a minority, namely 15 nodes, has no MUD capabilities. In this case, without additional contention resolution, weak nodes in the

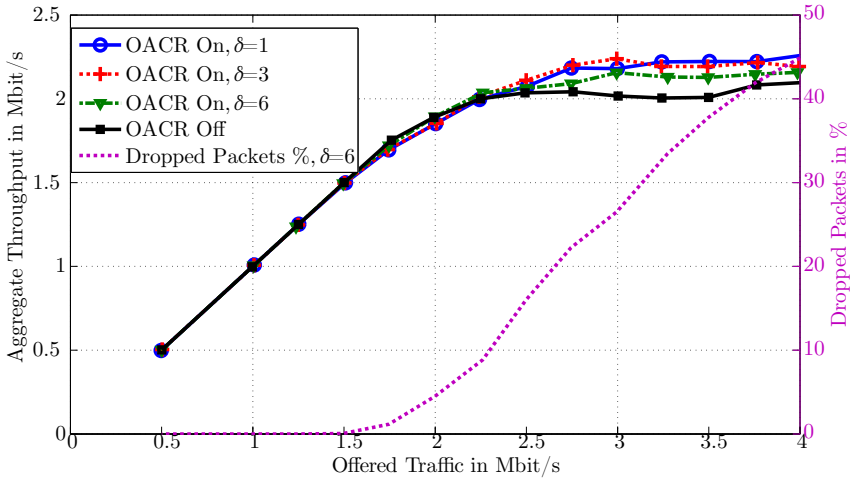

Figure 4.6.: Left axis: Aggregate throughput versus offered traffic for the OACR algorithm and different values for δ, and without the OACR algorithm. Right axis: corresponding dropped packet percentage.

MUD-MAC protocol block transmissions in their vicinity frequently. This leads to a reduced aggregate throughput, especially, if the contention is severe. The OACR algorithm is expected to increase the spectral efficiency in such overload situations without starving the weakly equipped nodes with no MUD capabilities completely. We further compare different values of δ (cf. Eqn. 4.3) regarding their influence on the system throughput and the per node fairness.

In Fig. 4.6, on the left ordinate, the aggregate throughput versus the offered traffic is shown for MUD-MAC with the OACR algorithm and different values of δ and without the OACR algorithm. The right ordinate shows the corresponding dropped packet percentages for MUD-MAC with OACR and $\delta = 6$. The aggregate throughput is evaluated as described by Eqn. 3.2. The irregularities of the curves are not due to a insufficient number of runs, as checked by the 95 % confidence interval (not shown). They are induced by the contention resolution mechanism at the beginning of the frames and corresponding variations in the per node backoff.

It can be observed that for very high offered traffic loads that exceed the highest supported throughput (for definition cf. Sec. 3.3.5), the aggregate system throughput is improved with the OACR algorithm for all values of δ compared with MUD-MAC without OACR applied. But the gains correspond to regions, where the offered traffic is that high that already a remarkable amount of packets is dropped from the packet queue, since the maximum delay restriction is violated. At the cross-over points, where the trends of the curves with the OACR algorithm applied start outperforming the pure MUD-MAC curve, already around 10 % of the packets are dropped.

For lower values of the offered traffic, the results with the OACR algorithm applied are slightly worse than without OACR. In the OACR algorithm, a receiver willing to protect its active reception has to content newly against transmitters in its vicinity for every block.

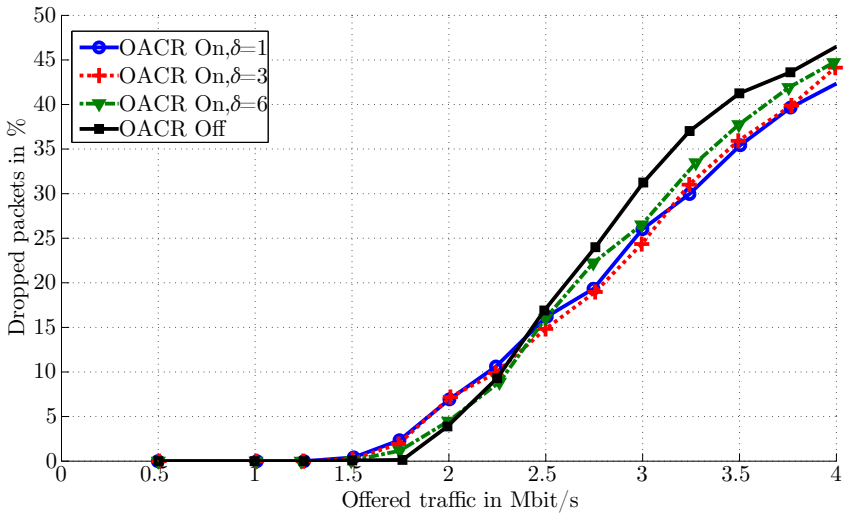

Figure 4.7.: Dropped packets in percent versus offered traffic for the OACR algorithm and different values for δ, and without the OACR algorithm.

Thus, an already started transmission might be interrupted after, e. g., two or three blocks, what makes the preceding transmission of these blocks useless. These increased losses for lower offered traffic values improve, however, the dropped packet percentages for high traffic load, as can be observed by Fig. 4.7.
There, all schemes with the OACR algorithm applied show a slightly increased dropped packet percentage for moderate offered traffic values compared with the pure MUD-MAC scheme without the OACR algorithm applied. These losses are compensated by reduced dropped packet percentages in regions where the offered traffic is very high and the system is in an overload situation.
In Fig. 4.8, the corresponding cdf curves of the throughput per nodes, as explained in Sec. 4.2, are presented for a very high offered traffic of 2.5 Mbit/s. The throughput per node is evaluated separately for each run, as explained by Eqn. 3.4. The stepwise increase of the cdf trends accounts for the increase of the per node throughput in multiples of the packet size.
All curves that apply the OACR algorithm trade off some fairness in the classical sense against improved system throughput compared with the pure MUD-MAC protocol without the OACR algorithm applied. This can be observed since the steepness of the curves is reduced compared with MUD-MAC without the OACR algorithm, leading to a minority of nodes that obtains a reduced per node throughput. But the majority of nodes can improve their throughput.
The amount of variation can be scaled by adapting the value of δ. For decreasing values, the variation increases, and the unfairness in the classical sense in the system grows as well. How to define appropriate values for δ in a practical system is a design parameter and out of scope of this work.

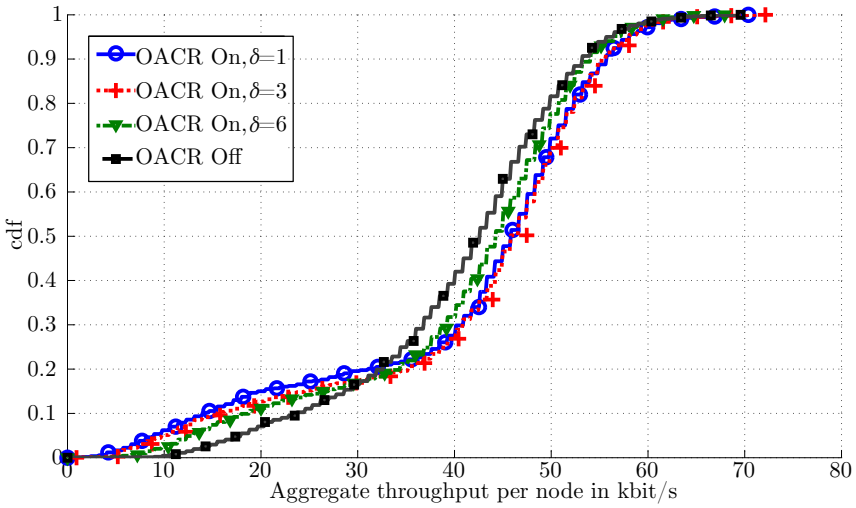

Figure 4.8.: Cumulative distribution function of the throughput per node for the OACR algorithm and different values for δ, and without the OACR algorithm for 2.5 Mbit/s aggregate offered traffic.

Remarkable for the trend of all curves is that no curve has a non-zero offset on the ordinate, i. e., by delay restrictions in the algorithm also the weakly equipped nodes are assured to get channel access. Even in very dense contention scenarios, a complete starving of these weak nodes is prevented.

4.5. Summary and Further Work

In this chapter, we addressed fairness issues in networks with heterogeneously equipped nodes. Our first contribution was the identification of this problem as a topic of interest. To the best of our knowledge, considering heterogeneously equipped nodes and their different prerequisites to access the channel was not addressed in fair contention resolution algorithms before.
Another contribution was a literature review of existing schemes regarding their adaptability to scenarios with heterogeneously equipped nodes. We subsequently formulated the requirement that receivers should be able to actively take part in contention resolution algorithms if heterogeneously equipped nodes exist.
As a third contribution, we derived a fairness understanding in scenarios with heterogeneously equipped nodes that varies from the fairness definition in the classical sense. We defined fairness in such scenarios as a trade-off. This trade-off is between, on the one hand, allowing better equipped nodes especially in overload situations to gain from their better equipment; and, on the other hand, to avoid a complete starving of weakly equipped nodes. We proposed a measure that represents this new understanding of fairness, since classical fairness measures like the Jain's fairness index cannot be applied.

As a main contribution, we presented an adaptive contention resolution algorithm that improves the system throughput in overload situations. The algorithm can especially be applied in scenarios with heterogeneously equipped nodes. Here it trades off aggregate system throughput and per node fairness in the classical sense.
By exchanging only a single parameter, the contention level, nodes obtain access to the medium depending on their successes and defeats in former contentions and depending on their per packet accumulated delays. This is achieved by two parameters, namely the utility index and the delay index. The parameters reflect successes and defeats in the past. By scaling the maximum value of the utility index with an additional weighting constant, different trade-offs between fairness and system throughput can be achieved.
Depending on the actual level of the utility index and the delay index, the contention level is adaptively adjusted after each contention. The algorithm not only takes transmitters into account. Moreover, also receivers are capable of contending in order to protect their ongoing transmissions against intolerable interference.
By means of simulations it was shown that the proposed OACR algorithm increases the aggregate throughput of the system for very high offered traffic loads without a complete starving of weakly equipped nodes. Furthermore, in these very high contention scenarios the percentages of packets that were dropped were shown to improve. These gains come at the cost of a slightly increased dropped packet ratio and a somewhat reduced system throughput for moderate offered traffic values. This restricts the applicability of the algorithm to overload situations.
In future work, the algorithm can be adapted to non-overload situations. This requires to adapt the duration of the contention window as well as the magnitude of the maximum utility index. Also, the behavior of the delay index regarding consecutive blocking, but not permanent blocking, has to be modified.
Further, investigations are required to derive analytical expressions for the influence of the weighting constant δ on the magnitude of the trade-off between fairness in the classical sense and system throughput.
The duration of the contention cycle was assumed to be known by all nodes in the network for our simulations. This requires that each node knows the individual equipment, e. g., the individual number of MUD branches of all other nodes in the network. In practical systems, the nodes can obtain the information on this equipment either locally by including this information into MAC control messages, or the routing protocol is modified accordingly. The practical realization of this modification has to be included into future investigations.

5. Multiple Antenna Communication in Ad Hoc Networks

Since the 1990s, one fundamentally new antenna technology, namely the Multiple Input Multiple Output (MIMO) technology, has obtained the attention of both, academia and industry. Instead of a conventional single antenna system that suffers from the detrimental effects of multipath fading, multiple antennas are applied at both ends of a transmission. The resulting MIMO system not only alleviates the fading effects, but additionally achieves gains, depending on the way, the multiple antennas are applied.
Although due to the huge variety of different MIMO strategies, it is not possible to give a complete overview here, we summarize in Sec. 5.1 some essential principles of MIMO communication that are important for the understanding of the work. In Sec. 5.2, we explain some basic principles regarding MIMO channel modeling and specify our concrete system model.
In the Chapters 5–8, we apply the following notation; a scalar value a is denoted by a lowercase letter. A vector $\boldsymbol{a}$ is denoted by a bold lowercase letter. A matrix $\boldsymbol{A}$ is denoted by a bold capital letter.

5.1. Multiple Antenna Techniques

Assuming frequency-flat fading, an exemplary MIMO point-to-point transmission is depicted in Fig. 5.1. The transmitter is equipped with M_t antennas and the receiver is equipped with M_r antennas. Between every transmit/receive antenna pair, a complex path gain describes the influences on the transmission between these two antennas. For the transmission from antenna i on the transmitter side to antenna j on the receiver side the channel transfer function is, e. g., summarized as $h_{i,j}$.
The complex path gain contains the influences of path loss, shadow fading, and multipath fading on the overall transmission attenuation between the antenna pair. Arranging the path gains from all receive to all transmit antennas to a matrix results in the complex channel matrix $\boldsymbol{H}$ of size $M_\mathrm{r} \times M_\mathrm{t}$. Since for a frequency flat channel, the received signal at any instant of time is independent on previous inputs, the resulting transmission can be described as

$$\boldsymbol{y} = \boldsymbol{H}\boldsymbol{x} + \boldsymbol{n}, \tag{5.1}$$

where $\boldsymbol{x}$ is a vector containing the M_t transmitted symbols, $\boldsymbol{n}$ is the M_r-dimensional noise vector and $\boldsymbol{y}$ contains the M_r received symbols. We assume the entries of $\boldsymbol{n}$ to be zero mean, complex Gaussian distributed, with a covariance matrix of $\sigma_\mathrm{n}^2 \boldsymbol{I}_{M_\mathrm{r}}$, where the variance of the noise, σ_n^2, is the product of the system bandwidth B and the thermal noise power spectral density N_0, $\sigma_\mathrm{n}^2 = BN_0$.
The complex channel matrix $\boldsymbol{H}$ describes the link qualities between all antennas in the system. If it is known on the transmitter side (Channel State Information at Transmitter (CSIT)),

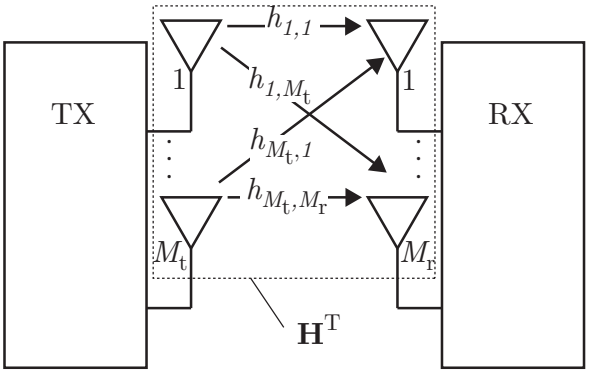

Figure 5.1.: Exemplary MIMO configuration with M_t transmit and M_r receive antennas.

the transmitter can precode the symbols both in phase and amplitude so that favorable path gains are exploited. Additionally, giving transmit power to those connections that undergo strong fading attenuations is prevented. This is performed by multiplying the symbols by a complex-valued *precoding matrix* $\boldsymbol{M}$

$$\tilde{\boldsymbol{y}} = \boldsymbol{H}\boldsymbol{M}\boldsymbol{x} + \boldsymbol{n}, \tag{5.2}$$

where $\boldsymbol{M}$ is of size $M_T \times s_t$, thus reflecting the parallel transmission of s_t symbols. The vector $\boldsymbol{x}$ is then of size $s_t \times 1$. $\tilde{\boldsymbol{y}}$ is a vector containing the received symbols after precoding. Similar to the transmitter, the receiver can exploit the knowledge of the channel matrix $\boldsymbol{H}$, the Channel State Information at Receiver (CSIR). It multiplies the received signal with a complex-valued *receiving matrix* $\boldsymbol{D}$

$$\hat{\boldsymbol{y}} = \boldsymbol{D}\boldsymbol{H}\boldsymbol{M}\boldsymbol{x} + \boldsymbol{D}\boldsymbol{n}, \tag{5.3}$$

where for the reception of s_r symbols the receiving matrix $\boldsymbol{D}$ is of size $s_r \times M_R$. $\hat{\boldsymbol{y}}$ contains the received symbols after precoding and subsequent decoding operations. As can be seen from Eqn. 5.3 each symbol experiences an individual attenuation and phase shift, the *spatial signature*.

In literature, in slow fading environments CSIR is commonly assumed; the knowledge of the complete channel matrix $\boldsymbol{H}$ on the transmitter side is often unavailable and, in case it can be achieved, likely to be falsified by delays in the estimation process. How the channel estimation in principle can be performed is out of scope of this thesis. For further information see, e. g., [PNG03], and references within.

A huge variety of different schemes proposes methods on how to design the precoding and decoding matrices. A fundamental distinction of the schemes is the availability of CSIT. We will give a top level overview of basic principles that are relevant for the remainder of the work that partly follows a classification from [Gol06].

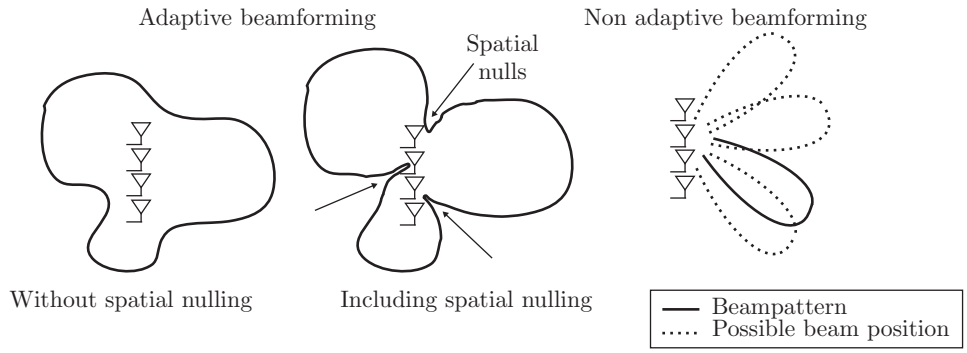

Figure 5.2.: Different technologies that all are referred to as beamforming in literature.

5.1.1. Beamforming

With beamforming, the same symbol is transmitted over each transmit antenna. The precoding matrix $\boldsymbol{M}$ reduces then to a precoding vector $\boldsymbol{m}$ that contains the complex factors for each antenna element. The receiving matrix $\boldsymbol{D}$ reduces accordingly to a receiving vector $\boldsymbol{d}$.
The terminology beamforming in principle is misleading, since it is commonly used not only in the sense that we describe in the following, i. e., as methods that adapt to the fading of the wireless channels. Also, non adaptive beams that are switched in order to find the best (fixed) beam direction to serve a user are called beamforming. These do not adapt to the wireless channel and can be realized, e. g., as phased antenna arrays. An example for such non adaptive beamforming is shown on the right of Fig. 5.2.
Adaptive beamforming, or simply beamforming, is applied if the multiple antennas at the transmitter and the receiver are used to obtain a *diversity gain*. This gain aims at improving the Frame Error Rate (FER) by increasing the Signal to Noise Ratio (SNR) for a fixed transmission rate. Correspondingly, if the SNR requirement is held fixed, the gain can improve the transmission range.
The diversity gain is achieved on the receiver side by combining the received symbols coherently. The magnitude in gain depends on wether or not CSI is available on the transmitter side. If the transmitter knows the channel matrix $\boldsymbol{H}$, the receive SNR can be optimized. In this case, a Singular Value Decomposition (SVD) of the channel matrix $\boldsymbol{H}$ is performed

$$\boldsymbol{H} = \boldsymbol{U}\boldsymbol{\Sigma}\boldsymbol{V}^H, \tag{5.4}$$

where $\boldsymbol{U}$ and $\boldsymbol{V}$ are unitary matrices, containing the left and right singular vectors of $\boldsymbol{H}$ and $\boldsymbol{\Sigma}$ is a diagonal matrix with the diagonal elements containing the singular values of $\boldsymbol{H}$. $\boldsymbol{A}^H$ refers to the hermitian transpose operator of $\boldsymbol{A}$.
The optimum strategy is to choose the precoding vector $\boldsymbol{m}$ and the receiving vector $\boldsymbol{d}$ as the left and right singular vectors belonging to the strongest eigenmode [PNG03]. All transmit power is thus allocated to the strongest eigenmode. The maximum diversity gain with an

optimal transceiver design is $M_\mathrm{r}M_\mathrm{t}$ [BCC+07].
If no channel state information is available on the transmitter side, the precoding vector $\boldsymbol{m}$ is a vector of ones, normalized to unit power, since the overall transmit power is fixed. The receiving vector $\boldsymbol{d}$ is chosen to maximize the receive SNR. In this case, the SNR reduces compared with full CSIT.
The before mentioned approach describes beamforming as a technology that is adaptive to the fading of the wireless channel, and aims at achieving the maximum diversity gain. It can also be combined with multiuser techniques like spatial nulling, explained later on in this section (cf. Sec. 5.1.3). Both methods are referred to as *adaptive beamforming* in literature. Two exemplary beam patterns, one without and one including spatial nulls, are shown in Fig. 5.2 on the left.
In Chapter 6 we focus on cross-layer designs that apply beamforming as a technology that adapts to the fading of the wireless channel. But since many challenges that arise on the MAC layer for directive transmission arise for both, the non adaptive beamforming as well as the adaptive beamforming, the non-adaptive beamforming is also partly included in Chapter 6.

5.1.2. Multiplexing

Another application of multiple antennas is to achieve a *multiplexing gain*. This gain aims at improving the data transmission rate for a fixed FER. Instead of transmitting one symbol over the MIMO channel, multiple symbols are transmitted in parallel. If the transmitter knows the channel matrix $\boldsymbol{H}$ (CSIT), the channel can be decomposed into independent, non interfering *sub-channels*. This is achieved by appropriately choosing the precoding and receiving matrices as the left and right singular vectors of the singular value decomposition of the channel matrix $\boldsymbol{H}$, cf. Eqn. 5.4. The transmit power is, optimally with respect to capacity, distributed among the sub-channels according to the *waterfilling mechanism* [CT91]. This algorithm suppresses eigenmodes that are below a certain performance level. The maximum multiplexing gain with an optimal transceiver design is $\min\{M_\mathrm{r}, M_\mathrm{t}\}$ [BCC+07], where $\min\{a, b\}$ returns the minimum of a and b.
In case only the receiver has knowledge of the channel matrix $\boldsymbol{H}$, the transmitter can neither arrange the sub-channels to fit to the dominant eigenmodes of the channel, nor optimize the power allocation among the sub-channels. Without CSIT, the transmitter divides the transmit power equally among all antennas and sends independent symbols over each antenna. Note that on the receiver side, to achieve a similar performance, the effort to demodulate the superimposed symbols is increased significantly compared with the case of CSIT.
A prominent example for spatial multiplexing without CSIT is the V-BLAST architecture [WFGA98]. There, the transmitter splits the data stream into substreams. Each substream is transmitted by one antenna. The receiver receives a substream on all its M_r receive antennas, thus achieving a diversity gain of M_r. In order to demodulate the streams, it applies symbol interference cancelation.
For symbol interference cancelation, the symbols of the different substreams are first ordered according to their receive SINRs, i. e., the SINR achieved if all other symbols are treated

as interference. The symbol with the highest receive SINR is estimated and subsequently subtracted from the received sum signal. This is performed successively until the symbols of all substreams are estimated.

The V-BLAST architecture is not restricted to the single user case, i. e., a transmitter can send multiple streams to different receivers. A receiver can apply interference cancelation for a sum signal consisting of streams from different transmitters. In this case, the V-BLAST receiver is applied as a multiuser detection receiver.

5.1.3. Spatial Nulling

In case multiple transmissions take place simultaneously, the nodes can apply their antennas not only to transmit or receive multiple streams, but also to avoid unattended interference from neighboring transmissions. This is achieved by exploiting the differences between the spatial signatures of the desired signal and interfering signals.

In the *spatial nulling* approach, a receiver experiencing strong interference from another transmitter than the desired one, determines its receiving matrix $\boldsymbol{D}$ so that besides receiving its own useful signals, the interfering components at different antennas cancel after combining.

This method is restricted by the number of receive antennas M_r at a receiver. If a receiver requires one antenna for receiving its useful signal, it can at most spatially null $M_\mathrm{r} - 1$ simultaneously impinging interferers. A transmitter can also apply spatial nulling to minimize the interference sent towards other nodes than the desired node. A more detailed mathematical description of this method is given in Chapter 6.

5.2. Channel Modeling

In order to simulate MIMO technologies, the channel matrix $\boldsymbol{H}$ has to be described by an appropriate channel model. Notice, however, that the main focus of this work is not solely on the physical layer part, but more on a joint design of physical and MAC layer. This requires to reduce the implementation effort for each layer. Thus, the affordable complexity of the channel model is limited. Moreover, since we do not simulate a predefined scenario as, e. g., the “indoor office environment” or the “suburban outdoor environment”, certain parameters are not clearly specified for the simulations. We set the parameters so that they apply for a variety of different scenarios. To reproduce the effects occurring in wireless environments, a

MIMO channel model is usually characterized by the following influences:

- path loss,
- shadow fading,
- fast fading,
- Rician K-factor distribution for line-of-sight,
- delay spread,
- Doppler shift, and
- transmit and receive antenna correlation.

We shortly summarize the theoretical background for each of the characteristics in the next sections. Besides the theoretical background, each section is complemented by a description of the practical implementation in the channel model.

5.2.1. Path Loss

Theoretical Background

Path loss describes the attenuation that the amplitude of an electromagnetic wave undergoes while propagating as a function of the distance. Besides the losses that each wave experiences in free-space propagation, path loss models can also include dependencies on other external parameters like building height or simulated environment. For further description see, e. g., [Mol05].

Practical Implementation

We model the path loss attenuation A_{PL} by the modified free-space path loss model described in Sec. 2.2.3. This attenuation is included into the channel model by multiplying the fading coefficient between each antenna pair with $\sqrt{A_{\mathrm{PL}}}$.

5.2.2. Fading and K-Factor

Additionally to path loss, the received signal suffers from variations in the signal level, called fading.

Theoretical Background

Fading can be classified in two multiplicative factors, namely *shadow fading* and *fast fading*.

Shadow Fading: Shadow fading describes the effect that the signal undergoes obstructions by obstacles, e. g., buildings, hills, or trees. It reflects long term variations of the receive signal power level, often also referred to as slow fading or macroscopic fading.

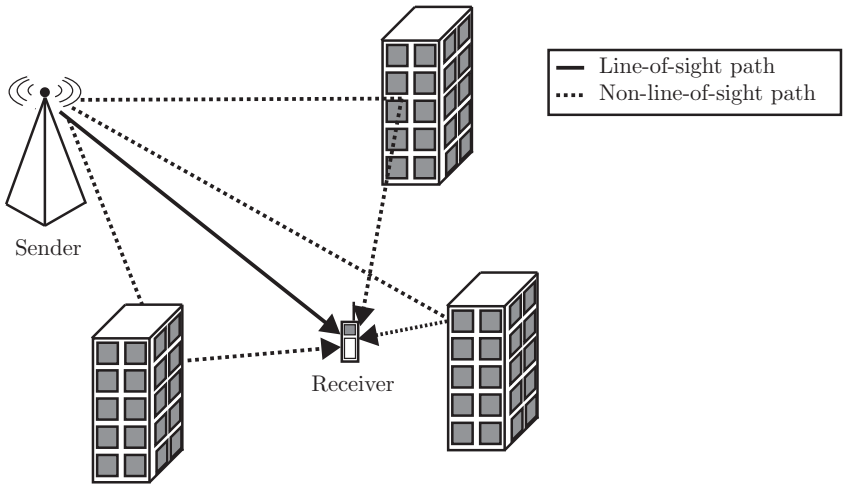

Figure 5.3.: Line-of-sight and multipath propagation.

Fast Fading and K-Factor: In contrast to shadow fading, effects of multipath propagation lead to *fast fading*. This occurs, since the transmitted signal is reflected and scattered by obstacles, as depicted in Fig. 5.3. The different paths (non-line-of-sight as well as line-of-sight) experience different attenuations and phase shifts each. Further, due to the varying path length they cover, they arrive at the receiver with different delays. Fast fading causes fluctuations of the received signal in time, frequency, and space.
If no line-of-sight path exists, and the quantity of independent fading paths is large, the in-phase (x_I) and the quadrature component (x_Q) of the received signal have an independent and identically (i. i. d) Gaussian distributed Probability Density Function (pdf) $f_{x_\mathrm{I}}(x_\mathrm{I})$ and $f_{x_\mathrm{Q}}(x_\mathrm{Q})$ with zero mean and variance σ^2

$$\begin{aligned} f_{x_\mathrm{I}}(x_\mathrm{I}) &= \frac{1}{\sqrt{2\pi\sigma^2}} e^{\frac{-x_\mathrm{I}^2}{2\sigma^2}}, \\ f_{x_\mathrm{Q}}(x_\mathrm{Q}) &= \frac{1}{\sqrt{2\pi\sigma^2}} e^{\frac{-x_\mathrm{Q}^2}{2\sigma^2}}. \end{aligned} \tag{5.5}$$

Since both components are independent, the joint distribution of x_I and x_Q, namely $f_{x_\mathrm{I},x_\mathrm{Q}}(x_\mathrm{I}, x_\mathrm{Q})$ is the product of the individual distributions

$$f_{x_\mathrm{I},x_\mathrm{Q}}(x_\mathrm{I}, x_\mathrm{Q}) = f_{x_\mathrm{I}}(x_\mathrm{I}) f_{x_\mathrm{Q}}(x_\mathrm{Q}). \tag{5.6}$$

$f_{x_\mathrm{I},x_\mathrm{Q}}$ is complex Gaussian distributed with zero mean and variance $2\sigma^2$

$$f_{x_\mathrm{I},x_\mathrm{Q}} \sim \mathcal{CN}(0, 2\sigma^2).$$

For practical implementation, the channel matrix $\boldsymbol{H}_\mathrm{iid}$ can thus be modeled as

$$\boldsymbol{H}_\mathrm{iid} = \frac{1}{\sqrt{2}}(\boldsymbol{H}_\mathrm{Re} + i\boldsymbol{H}_\mathrm{Im}), \tag{5.7}$$

where $\boldsymbol{H}_{\mathrm{Re}}$ and $\boldsymbol{H}_{\mathrm{Im}}$ contain the real and imaginary parts of the entries of $\boldsymbol{H}_{\mathrm{iid}}$. All entries of $\boldsymbol{H}_{\mathrm{Re}}$ and $\boldsymbol{H}_{\mathrm{Im}}$ follow a Gaussian distribution as described in Eqn. 5.5, with zero mean and variance $\sigma^2 = 1$ (standard normal distribution).
Note that to achieve a joint distribution $f_{x_{\mathrm{I}},x_{\mathrm{Q}}}$ with zero mean and variance $\sigma^2 = 1$ instead of $2\sigma^2 = 2$, a scaling factor of $\frac{1}{\sqrt{2}}$ is included. The resulting value of the received signal amplitude has a Rayleigh distributed probability density function.
If there is a dominant path, e. g., a direct line-of-sight, the signal amplitude is modeled to be Rician distributed instead. The ratio of the signal power in the dominant path over the power in the other, scattered paths is described by the K-factor.

Practical Implementation

We assume non-line-of-sight conditions in our simulations, i. e., the K-factor is set to zero, resulting in Rayleigh fading receive signal amplitudes and a fading channel matrix modeled as described in Eqn. 5.7. Assuming a non-line-of-sight transmission reflects a more general channel assumption and thus more general simulation scenarios, since line-of-sight connections can only be assumed in specific cases.
Furthermore, we do not take shadow fading into account. Shadow fading has the same impact on a transmission than a reduced or increased transmission range. Since we model variable transmission ranges and do not simulate a predefined scenario, the modeling of shadow fading will not offer new insights into the system performance.

5.2.3. Delay Spread and Doppler Shift

In the previous section we explained how to derive one realization of $\boldsymbol{H}$. In principal, $\boldsymbol{H}$ depends on time and frequency, $\boldsymbol{H} = \boldsymbol{H}(t, f)$. For a practical implementation the question arises, for how many temporal snapshots (how long in time) one channel realization is valid until a new realization has to be created. Related to this, it has to be defined, which bandwidth in a simulation environment experiences the same channel realization $\boldsymbol{H}$, and at which bandwidth a new channel realization has to be simulated instead. These two questions lead to a radio-channel classification as shown in Fig. 5.4, taken from [Big05]. There, the author splits the resources in time and frequency into four blocks, depending on the *coherence time* T_{c} on the time axis and the *coherence bandwidth* B_{c} on the frequency axis. These two parameters approximately describe bounds. Within these bounds the same channel realization is valid in time and frequency.
If the transmission time exceeds the coherence time of the channel, a new channel realization is required, and the channel is set to be selective in time. Likewise, if the system bandwidth goes beyond the coherence bandwidth, the channel has to be modeled by a new channel realization, resulting in a frequency selective channel behavior.

Theoretical Background

The time between the arrival of the first multipath component, normally the line-of-sight path if it exists, and the last multipath component is called maximum delay spread. Related

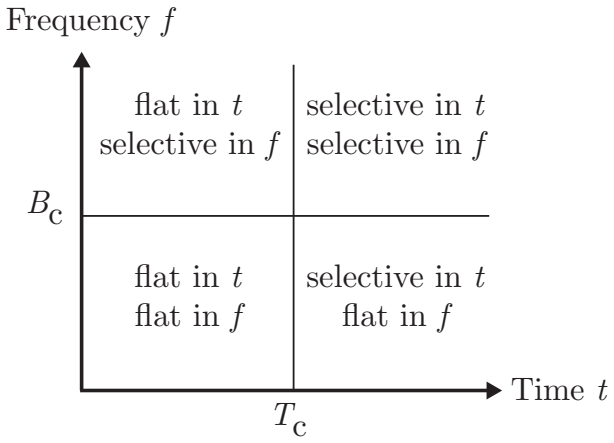

Figure 5.4.: Radio-channel classification [Big05].

to the maximum delay spread, based on a power delay profile, i. e., the average power as a function of the delay, the Root Mean Square (RMS) delay spread can be defined (for definition see, e. g., [PNG03, Gol06]).

The coherence bandwidth B_c is defined in [PNG03] to be approximately the inverse of the RMS delay spread of a channel. If the RMS delay spread is smaller than the inverse of the system bandwidth, the different multipath components cause *narrow band (flat) fading*, corresponding to the lower row of the four areas in Fig. 5.4. Otherwise, frequency selective (wide band) fading occurs (upper row of Fig. 5.4). For further information about wide band channel modeling, please refer to, e. g., [BCC+07, Gol06].

The movement of a sender or a receiver causes a single frequency to be spread over a finite spectral bandwidth. The distribution of the receive power as function of these *Doppler frequencies* is the *Doppler power spectrum* For further definition see, e. g. [PNG03]. The Doppler spread f_d is the maximum frequency for which the absolute value of the Doppler power spectrum of a signal is approximately non-zero. According to [Gol06], it is determined by the velocity v_m of the moving node and the wavelength λ of the carrier frequency and can be approximated as follows

$$f_d \leq \frac{v_m}{\lambda}. \tag{5.8}$$

The Doppler spread in the frequency domain results in time selective fading in the temporal domain. This changes get significant if the time investigated exceeds the inverse of the Doppler spread (Right column of Fig. 5.4). More precisely, the time for which the channel characteristics can be assumed to stay fairly constant, namely the coherence time T_c, is approximately the inverse of the Doppler spread [PNG03].

Practical Implementation

We restrict our simulations regarding the delay spread of the channel and the resulting frequency selective fading to the narrow band case. In [Mol05], typical values for the RMS delay spread are shown. There, the RMS delay spread for indoor residential buildings ranges from 5 ns–10 ns, in indoor office environments depending on the room size from 10 ns–100 ns, in factories and airport halls from 50 ns–200 ns, in microcells for non-line-of-sight from 100 ns–500 ns, and in urban and suburban environments from 100 ns–800 ns.
All simulations in Chapter 6 and Chapter 8 are performed with 1 MHz system bandwidth. The maximum RMS delay spread to achieve a coherence bandwidth of 1 MHz is $\approx 1\,\mu$s and thus fits to all of the above listed scenarios. In Chapter 7 for some simulations, nodes are not solely separated by multiple antenna signal proccessing, but additionally by CDMA. Depending on the spreading code length, the bandwidth requirement is increased accordingly. The maximum bandwidth requirement is 31 MHz, corresponding to a maximum RMS delay spread of ≈ 30 ns. Thus, the results in Chapter 7 are restricted to those scenarios where this RMS delay spread is met.
We model the changes in time with respect to the Doppler spread of the channel and the resulting time selective fading by a *block fading channel model*. In this model, the channel matrix $\boldsymbol{H}$ remains constant within a block[1] and changes only between different blocks. The block duration is significantly smaller than the coherence time of the channel.
According to Eqn. 5.8, the Doppler spread at 2.4 GHz carrier frequency is around 11 Hz for a mobile user with pedestrian speed of 5 km/h, corresponding to a coherence time of ≈ 0.09 s. With respect to the assumption that a block duration is clearly smaller than the coherence time of the channel, we model a block duration of 0.01 s. We do not assume the blocks to fade independently, but according to a spatio-temporal correlation model, i. e., a model that assumes correlation in time and space. The practical realization of the temporal correlation between the blocks is thus explained together with the practical realization of the spatial correlation in Sec. 5.2.4.

5.2.4. Transmit and Receive Antenna Correlation

If the amplitudes between different antenna pairs of transmitter and receiver are modeled independently, there is no correlation between antennas belonging to the same antenna array. This is also assumed for the generation of $\boldsymbol{H}_{\text{iid}}$ in Eqn. 5.7.

Theoretical Background

In reality, this might not be the case due to insufficient antenna spacing, co-polarized antennas, or scattering that leads to a spatial correlation. Since the signals reflected by scatterer clusters arrive at the individual antennas of one array with almost the same angle, the changes in phase and amplitude are only depending on the relative distance as seen by the impinging wave, leading to a certain correlation in the path coefficients of these elements.

[1] The term block is not to be associated with a block of the MUD-MAC protocol as described in Sec. 3.2.2.

In order to take these antenna correlations into account, a correlation matrix at the transmitter ($\boldsymbol{R}_{\mathrm{TX}}$) of size $M_{\mathrm{t}} \times M_{\mathrm{t}}$ as well as at the receiver ($\boldsymbol{R}_{\mathrm{RX}}$) of size $M_{\mathrm{r}} \times M_{\mathrm{r}}$ is introduced. Both matrices are symmetric, since the correlation between antenna element i and antenna element j is the same as between antenna element j and antenna element i.
Based on these correlation matrices the resulting channel matrix $\boldsymbol{H}$ of size M_{r} by M_{t} can be calculated by the Kronecker model ([OCB05] and references within) as

$$\boldsymbol{H} = \frac{1}{\sqrt{\mathrm{TR}(\boldsymbol{R}_{\mathrm{RX}})}} \boldsymbol{R}_{\mathrm{RX}}^{1/2} \boldsymbol{H}_{\mathrm{iid}} \left(\boldsymbol{R}_{\mathrm{TX}}^{1/2}\right)^{T}. \tag{5.9}$$

$\boldsymbol{A}^{1/2}$ is the square root of $\boldsymbol{A}$ that satisfies $\boldsymbol{A}^{1/2} \cdot \left(\boldsymbol{A}^{1/2}\right)^{H} = \boldsymbol{A}$ and $\mathrm{TR}(\boldsymbol{A})$ is the trace of $\boldsymbol{A}$. $\boldsymbol{H}_{\mathrm{iid}}$ is a matrix with zero mean, unit variance, complex Gaussian entries ($\sim \mathcal{CN}(0,1)$) of size M_{r} by M_{t}, as defined by Eqn. 5.7.

Practical Implementation

The transmit and receive correlation matrices are modeled according to model "A" for these matrices in the 802.11n standard [ESK+04]. In [SPM02] a detailed description of how to calculate cross correlation functions depending on the distance between the antenna elements can be found.
With the transmit and receive correlation matrices, a **spatial correlation** is introduced into the channel model as described in Eqn. 5.9. But the **temporal correlation** between the blocks of the block fading model still has to be included.
In order to obtain a spatio-temporal correlated model, we apply a method described in [NAP04]. There, the (t_0+t)-th channel realization is derived from the t_0-th channel realization as follows

$$\boldsymbol{H}(t_0 + t) = \rho(t)\boldsymbol{H}(t_0) + \sqrt{1 - \rho(t)^2}\boldsymbol{E}, \tag{5.10}$$

where $\boldsymbol{H}(t_0)$ and $\boldsymbol{E}$ are spatially correlated channel matrices which are generated as described above. ρ is the correlation coefficient that can be calculated according to the Jakes' model [JE94] as

$$\rho(t) = J_0(2\pi f_d t), \tag{5.11}$$

with J_0 the Bessel function of the first kind and 0-th order. The correlation matrices $\boldsymbol{R}_{\mathrm{RX}}$ and $\boldsymbol{R}_{\mathrm{TX}}$ are the same for all temporal channel realizations that are generated according to Eqn. 5.10.

6. Beamforming Based Cross-Layer Design

During the last years, beamforming was adapted to the field of wireless ad hoc networks. This technique promises a strong coverage extension by diversity gains. It also offers large gains in spatial reuse if it is combined with multiuser technologies like, e. g., spatial nulling. Still, to obtain the gains offered by the physical layer strategy, appropriate MAC layer solutions are required since the application of beamforming in ad hoc networks is not straight forward.
The term beamforming refers to channel adaptive beamforming as well as the switching of a beam by means of a phased array, cf. Sec. 5.1.1. The latter technique performs satisfactorily if there is one distinct direction like a line-of-sight to the communication partner. In multipath environments such schemes are likely to perform insufficiently. Within the chapter, we aim at cross-layer designs that apply adaptive beamforming and are thus applicable in multipath environments without line-of-sight connection. For the development of a new appropriate MAC protocol design, we focus on a combination of beamforming and spatial nulling that reduces the Multiple Access Interference (MAI) on the physical layer.
The structure of this chapter is as follows. We start with challenges and related work of beamforming based cross-layer designs in Sec. 6.1. Some challenges known from non-adaptive directional transmission also arise for adaptive beamforming. Thus, in Sec. 6.1.1 we include known challenges from non-adaptive beamforming as well. In Sec. 6.2 and Sec. 6.3 we summarize two existing beamforming based cross-layer designs. By exploiting the advantages of both protocols but avoiding their disadvantages, we develope our proposed Channel Information Exchange (CIE)-MAC protocol in Sec. 6.4. We show related simulation results in Sec. 6.5, and Sec. 6.6 summarizes the chapter.
Parts of the results published here have earlier been published in [KWH+10].

6.1. Beamforming in Ad Hoc Networks

6.1.1. Challenges for Beamforming Based Cross-Layer Design

To support a beamformed data transmission, many approaches also transmit the preceding control messages in a beamformed manner. Three major problems related to directional control message transmission are listed in [CYRV06], namely underutilization, deafness, and an impaired hidden terminal problem.
Underutilization is related to coverage extension that is a strong advantage of directional transmission. A node obtains a certain antenna gain G_0 in case it transmits or receives omnidirectionally. This gain can be increased to G_B ($G_\mathrm{B} \geq G_0$) if the node directs its beam pattern to its associated communication partner. The resulting overall directional communication gain if both nodes of a transmission orientate their antennas to their associated

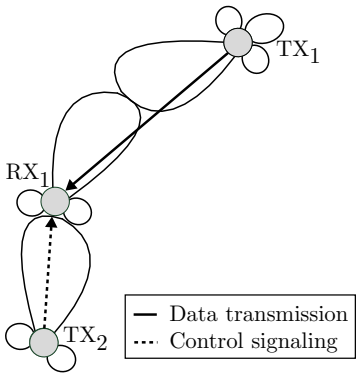

Figure 6.1.: Deafness against control messages during an ongoing data transmission.

partner is $G_B \times G_B$. This increases the communication range compared with the overall omnidirectional gain of $G_0 \times G_0$, leading to a coverage extension.
If during the control message transmission, one node or both nodes do not direct their beam pattern to the communication partner, but transmit or receive omnidirectionally, the whole transmission is bounded to the range of this control message. This leads to a reduction in the maximum possible coverage extension, the *underutilization*.
Deafness describes that a node that is beamformed towards a communication partner is not able to reply to a control message sent by another node that is placed in a different spatial direction than the communication partner. An exemplary situation is shown in Fig. 6.1. For simplification, Fig. 6.1 and Fig. 6.2 represent the beams by a uniform pattern, as expected for non-adaptive beamforming. The presented scenarios hold, however, for adaptive beamforming as well. The pattern then change as explained by Fig. 5.2.
Assuming that in Fig. 6.1 TX_1 and RX_1 agreed on a data transmission by exchanging directional control messages. Assuming further that node TX_2 that is in another spatial direction than TX_1 is not able to overhear this control message exchange. Subsequently, since it has also a packet for RX_1 in its queue, it sends a directional control message to RX_1. Since RX_1 is beamformed towards TX_1, it cannot receive the control message from TX_2. This is even the case if it is at the moment not busy with receiving a data packet, e. g., if the control message exchange is in specific reserved time slots as in MUD-MAC. Thus, it will not reply to TX_2. The described failure of this control message exchange can result in misinterpretations on higher layers of TX_2. On these layers the unsuccessful control message is interpreted as congestion or link failure if occurring multiple times.
The inability of RX_1 to receive control messages from TX_2 can even lead to packet losses if RX_1 is not the addressee of the control message sent by TX_2. In this case, RX_1 is not aware that TX_2 starts a new transmission to another node. If RX_1 started a new transmission on its own after it finished the reception of packets from TX_1, it would probably interfere the transmission of TX_2. Corresponding to a similar problem in omnidirectional transmissions, this problem is termed *hidden terminal problem due to beamforming*.
Another problem that also falls in the category of a hidden terminal problem is the *hidden*

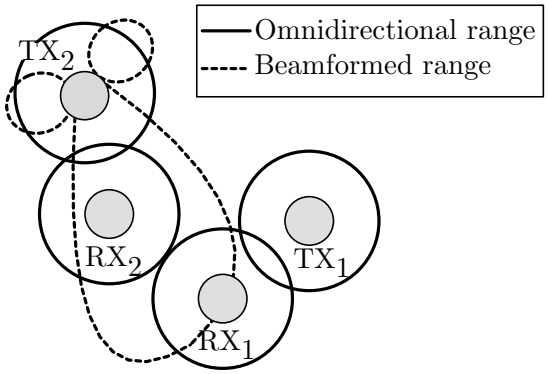

Figure 6.2.: Hidden terminal problem due to asymmetry in gain between omnidirectional control messages and directive data transmission.

terminal problem due to asymmetry in gain. It is related to the differences in the directional gain G_{B} of a beamformed data transmission to the omnidirectional gain G_0 in case of an omnidirectional control message transmission. This is shown in Fig. 6.2. If control messages are transmitted omnidirectionally, as during the control message exchange between TX_1 and RX_1, only nodes that are in the omnidirectional range of these nodes overhear the control messages. Thus, in the example, TX_2 does not overhear the control message exchange from TX_1 and RX_1. Although it is not in the omnidirectional range of RX_1, it might cause interference to RX_1 in case it transmits directionally to its associated partner RX_2. This can happen since the range of the data transmission is increased compared with the omnidirectional control message range.

In [CYRV06] it is argued that the hidden terminal problem due to asymmetry in gain might not appear very frequently. It requires that the interfering node must be out of omnidirectional communication range to both, the transmitter as well as the receiver, during the preceding control message exchange; then the interference might not be so large if the transmitter changes its gain from G_0 to G_{B}.

The authors describe the problem implicitly assuming that all nodes are equally equipped, i. e., all nodes have the same number of antennas. If the nodes are heterogeneously equipped also the beamforming gain G_{B}, which is a function of the number of antennas, and thus the communication range, changes individually. This poses additional challenges to the design of a new MAC protocol. Specific considerations are also required if different beamforming vectors are applied at a node for transmission and reception as well as for control messages and data transmission. Moreover, also if all nodes are equally equipped, the problem gets severe if the number of antennas applied during the data transmission phase varies strongly from the number of antennas applied during control message transmission.

Besides the before mentioned challenges related to directional control message transmission, for channel adaptive beamforming based cross-layer designs an additional challenge arises. If a protocol aims at full applicability in time-varying environments, it requires to obtain

spatial information like a certain channel knowledge or the knowledge of a node's spatial signature (cf. Sec. 5.1) in a fully distributed manner. Moreover, this information has to be obtained on a short temporal basis since it is only valid for a time period that lies on the order of the coherence time T_c of the channel, cf. Sec. 5.2.3.
Multiple approaches assume that there is a certain pre-knowledge of Direction of Arrival (DoA), Direction of Departure (DoD), or spatial signatures that is, e. g., provided by higher layers. Since higher layer information, like, e. g., routing information is not exchanged as frequently as required for a time-varying channel, these protocols are restricted to static channels. We formulate the corresponding challenge that has to be overcome as *static channel assumption* in the following.
Even in case a protocol provides the required channel information or information about spatial signatures by an appropriate control message exchange, estimating the channel is prone to channel estimation errors. Moreover, the information about channels and spatial signatures that is included in control messages can be lost in case of control packet losses. Thus, we raise the robustness of a protocol against protocol failures like control messages losses or channel estimation errors as a last challenge. This challenge is called *vulnerability against control message failures*.
Summarizing, we identified the following six challenges (**CH1**–**CH6**) that have to be overcome by an appropriate cross-layer design that assumes beamforming as physical layer strategy:

- underutilization (**CH1**),
- deafness (**CH2**),
- hidden terminal problem due to beamforming (**CH3**),
- hidden terminal problem due to asymmetry in gain (**CH4**),
- static channel assumption (**CH5**), and
- vulnerability against control message failures (**CH6**).

In this chapter, we present a new MAC protocol design that combines adaptive beamforming with spatial nulling and takes all above-mentioned challenges into account. We develop our new CIE-MAC protocol for a time-varying environment, i. e., no a priori knowledge of DoDs, DoAs, or channels is assumed.

6.1.2. Related Work

Multiple surveys on beamforming based MAC protocol designs exist in literature [DNW04, BJ11]. An up to date and detailed survey can be found in [BJ11]. The authors compare 38 protocol designs regarding different features. Besides others, they also investigate the way the protocols learn beamforming information of neighbors, corresponding to **CH5**. We shortly summarize the outcome regarding this challenge in the following.
From the compared schemes, almost half of the schemes, namely 17, fail to overcome **CH5** since they assume the information to be available (10), to be provided by upper layers (4), or

to be learned by Global Positioning System (GPS) (3). The latter as a pure location based information is in principle inappropriate if channel effects like reflections and shadowing are included in the signal propagation. The SpotMAC protocol [Chi07] is listed in [BJ11] as a protocol that achieves the information about the DoA from neighboring transmissions appropriately; but the approach does not explain how a node, willing to transmit, obtains the information about the spatial signature to the communication partner. This is required, since already the announcement of the transmission is beamformed to the partner. Thus, it also fails to overcome **CH5**.

From the remaining schemes, only 8 schemes apply adaptive beamforming. All other schemes rely on switched beam antennas and are thus out of scope of this work. Since we focus on schemes that combine beamforming with spatial nulling, only the references [FDA09, BHHT01, MRV07] are further considered. We shortly summarize them in the following.

In the BMAC protocol [FDA09], each node periodically transmits a training sequence that allows neighbors to estimate the channel to this node. The neighbors include the channel and this node's identifier into a table. In case of a transmission, the beamforming weights are calculated based on the table entries. The update period is chosen to be a function of the coherence time of the channel.

Similar to the argumentation in multiuser detection based cross-layer design (cf. Sec. 3.2.1), we argue that estimating the channel to all neighbors periodically in a proactive manner introduces a non negligible overhead that is only partly required; in high node density scenarios, the majority of channel estimations is expected to stay unused. The authors address this issue and state that due to the periodic update they assume low mobility scenarios as most suitable.

Similar to the BMAC protocol, the authors of [BHHT01] assume that nodes keep track of spatial directions to other nodes by *Angle-SINR* tables. Each node periodically performs a directional broadcast, sequentially in all directions. Neighboring nodes measure the SINR for each direction. After the directional broadcast is finished, they return the measured values to the broadcasting node. The node includes these values into its Angle-SINR table. By evaluating the information of the table, the best communication direction to each neighbor is decided. The approach is expected to face the same shortcomings as the BMAC protocol.

Instead of updating the spatial information in the whole neighborhood periodically, the NULLHOC protocol [MRV07] includes a channel estimation phase into the control message exchange that precedes a data transmission. Thus, the channel is only estimated to those nodes that at the estimation time take actively part in a transmission. This reduces the overhead and ensures the information to stay updated.

The NULLHOC protocol is applicable in fading environments, but it fails to overcome the challenges **CH1**, **CH3**, **CH4**, and **CH6**. Still, since the most difficult challenge to be overcome is **CH5**, it is a very promising approach. We further extend its ideas by our newly proposed cross-layer design. More precisely, our protocol design is based on two existing protocols, namely the NULLHOC protocol, and the BeamMAC protocol [VBH06]. The latter solves the challenges **CH1**, **CH3**, **CH4**, and **CH6**, but fails to overcome **CH2** and, as a major drawback, **CH5**.

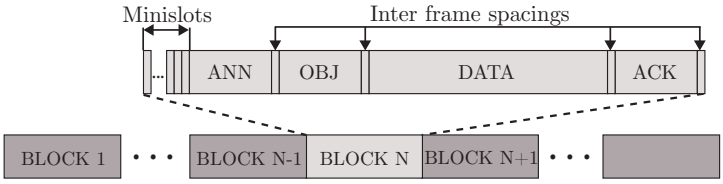

Figure 6.3.: One block of the BeamMAC protocol.

By exploiting the advantages of both protocols but avoiding their disadvantages, the newly developed Channel Information Exchange (CIE)-MAC protocol solves the described hidden terminal problems, takes all specific challenges into consideration that arise for heterogeneously equipped nodes, and is applicable in fading environments.
We summarize the BeamMAC and the NULLHOC protocol in the following.

6.2. The BeamMAC Protocol

Originally, the BeamMAC protocol [VBH06] was developed as a MAC-layer-asynchronous protocol (cf. Sec. 2.3.1). Later the authors adapted BeamMAC to the time slotted frame structure that they developed for MUD-MAC.

6.2.1. Functional Description

This frame structure is depicted in Fig. 6.3. The different slots of the frame structure serve for the same purposes as described for the MUD-MAC protocol in Sec. 3.2.2. Also, a data packet to be transmitted is split into up to N_B blocks and transmitted over the course of N_B consecutive frames (blockwise parallel transmission, cf. Sec. 3.2.2).
In contrast to MUD-MAC, in the BeamMAC protocol control messages as well as data packets are transmitted directionally. The beam pattern deployed at a node points the main lobe to the associated partner, but does not include additional multiuser technologies like spatial nulling. Receivers that already apply individual beam patterns for data transmission stay with this beam patterns also during subsequent control message exchanges, until they finished the reception of all N_B blocks. Idle nodes receive omnidirectionally.
Since, as a prerequisite of the BeamMAC protocol, a potential transmitter already knows the direction to its associated receiver, it applies the same beam pattern for transmission of the ANN message as it plans to use during data transmission. Thus, neighboring receivers can estimate the amount of additional interference by analyzing the beamformed signal and thus decide on the necessity of objecting to the planned transmission.

6.2.2. Advantages and Drawbacks

Allowing the receivers instead of potential transmitters to determine the amount of actual interference resulting from a new transmission is a major advantage of the BeamMAC

protocol. Difficult and imprecise estimations on the transmitter side are thus dispensable. Corresponding, heterogeneously equipped receivers are able to control the interference to not exceed their individual tolerance level.
Moreover, receivers are allowed to object to an announced transmission in case it would harm their ongoing reception. This receiver objection capability is a very important feature since it accounts for all kind of control message failures and thus is a possibility to overcome **CH6**. Also, a negative influence of the hidden terminal problem due to beamforming (**CH3**) is prevented. Its impact is resolved, since nodes that miss control messages do not harm the corresponding transmissions later on. In case a transmitter that is unaware of an ongoing transmission announces a new, harmful transmission, the affected receiver objects, thus avoiding packet losses.
Since all messages are transmitted in a directional manner with all antennas, the hidden terminal problem due to asymmetry in gain (**CH4**) does not occur. Further, the full coverage extension is exhausted, thus avoiding any underutilization (**CH1**). But this is only possible since a potential transmitter holds the a priori knowledge of the beam pattern required to serve its partner. Obtaining this kind of information seems suitable for static channels. But, it makes the protocol unapplicable in fading environments (**CH5**).
Deafness (**CH2**) is an issue with the BeamMAC protocol, since nodes involved in ongoing data transmissions stay beamformed also during intermediate control message slots. Thus, they are likely to fail to decode these control messages.

6.3. The NULLHOC Protocol

In the following, we shortly summarize the NULLHOC protocol [MRV07].

6.3.1. Functional Description

The NULLHOC protocol is a MAC-layer-asynchronous protocol design. It combines adaptive beamforming as described in Sec. 5.1.1 with spatial nulling as a multiuser technology.
Its basic idea is that all nodes that plan to take part in a new transmission must handle interference to or from already ongoing transmissions, i. e.,

- potential transmitters form their individual beam pattern so that, besides serving their associated partner, they put spatial nulls into the direction of all active receivers in their vicinity.

- Potential receivers form their beam pattern to, on the one hand, exploit as much energy from their associated partner as possible, and, on the other hand, to suppress all interference by spatially nulling all active transmitters.

Spatial nulling at the transmitter avoids that a new transmission strongly interferes already existing transmissions between other nodes; spatial nulling at the receiver assures that the receiver of a new transmission can receive interference free.

Note that nodes are only allowed to take part in a new transmission if they have enough *degrees of freedom* to null their active neighbors. The degree of freedom of a node equals its individual number of antennas. Since one degree of freedom is required for the wanted (own) data transmission or reception, a node needs at least one antenna more than the overall number of neighbors to be nulled to take part in a new transmission.
As stated in Sec. 5.1.1, for beamforming based signal processing, the precoding matrix $\boldsymbol{M}$ reduces to a precoding vector $\boldsymbol{m}$, and the receiving matrix $\boldsymbol{D}$ accordingly reduces to a receiving vector $\boldsymbol{d}$. Instead of differentiating between receiving vector and precoding vector in the following, we summarize both as a *weight*. We explain the computation of this weight for beamforming combined with spatial nulling, regardless of the node being a transmitter or a receiver. In Sec. 5.1 we defined the channel matrix $\boldsymbol{H}$ so that the rows always correspond to the receive antennas and the columns always correspond to the transmit antennas. We now, in contrast to this, introduce a channel between two nodes i and node k as $\boldsymbol{H}_{i,k}$, i. e., the rows of $\boldsymbol{H}_{i,k}$ correspond to the antennas of node i while the columns correspond to the antennas of node k, regardless of node i and node k being a transmitter or a receiver.
The calculation described in the following is based on a certain information about channels and weights. How the information required during the calculation is obtained by an appropriate MAC protocol design is subsequently explained.
Assuming $\mathcal{K}_\mathcal{N}$ is the set of K_N neighbors that a node k has to spatially null by its beam pattern. Then, the calculation of a weight $\boldsymbol{w}_k$ for this node k proceeds as follows:

1. Compute the effective channel vector $\boldsymbol{h}_{k,i}$ for each node i from the set of nodes $\mathcal{K}_\mathcal{N}$ to node k. The effective channel vector is the product of the weight node i uses, $\boldsymbol{w}_i$, and the channel between this node i and node k, $\boldsymbol{H}_{i,k}$,

$$\boldsymbol{h}_{k,i}^T = \boldsymbol{w}_i^T \boldsymbol{H}_{i,k}.$$

2. Calculate the effective channel $\boldsymbol{h}_{k,d}$ to the desired partner d that plans to apply weight $\boldsymbol{w}_d$ during the transmission

$$\boldsymbol{h}_{k,d}^T = \boldsymbol{w}_d^T \boldsymbol{H}_{d,k}. \tag{6.1}$$

3. All effective channels (effective channel of own partner d and effective channels of all K_N nodes to be nulled) are stacked to build an effective channel matrix $\boldsymbol{H}_{\mathrm{eff}_k}$

$$\boldsymbol{H}_{\mathrm{eff}_k} = [\boldsymbol{h}_{k,d} \;\; \boldsymbol{h}_{k,1} \;\; ... \;\; \boldsymbol{h}_{k,i} \;\; ... \, \boldsymbol{h}_{k,K_\mathrm{N}}].$$

4. The desired weight $\boldsymbol{w}_k$ is the minimum norm solution to the equation

$$\begin{aligned} \boldsymbol{H}_{\mathrm{eff}_k}^T \boldsymbol{w}_k &= \boldsymbol{c}, \text{ with } \boldsymbol{c} = [1 \;\; 0 \;\; ... \;\; 0]^T. \\ \boldsymbol{w}_k &= \left(\boldsymbol{H}_{\mathrm{eff}_k}^T\right)^+ \boldsymbol{c}, \end{aligned} \tag{6.2}$$

where $\boldsymbol{A}^+$ denotes the Moore-Penrose pseudoinverse of a matrix $\boldsymbol{A}$. Transmit weights are subsequently normalized to unit norm.

The calculation of the weight requires knowledge of the weights deployed by the partner as well as all nodes that have to be spatially nulled. Moreover, also the channels to these nodes have to be known. The information is obtained by the NULLHOC protocol by an appropriate MAC protocol design. The control message exchange comprises – similar to 802.11 – RTS and CTS messages. Additionally, in NULLHOC a third control message, namely a Data Send (DS) message, is exchanged. A successful transmission is acknowledged by the receiver with the help of an ACK message.
Data as well as acknowledgement messages are transmitted directionally. RTS, CTS, and DS are transmitted omnidirectionally. Before the control message *information* is transmitted, there is a phase for channel estimation included into each of these messages. Here, the nodes transmit successively with each antenna, but for the actual control *information* exchange they only transmit with one antenna.
By the channel estimation phase it is possible for all nodes that overhear the control messages to estimate the channel to the message originator. The control *information* contains mainly the transmission weights that will be applied by the message originator during the upcoming transmission.
More precisely, the RTS contains the weight, the potential transmitter will deploy for the reception of the ACK message. The CTS is sent by the potential receiver to inform its neighbors of the weight it will apply during data reception. Corresponding, the potential transmitter lets the vicinity know with the DS message, which weight it will apply during the data transmission.
By overhearing control messages of neighboring transmissions, nodes are aware of the channel to the signaling node as well as the weights applied during these transmissions. Thus, they know the effective channels to all nodes in the set of nodes to be nulled $\mathcal{K}_{\mathcal{N}}$.
From the RTS message, a potential receiver can estimate the channel to its partner. Still, the weight $\boldsymbol{w}_d^T$ to calculate the effective channel to its partner (cf. Eqn. 6.1) is not known yet by the potential receiver. Thus, it assumes the weight to be omnidirectional, i. e., simply a vector of ones, normalized to unit power.
Using the resulting estimate of the effective channel to its partner together with the knowledge of the effective channels to all active transmitters, the potential receiver determines its weight according to Eqn. 6.2. It includes this weight into the CTS message.
Based on this weight and the channel information estimated from the CTS message, the transmitter calculates the effective channel to its partner. Including also information on the effective channels to active receivers in its vicinity, it determines its actual weight that it will apply during the data transmission according to Eqn. 6.2. It informs its partner as well as neighbors of this weight by means of the DS message.

6.3.2. Advantages and Drawbacks

The major advantage of the NULLHOC protocol is its applicability in fading environments (**CH5**). By the described control message exchange, information on channels and weights is provided on a short and thus up-to-date temporal basis. This information is exploited by spatial nulling to increase the spatial reuse.

Table 6.1.: Drawbacks of the BeamMAC and the NULLHOC protocol.

Drawback	BeamMAC	NULLHOC
CH1: underutilization		X
CH2: deafness	X	
CH3: hidden terminal problem due to beamforming		X
CH4: hidden terminal problem due to asymmetry in gain		X
CH5: static channel assumption	X	
CH6: vulnerability against control message failures		X

In accordance with the IEEE 802.11 protocol, the NULLHOC protocol is designed as a MAC-layer-asynchronous protocol. Thus, control packets can collide with ongoing data transmissions. But since the control messages are transmitted omnidirectionally, deafness (**CH2**) as explained by Fig. 6.1 is not expected to happen. By omnidirectional control messages, TX_2 in Fig. 6.1 already got informed of the transmission between TX_1 and RX_1, and would thus not start to signal to RX_1.
Degradations by the hidden terminal problem due to beamforming (**CH3**) could be expected, since the nodes are beamformed during data transmissions and thus blind against control messages from other directions. Also, the hidden terminal problem due to asymmetry in gain as explained in Fig. 6.2 has to be taken into account, since control messages and data transmission differ in their antenna gains (**CH4**).
Both problems might degrade the performance significantly, as they lead to nodes being not aware of some neighbors to be nulled. Since additionally the authors assume no possibility for a receiver to object to an announced transmission, the unawareness of these nodes, e. g., by control message losses, will lead to corruptions of already ongoing transmissions. Also channel estimation errors that lead to an increased interference at receivers of ongoing transmissions cannot be overcome (**CH6**). The coverage is restricted to the omnidirectional range, because control messages are transmitted omnidirectionally, resulting in underutilization (**CH1**).
In Tab. 6.1 the drawbacks for the BeamMAC protocol as well as for the NULLHOC protocol are summarized.

6.4. The CIE-MAC Protocol

In this section, we present the CIE-MAC protocol that is a combination of the NULLHOC and the BeamMAC protocol. The goal of the CIE-MAC protocol is to exploit the advantageous strategies of the previously summarized protocols while avoiding as many of their disadvantages as possible.
In the end, the only disadvantage remaining for CIE-MAC is the underutilization (**CH1**), which is due to the design decision to transmit and receive control messages omnidirectionally. This is, however, required if the protocol should be applicable in fading environments.
As in the NULLHOC protocol, the CIE-MAC protocol combines beamforming and spatial nulling. Also, the strategy that all nodes that plan to take part in a new transmission have

to handle interference to or from already ongoing transmissions is adopted by CIE-MAC. Further, the CIE-MAC protocol incorporates a receiver objection capability as in the BeamMAC protocol. We develop the CIE-MAC protocol as a time-slot-synchronous protocol.

6.4.1. Frame Structure

The newly developed frame structure of the CIE-MAC protocol is shown in Fig. 6.4. The control message part consists of minislots, an ANN message, an Allowance (ALL) message, a DS message, and, after the data transmission, an ACK message. Control messages are transmitted with BPSK modulation.

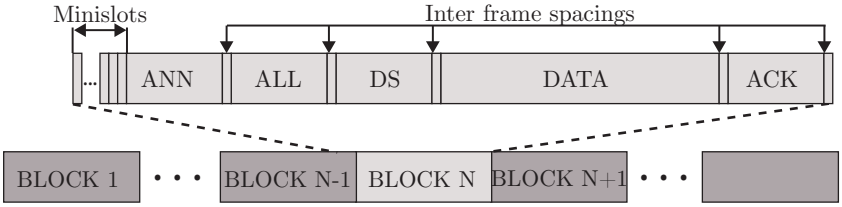

Figure 6.4.: One block of the new CIE-MAC protocol.

Similar to BeamMAC and MUD-MAC, the data packet to be transmitted is split into up to N_B blocks, allowing for up to N_B blockwise parallel transmissions. The duration of N_B blocks is significantly smaller than the block duration of the block fading channel model described in Sec. 5.2. Thus, the channel is constant for the whole transmission of a data packet. Data is transmitted in the CIE-MAC protocol with QPSK modulation.
All control messages are transmitted omnidirectionally, i. e., in contrast to NULLHOC, also the ACK message is transmitted in a non-directive manner. This is possible, since the transmissions start one after the other and each last for the same duration of N_B blocks. In this way, the probability of ACK collisions is quite low, even for omnidirectional transmissions.

6.4.2. Protocol Description

As in the NULLHOC protocol, the ANN, ALL, and DS messages are split into a channel estimation phase where the channel to all antennas is estimated, and the actual control information exchange operated with a single antenna. The procedure to start a transmission in the CIE-MAC protocol can be summarized as follows:

1. A potential transmitter that has enough degrees of freedom chooses one minislot randomly. If it senses a signal in one of the preceding slots, it backs off.

2. In case of success, it transmits an ANN message. The ANN message contains a preliminary weight. This weight is, in contrast to the weight included in the RTS message of NULLHOC, not for the reception of an ACK message. It is included instead to allow the associated receiver to adapt its weight for the data transmission better.

Also other active receivers in the vicinity can check if they experience high interference by the new transmission.

The preliminary weight is calculated by the transmitter according to Eqn. 6.2. The effective channel to the receiver that is not known yet by the potential transmitter is set to be a vector of ones, normalized to unit power. Thus, the preliminary weight does not include any orientation that improves the channel to the partner. But it already includes the spatial nulls to active receivers, making interference estimations possible. this is required, since due to channel estimation errors or control message failures, a potential transmitter might fail to null receivers in its vicinity perfectly.

3. Active receivers estimate the actual interference expectable by the new transmission. If the interference exceeds the amount they can tolerate, they transmit an ALL containing an error ID, referred to as *receiver objection* in the following.

   The addressed receiver transmits an ALL in case it is ready for a new reception, i. e., it is not busy and has enough degrees of freedom. The ALL contains the transmitter's ID as well as the final weight the receiver employs during the data reception. The weight is calculated according to Eqn. 6.2. The effective channel to the partner is calculated by Eqn. 6.1, with the channel estimated from the partner's ANN and the weight set to the preliminary weight contained in the ANN message.

   If the intended receiver is not ready for a new reception, it transmits an ALL containing an error ID.

   In case of an additional receiver objection by a receiver other than the intended receiver, both ALL messages collide with a high probability. If the potential transmitter senses, but not decodes an ALL message, or it decodes an ALL message containing an error ID, it backs off. The same holds if no receiver sends an ALL message.

   If only the addressed receiver transmits an ALL as a positive reply, the transmitter can decode the message, and goes on transmitting the DS message.

4. The transmitter adapts the preliminary weight based on the knowledge of the effective channel to the associated partner that is obtained by the ALL message. It includes its final weight into the DS message. The DS message informs neighbors of the updated weight. Further, they are informed that the transmission indeed takes place.

The transmitter reaction during the ALL slot and the reactions of receivers during the ANN slot are shown for further clarification as flowcharts in Fig. 6.5.
After the control message part, the data transmission starts with the predefined weights and lasts N_{B} consecutive blocks. If all blocks are received error free, the receiver acknowledges the transmission by sending an ACK message.

6.4.3. Advantages

The CIE-MAC protocol is fully applicable in fading environments, since it does not assume any a priori knowledge of channels, DoDs or DoAs (**CH5**). As in the NULLHOC protocol

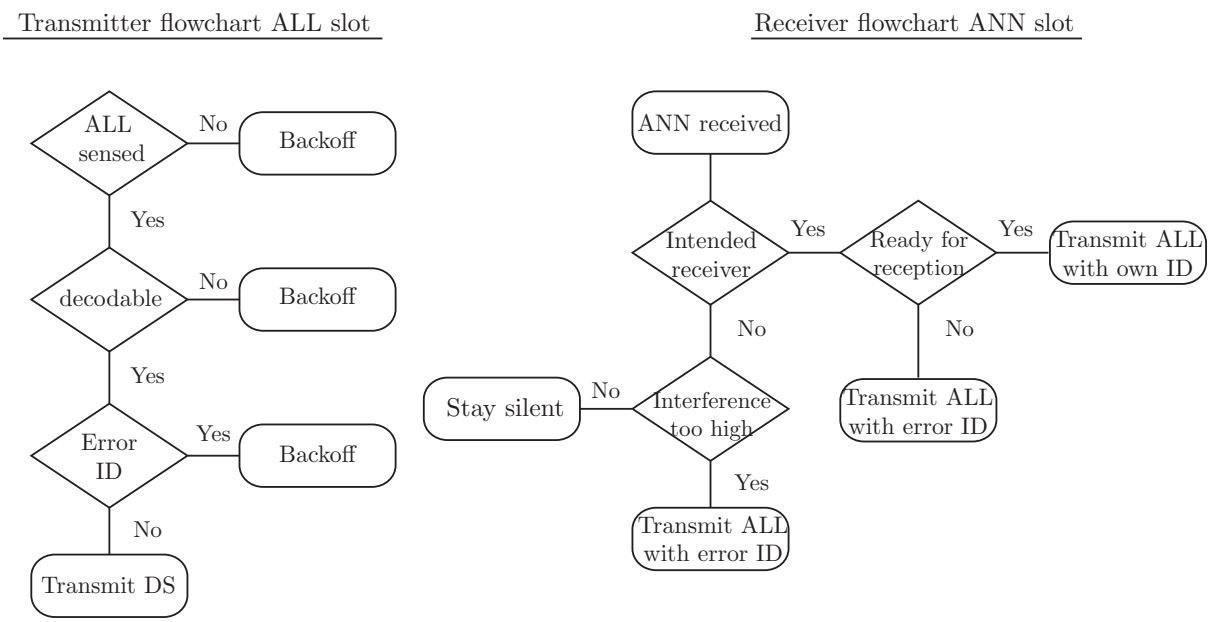

Figure 6.5.: Flowcharts of transmitter reaction during ALL and receiver reaction during ANN.

information on channels and weights is provided in time. It further does not suffer from the deafness problem (**CH2**) since it transmits all control messages omnidirectionally (see also Sec. 6.3.2 for explanation).
By the time slotted structure and by nodes receiving omnidirectionally during the control slots, the hidden terminal problem due to beamforming is solved (**CH3**). The receiver's objection capability prevents negative impact on the system performance by the hidden terminal problem due to asymmetry in gain (**CH4**). Further, the occurrence of this problem is reduced. This is, because the control message is transmitted with a lower order modulation scheme, i. e., an increased transmission range, compared to the data transmission. Thus, differences in gain between the omnidirectional control message transmission and the beamformed data transmission are diminished. That this is indeed required is shown by Fig. 6.6.
Fig. 6.6 shows the cdf of the gain in SNR achieved for a beamformed data transmission with four antennas compared to an omnidirectional control message transmission with one antenna. The simulations are performed for the CIE-MAC protocol if one, two, or three interferers are in static communication range of both, transmitter as well as receiver. For each curve, 10000 realizations of different transmitter positions, receiver positions, interferer positions, and channels are simulated.
As can be seen, if except one antenna, all other antennas are applied to null interferers in the vicinity (three interferers, solid line), on the average there is no gain. The median of the curve lies at 0 dB. The gain improves if the number of interferers in the communication range decreases and the additional degrees of freedom can be used to serve the communication

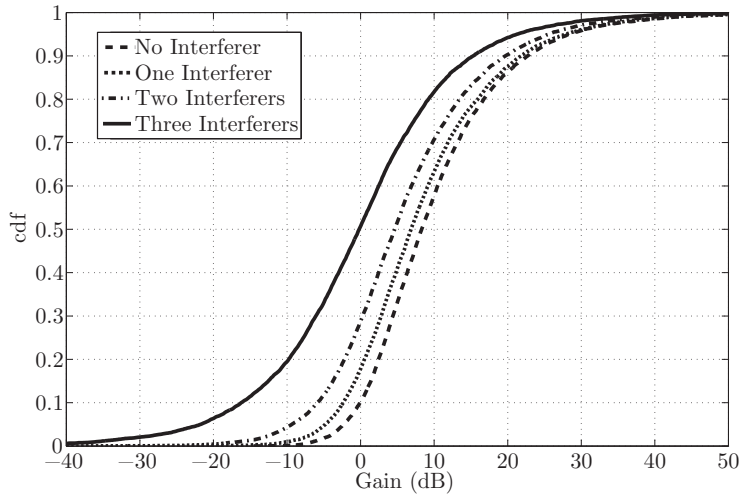

Figure 6.6.: Gains of directional transmission with four antennas compared to omnidirectional transmission with a single antenna in the presence of one, two, or three interferers.

partner. Obviously, the gain to be expected during the data transmission is a function of the number of nodes to be nulled as well as the correlation between interferers' channels and the channel to the partner. Thus, it can hardly be predicted.
The curves underline the necessity of a receiver objection capability. Even if the control signal range is improved by a lower order modulation scheme, this can only reduce, but not completely balance the differences compared with the beamformed data transmission range. Without a receiver objection capability, the losses from the hidden terminal problem due to asymmetry in gain are likely to get severe.
The receiver objection capability also allows active receivers in the CIE-MAC protocol to protect their receptions against control message failures like channel estimation errors (**CH6**).

6.5. Simulation Results

After a detailed functional description of the CIE-MAC protocol we now present simulation results. The CIE-MAC protocol is simulated with the channel model described in Sec. 5.2. The scenario under investigation is the 50 m × 50 m scenario with 50 nodes randomly and uniformly distributed, as described in Sec. 3.3.3. Since this scenario is very dense, resulting in very high contention for high offered traffic loads, we assume that a node willing to transmit only starts to contend with a probability of 25 %. Note that we do not further adapt this percentage to varying traffic loads, since this would require additional system information at each node.
The influence of heterogeneously equipped nodes is investigated by differently equipping subgroups of the 50 nodes with 1, 2, 3, or 4 antennas. We simulate varying sizes of these subgroups called Heterogeneous Node Constellation (HNC)s. These are listed in Tab. 6.2.

Table 6.2.: Simulated heterogeneous node constellations (HNC)s.

number of antennas	1	2	3	4	$\sum$
HNC-1	0	0	0	50	50
HNC-2	12	13	12	13	50

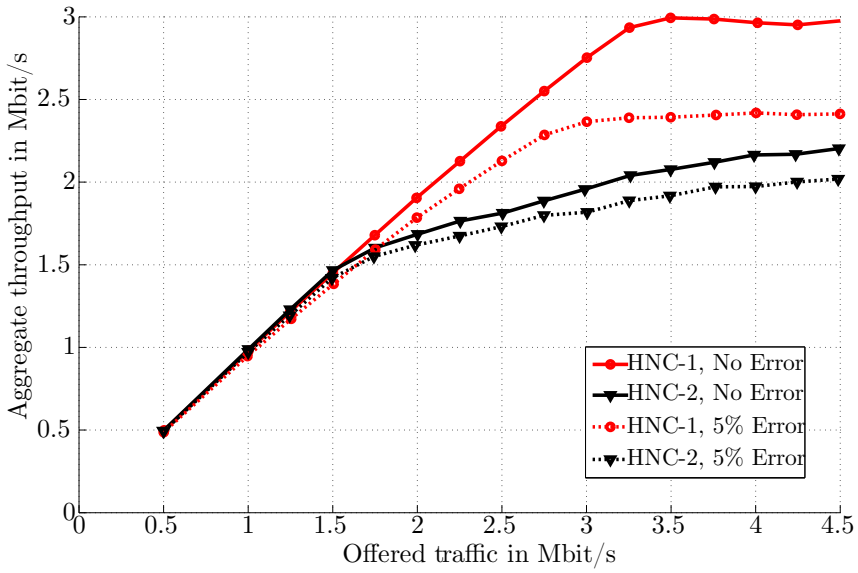

Figure 6.7.: Aggregate throughput versus offered traffic in the 50 m × 50 m scenario for different HNCs without channel estimation error and with 5 % error.

All other system parameters are set as in Tab. 3.2.
We further want to investigate the influence of channel estimation errors on the control message exchange and the system performance. Thus, we model a Gaussian distributed channel estimation error with a power of 5 % of the channel power that is added to the perfect channel estimate.
The aggregate throughput versus the offered traffic with and without channel estimation error is depicted for the two HNCs in Fig. 6.7. Without channel estimation errors, HNC-1 improves the aggregate system throughput significantly compared with HNC-2. For 5 % channel estimation error HNC-1 still outperforms HNC-2. But the additional achievements are reduced compared with the case of no estimation error.
To further investigate the behavior of the curves we look more detailed into the statistics of the control message exchange. More precisely, we investigate the following two points:

- Improvements of HNC-1 compared with HNC-2: how do they show during the control message exchange?

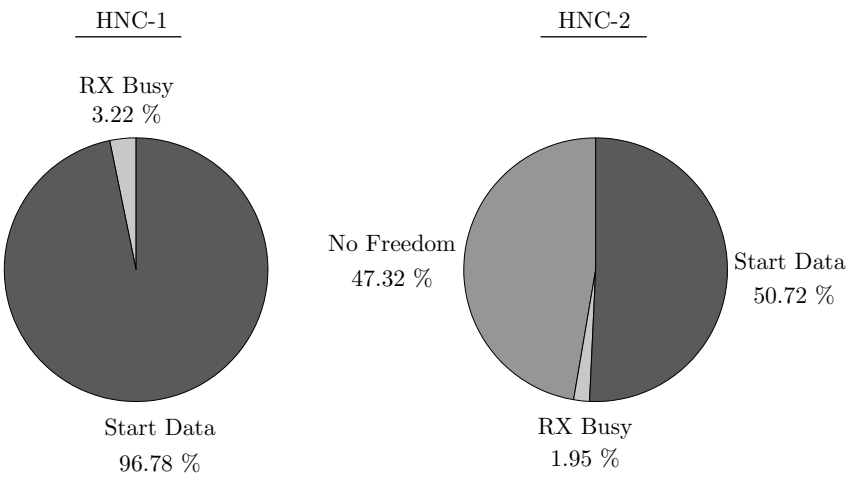

Figure 6.8.: Percentages of ALL messages that are sent to accept a data transmission (Start Data), to object since the receiver is busy (RX Busy), and to object since the receiver has not enough degrees of freedom (No Freedom) for HNC-1 and HNC-2.

- Influence of channel estimation errors: Why are the improvements shrinking in case of channel estimation errors?

6.5.1. Improvements of HNC-1 Compared With HNC-2

To investigate the improvements of HNC-1 compared with HNC-2, we investigate the statistics of the ALL messages sent by the announced receiver as a reaction to a correctly received ANN message for an offered traffic of up to 3 Mbit/s.
We evaluate the percentages of ALL messages that are sent as a positive reply to start a data transmission (*Start Data*), ALL messages that are sent to drop the transmission since the receiver has not enough degrees of freedom to null neighbors and accept the new transmission (*No Freedom*), and ALL messages that are sent to drop the transmission since the receiver is already busy with receiving another transmission (*RX Busy*).
The resulting percentages are depicted in Fig. 6.8. For HNC-1, almost all correctly received ANN messages result in a positive reply by the receiver. The remaining messages are dropped, because the receiver is already busy with receiving another message. It never happens that a receiver has not enough degrees of freedom to accept a new transmission.
This changes if some nodes are weakly equipped, as it is the case for HNC-2. Here, nearly half of the ANN messages result in dropped transmissions since the receiver has not enough degrees of freedom to spatially null neighbors in its vicinity and start a new reception.
Still, by the appropriate MAC protocol design, a dropping of ANN transmission requests at the receiver does not lead to packet corruptions. The transmitter requires a positive reply of its associated partner to start with the actual data transmission. If it receives a negative reply by its partner, or even no reply, it stops its transmission attempt and backs off. This

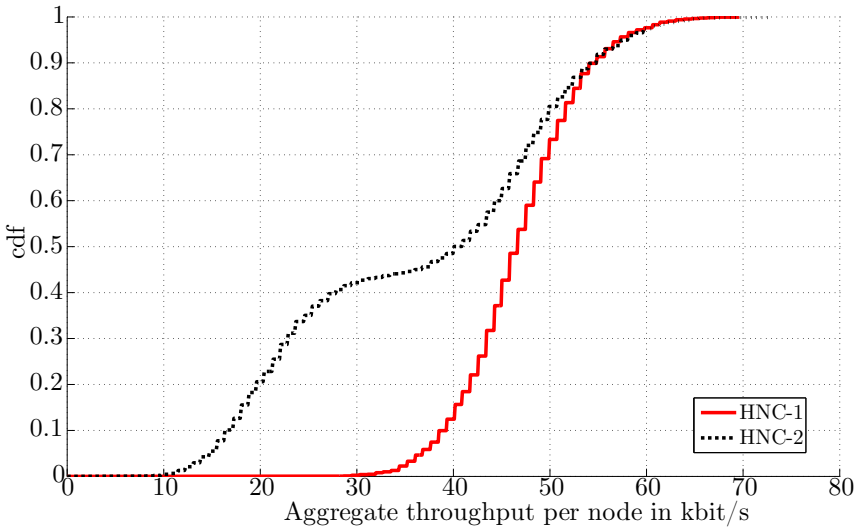

Figure 6.9.: Cumulative distribution function of aggregate throughput per node for an offered traffic of 2.5 Mbit/s for HNC-1 and HNC-2.

shows that tracking the actual amount of interference on the receiver side instead of on the transmitter side allows for accurate reactions, especially in case of heterogeneously equipped nodes.
The principle strategy extended from NULLHOC that all nodes require to null active neighbors in their vicinity comes at the cost of a strongly reduced fairness for heterogeneously equipped nodes, as shown by Fig. 6.9. The figure shows the cdf of the aggregate throughput per node that we already applied as fairness indicator in Sec. 4.2 for an offered traffic of 2.5 Mbit/s. For HNC-1 the cdf has a steady trend. For HNC-2 there is a break and shift to the right at a percentage of about 42 % of the nodes. These nodes achieve significantly less throughput than the other nodes in the network, since they have not enough degrees of freedom to null neighbors in their vicinity.

6.5.2. Influence of Channel Estimation Errors

To motivate the necessity of receiver objections to overcome **CH6**, we further look into the statistics for the control message exchange in case channel estimation errors occur. From Fig. 6.7 it can be observed that these errors influence the HNCs differently. In case of channel estimation errors, HNC-1 still outperforms HNC-2 in terms of aggregate throughput; but the difference between the two HNCs shrinks compared with the case without estimation errors. This happens, since the interference resulting from estimation errors from different simultaneously transmitting nodes sum up at a receiver. Thus, if more parallel transmissions exist, the interference is increased.
This can also be observed by looking into the percentages of DS messages resulting from ALL messages that are sent **as a positive reply by the associated parter** to start a data

Table 6.3.: Percentages of DS messages resulting from ALL messages that are sent as positive reply by the associated partner in the case of no estimation error, 5 % estimation error, and 10 % estimation error.

	Channel estimation		
	No Error	5% Error	10% Error
	in %	in %	in %
HNC-1	93.56	83.89	81.24
HNC-2	98.16	96.58	95.79

transmission. If no other receivers objected simultaneously, almost all positive ALL messages would result in a DS message. In case other receivers frequently object, the percentage of DS messages resulting from positive ALL messages is reduced. This percentage is shown for no estimation error, 5 % estimation error, and 10 % estimation error (not shown in Fig. 6.7) in Tab. 6.3.
If the channel is estimated perfectly, for both HNCs more than 90 % of the ALL messages that are started for data transmissions result in a DS message. But, for HNC-1 already more than 5 % of the ALL messages that are started as positive reply are blocked by colliding receiver objections.
The necessity of receiver objections becomes obvious for channel estimation errors. Already for 5 % channel estimation error, the percentages of DS messages is further reduced for both HNCs. While for HNC-2, even in case of 10 % estimation error, still more than 95 % of the ALL messages are successful, for HNC-1 about 20 % of the transmissions are blocked in order to protect ongoing receptions.
Channel estimation errors are likely, since the estimation process itself is prone to errors. Further, the weights included into the control messages are digitized with a finite number of bits, resulting in an additional quantization error. Moreover, even if the channel estimation is performed perfectly, and estimation and data transmission are within the coherence time, the real channel might undergo slight changes.

6.6. Summary and Further Work

Beamforming, optionally combined with multiuser signal processing for interference suppression, is an interesting physical layer strategy for cross-layer designs in wireless ad hoc networks. In this chapter, we presented a new PHY-MAC cross-layer design that supports beamforming combined with spatial nulling. As a first contribution, we complemented known challenges arising for directive transmission by an additional challenge that arises if time-varying environments are considered, and a challenge that corresponds to control message failures.
The second contribution was the design of the CIE-MAC protocol. It combines two existing protocol designs, namely the BeamMAC protocol, and the NULLHOC protocol, that both suffer from certain disadvantages. By appropriately combining major ideas of BeamMAC

and NULLHOC, most of the disadvantages known from directive transmission are overcome. The new CIE-MAC protocol design is applicable in time-varying environments and has a mechanism to reduce the negative impact of control message failures like channel estimation errors.
As another contribution all simulations were performed with a sufficiently detailed channel model. The model takes fading influences, temporal, and spatial correlation into account. The system performance was investigated in terms of aggregate throughput with perfect channel estimates and under the assumption that the channel estimates experienced a certain estimation error. The antenna configuration of the nodes was varied in order to see the influence of heterogeneously equipped nodes on the system performance.
To get further insight into the protocol behavior, the statistics of certain control messages were recorded during runtime and evaluated afterwards. Thus, also the necessity of a receiver objection capability could be shown. This receiver objection capability turned out to be essential if multiple parallel transmissions take place and channel estimation errors lead to increasing interference in the system. Even for perfect channel estimates it, however, overcomes packet losses related to the hidden terminal problem due to beamforming.
Further investigations are needed to assure that receiver objections lead reliably to a blocking of the interfering transmission. Since at the potential transmitter the packet of an objecting receiver collides with the packet of an intended receiver only with a certain probability such that the packets cannot be decoded, packet losses due to control message failures are still possible.
Another point to be investigated in future work is how nodes in the network might capitalize from other nodes' degrees of freedom in case they cannot participate in new transmissions since they have not enough degrees of freedom on their own. An advanced strategy might, e. g., shift the responsibility from a potential receiver with no degrees of freedom to an already active transmitter that has still some degrees of freedom left. This can help to alleviate the main drawback of CIE-MAC, namely the reduced fairness, if nodes are heterogeneously equipped. Alternatively, the OACR algorithm can be adapted to balance spatial reuse and fairness.

7. Spatial Multiplexing Based Cross-Layer Design

In Chapter 6, we presented the CIE-MAC protocol that applies MIMO beamforming combined with spatial nulling. It requires channel state information at the transmitter and the receiver. This introduces additional control overhead.
If the multiple antennas are exploited to apply spatial multiplexing combined with appropriate receiver technologies like V-BLAST[1] [WFGA98], channel state information is only required on the receiver side (cf. Sec 5.1.2). Channel information at the receivers is commonly assumed and can be learned more accurately than at the transmitters. This makes the technique a very promising candidate for its application in wireless ad hoc networks. Challenges related to the directional transmission of control and data packets, like e. g., deafness or an increased hidden terminal problem, do not occur for spatial multiplexing. But compared to the huge variety of beamforming based cross-layer designs in wireless ad hoc networks, a significantly smaller number of schemes proposes spatial multiplexing as the physical layer strategy.
The capabilities of a receiver like the V-BLAST receiver can be exploited to handle multiple streams from different transmitters simultaneously. The receiver then functions as a multiuser detector to overcome Multiple Access Interference (MAI) in ad hoc networks. In this chapter, we focus on cross-layer designs that apply spatial multiplexing at the transmitters combined with MUD at the receivers as the physical layer strategy. For simplification, we refer to this combination solely as *spatial multiplexing* in the following, although generally spatial multiplexing would also contain schemes that require channel state information at the transmitters. These are, however, out of scope of this work.

7.1. Spatial Multiplexing in Ad Hoc Networks

7.1.1. Transmissions with Multiple Streams

The multiple degrees of freedom offered by the multiple antennas at the transmitters and receivers can be exploited manifoldly. This is explained by Fig. 7.1. There, two transmitters and two receivers are shown that are equipped with two antennas respectively. Assuming that each transmitter has packets for both receivers in its queue, different strategies to distribute the degrees of freedom at the different nodes exist.
In example A and example B, one of the two transmitters transmits with all of its available streams to one of the receivers. Thus, the other transmitter abstains completely from transmitting, since no receiver has degrees of freedom remaining to receive additional streams. Either, a receiver already exploited its degrees of freedom to receive *wanted* streams, i. e.,

[1] Also other interference cancelation receiver technologies would be possible. The V-BLAST receiver is considered as an example for BLAST receivers. They offer a reduced complexity compared with the Maximum Likelihood receiver and an improved performance compared with linear receivers.

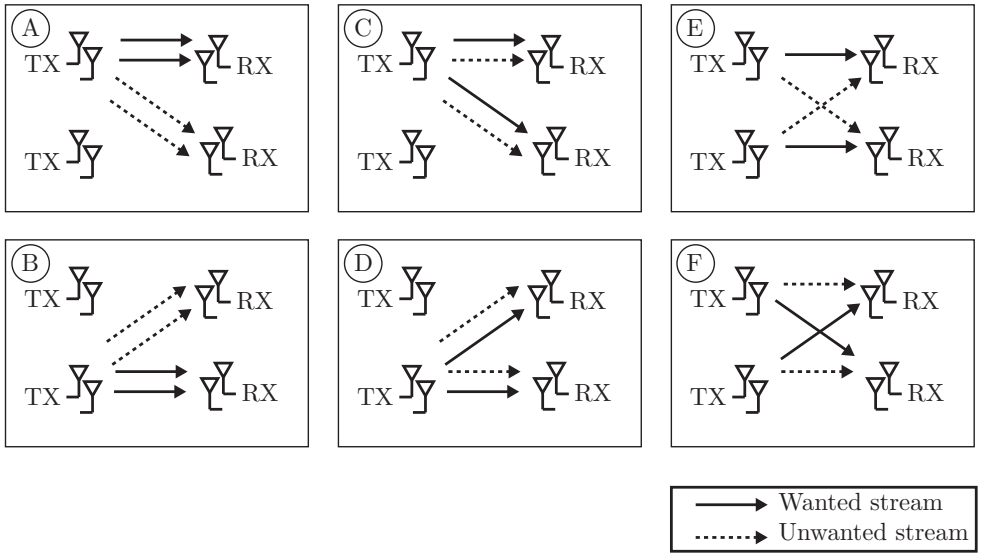

Figure 7.1.: Different possibilities to exploit the degrees of freedom at the senders and the receivers.

streams where it is the addressee; or the receiver would require its degrees of freedom to cancel *unwanted*, i. e., interfering streams, and thus could not receive any wanted streams additionally.
In example C and example D, one of the two transmitters transmits one wanted stream to both receivers. This also exploits all degrees of freedom at the receivers, since this results in one wanted and one unwanted stream at each receiver. In example E and example F, both transmitters transmit one stream to one of the receivers.
Obviously, multiple different strategies how to exploit the degrees of freedom at the transmitters and the receivers exist. Also, these strategies have to be decided fully distributed, i. e., by an appropriate MAC protocol design. In literature, several approaches exist that differ in their respective strategies and assumptions. We summarize such cross-layer designs in the following. Moreover, in the course of the summary, we elaborate requirements that we assume to be essential for a newly developed cross-layer design that applies spatial multiplexing. These requirements are emphasized by bold print of the respective clauses.

7.1.2. Related Work

We summarized methods that apply multiuser detection at the receivers in Sec. 3.2.2. Although the objective there was solely to support multiple streams at the receiver by means of MUD, we referenced several schemes that assume multiuser detection with MIMO on the physical layer [CLZ06, CLZ08, CW10]. These schemes **support multiple streams at the receivers as well as at the transmitters.**
We pointed out that the approach in [CW10] is restricted to a limited node density due to

strongly increasing overhead with increasing number of nodes. The approaches proposed in [CLZ06, CLZ08] require a separate proactive channel estimation phase that is repeated periodically. Still, the approach in [CLZ08] offers interesting insights into cross-layer designs that do not solely support multiple streams at the receiver by means of MUD, but also at the transmitter by spatial multiplexing. The proposed protocol matches the requirements of the underlying V-BLAST receiver technique well. It applies a control message exchange similar to the RTS/CTS handshake of IEEE 802.11, but in a time-slot-synchronous manner. The authors propose specific RTS and CTS *policies* to exploit the degrees of freedom at the senders and **allocate a receiver's branches to wanted and unwanted streams**. With the proposed RTS policy, a transmitter estimates the additional number of streams its partner as well as unintended neighboring receivers can tolerate as a function of its distance to these nodes. Not only is this a complex procedure, it is also expected to work inaccurately in case the receivers receive streams from other transmitters simultaneously.

Another strategy to decide how many streams a potential transmitter should send to its partner is presented in [LTZ08]. In the proposed protocol, a potential transmitter sends a *request packet* in one slot. If the associated partner is not already busy, it replies with a *grant packet* in the following slot. The partner thereby determines the number of streams to be sent by additional information contained in this grant packet. This information exchange **avoids complex estimations with respect to the interference situation at the intended receiver by a potential transmitter**. All neighboring nodes that overhear the grant packet include the receiver in an *occupancy table*. They delay own transmissions to this receiver until the other transmission ends. Thus, the granted transmission is protected against other newly starting transmissions to this receiver. Transmissions in the vicinity of the receiver to other receivers are, however, not influenced by the grant packet. Thus the approach fails to **protect ongoing transmissions against interference from newly starting transmissions** by the MAC protocol design. The authors argue that the underlying LAyered Space Time MultiUser Detector (LASTMUD) receiver [SML03] handles interference by combining a V-Blast type multiuser detector with CDMA. Moreover, they precautionary include a specific backoff. But by exploiting MAC layer capabilities additionally, it would be possible to aid the interference suppression on the physical layer significantly.

Another important drawback of the proposal in [LTZ08] is that it, in contrast to the proposal in [CLZ08], does not explicitly **support wanted streams from different transmitting nodes at a receiver**.

From the discussion of existing approaches it is obvious that dealing with the degrees of freedom at both ends of the transmission is a challenging task. It gets even more difficult if **heterogeneously equipped nodes** exist, i. e., nodes that offer a varying number of antennas or even only a single antenna. In this case, the amount of streams to be handled differs for each individual node. Strategies to exploit the multiple antennas at the receivers as well as at the transmitters then have to be accordingly adapted.

For a cross-layer design that applies spatial multiplexing as the physical layer strategy we thus identify the following six requirements (**R1**–**R6**):

- **R1**: support of multiple streams at both ends of a transmission,

- **R2**: allocation of a receiver's multiuser detection branches to multiple wanted and unwanted streams,
- **R3**: decision of the number of parallel transmitted streams at the receivers, not at the transmitters,
- **R4**: support of different simultaneously transmitting senders at a receiver and support of different simultaneously served receivers at a transmitter,
- **R5**: protection of ongoing transmissions against interference from newly starting transmissions, and
- **R6**: support of heterogeneously equipped nodes.

As the main contribution of this chapter, we propose a new cross-layer design that is developed to meet the elaborated requirements. Our proposed FDSM-MAC protocol further extends basic ideas of the MUD-MAC protocol, like the frame structure, the receiver objection capability, and the blockwise parallel transmission. The interfering streams are, in contrast to the MUD-MAC protocol, not solely detected by means of spreading signatures. Multiple simultaneous transmissions are rather separated by both, advanced signal processing that exploits the differences in the spatial signatures of the transmissions, as well as by pseudo-random code sequences. This is achieved by a LASTMUD detector [SML03] on the receiver side that we, similar to the approach in [LTZ08], suppose for the FDSM-MAC protocol.
This chapter is organized as follows. In Sec. 7.2 we present mathematical details of the underlying LASTMUD detector. Protocol aspects of the FDSM-MAC protocol are introduced in Sec. 7.3. We show a physical layer approximation to model the SINRs of the received streams in a fading environment in Sec. 7.4. Simulation results for the FDSM-MAC protocol are shown in Sec. 7.5. In Sec. 7.6 we summarize this chapter and indicate possible directions for further work.
Parts of the results presented here have earlier been published in [KH11].

7.2. The FDSM-MAC Protocol - Physical Layer Reception Strategy

In the MUD-MAC protocol, nodes apply individual spreading sequences for the transmission of their streams. The underlying multiuser detector applies Successive Interference Cancelation (SIC) to suppress interference caused by the non-optimal cross-correlation properties of the codes and the effects of imperfect synchronization. All nodes are equipped with a single antenna only.
For the FDSM-MAC protocol, the nodes employ pseudo-random spreading codes with moderate spreading code length and are equipped with a variable number of antennas. The latter allows to exploit the differences in the spatial signatures of interfering streams by means of spatial multiplexing. These differences are exploited solely on the receiver side, since for the FDSM-MAC protocol, channel state information on the transmitter side is not assumed.

As explained in Sec. 5.1.2, if spatial multiplexing is performed without CSIT, the computational complexity at the receivers is increased to obtain a similar performance than in the case of CSIT. In the following, we explain the detection process of the LASTMUD receiver [SML03] that we suppose for the FDSM-MAC protocol.
In a scenario with heterogeneously equipped nodes, each transmitting node k is equipped with an individual number of antennas M_k. Since there exists no channel state information on the transmitter side, the nodes' overall transmission power (p_{tot}) is distributed equally among all M_k transmit antennas. Node k transmits u_k data streams in parallel using u_k of its M_k transmit antennas. All symbols belonging to one data packet are sent over the same antenna, i. e., a data packet is not split over the u_k streams of node k. Before transmission, node k applies its spreading sequence $\boldsymbol{s}_k$ on all u_k streams. The length of the spreading sequences is S_{N} and the same for all nodes. Note that we do not assume that each node has an individual spreading sequence. Thus, the spreading sequences of multiple nodes can be identical.
In case K nodes are transmitting in parallel, the overall amount of active transmit antennas M_{tot} is $M_{\text{tot}} = \sum_{k=1}^{K} u_k$. The data streams of all M_{tot} antennas superimpose at the receivers. We describe the channel from all active transmit antennas to the receive antennas of a node r as $\boldsymbol{H}_r^T$, where $\boldsymbol{H}_r$ is of size $M_r \times M_{\text{tot}}$.
In order to describe the superposition of all transmit signals at each receive antenna, we denote the channel gain among all transmit antennas and the j-th receive antenna of a receiving node r as $\boldsymbol{h}_r^{(j)}$, where $\boldsymbol{h}_r^{(j)}$ is a $1 \times M_{\text{tot}}$ row-vector. Furthermore, we generate a spreading matrix $\boldsymbol{S}$ of size $S_{\text{N}} \times M_{\text{tot}}$ that consists of the spreading sequences $\boldsymbol{s}_k$ ($k \in \{1, \ldots, K\}$) applied by each active transmit antenna columnwise stacked: $\boldsymbol{S} = [\boldsymbol{s}_1, \ldots \boldsymbol{s}_1,\ \boldsymbol{s}_2, \ldots \boldsymbol{s}_2,\ \ldots\ \boldsymbol{s}_K, \ldots \boldsymbol{s}_K]$. Note that there exist multiple identical entries $\boldsymbol{s}_k$ that belong to different antennas of the same transmitting node k. The received signal $\boldsymbol{y}_r^{(j)}$ at the j-th receive antenna of receiver r is of size $S_{\text{N}} \times 1$ and can thus be expressed as

$$\boldsymbol{y}_r^{(j)} = \boldsymbol{S}\,\text{diag}(\boldsymbol{h}_r^{(j)})\,\boldsymbol{x} + \boldsymbol{n}_r^{(j)}.$$

$\boldsymbol{x}$ is a $M_{\text{tot}} \times 1$ symbol vector containing the bits transmitted by all transmit antennas, $\boldsymbol{n}_r^{(j)}$ is a zero mean, complex Gaussian noise vector of size $S_{\text{N}} \times 1$, and diag($\boldsymbol{a}$) describes the generation of a matrix that contains the entries of a vector $\boldsymbol{a}$ on the main diagonal and zeros otherwise.
In order to apply an iterative detection algorithm for receiver r, in a first step, a space-code cross-correlation matrix $\boldsymbol{R}_r$ of all streams arriving at receiver r is calculated as follows

$$\boldsymbol{R}_r = \sum_{j=1}^{M_r} \text{diag}(\boldsymbol{h}_r^{(j)})^H \boldsymbol{S}^H \boldsymbol{S}\,\text{diag}(\boldsymbol{h}_r^{(j)}).$$

Building $[\boldsymbol{R}_r]^+$, where $\boldsymbol{A}^+$ denotes the Moore-Penrose pseudoinverse of a matrix $\boldsymbol{A}$, the stream with the highest SINR that is not yet detected can be identified. This results in an ordered detection of all M_{tot} transmit antennas, where the transmit antenna index TA_s for a stream s is an integer number out of the total numbers of transmit antennas M_{tot}.

Assume that stream s is to be detected during the first iteration. It is sent by a transmit antenna with antenna index TA_s. The weight applied in order to detect this stream during iteration "1" at receiver r, $\boldsymbol{w}_r(1)$, is the TA_s-th row of $[\boldsymbol{R}_r]^+$.
The detected stream is subtracted from the received signal. After deleting the TA_s-th row and column of $\boldsymbol{R}_r$, the next stream can be detected, resulting in an iterative detection process. Further details on the LASTMUD receiver can be found in [SML03].

7.3. The FDSM-MAC Protocol - Protocol Aspects

By applying spatial multiplexing at the transmitters, each transmitter can inherently serve multiple receivers. Thus, requirement **R4** reduces to receivers supporting different simultaneously transmitting senders. To meet the other requirements, the FDSM-MAC protocol further extends basic ideas from the MUD-MAC protocol. By the *objection capability* of MUD-MAC, which was introduced to protect receivers with a single detector branch, **R5** is covered. Further, although for MUD-MAC only one wanted stream is supported at a receiver at a time, this objection capability in principle allows for deciding on the number of supportable streams at a receiver (**R3**). We adapt the objection criterion to suit the capabilities of the LASTMUD detector as further explained in Sec. 7.3.1.
The *blockwise parallel transmission* avoids that advanced physical layer capabilities are required during the control message exchange, but it supports multiple parallel transmissions during the data transmission phase, cf. Sec. 3.2.2. It allows heterogeneously equipped nodes to follow the control message exchange and is thus useful to achieve **R6**. Still, for a full support of heterogeneously equipped nodes by a spatial multiplexing based cross-layer design, further points have to be considered. Theses points are related to the requirements **R1**, **R2**, and **R4**. We give an in-depth explanation of the necessary adaptations in Sec. 7.3.2 and Sec. 7.3.3.

7.3.1. Objection Criterion

The LASTMUD receiver exploits both, the advantages of spread spectrum communication as well as the advantages of advanced signal processing with multiple antennas. Combining both technologies allows for spreading codes with moderate code length, i. e., a limited amount of different spreading sequences that is significantly lower than the overall number of nodes in communication range. In case no additional separation of the nodes by pseudo-random spreading sequences is applied, the LASTMUD receiver performs like a V-BLAST receiver. Without additionally exploiting the spatial information available from multiple antennas, streams that apply the same spreading sequence cannot be separated by a receiver. In case of MUD-MAC, two streams would sum up at a receiver inseparably if two transmitting nodes randomly chose the same spreading sequence. In this case, the only strategy for a receiver is to object to one of the transmissions.
For the FDSM-MAC protocol, streams with identical spreading code can still be separated at a receiver as long as the number of streams with the same code does not exceed the number of receive antennas. Thus, the objection criterion is defined so that a receiver only

objects if the latter condition is not fulfilled. This functionality allows receivers to decide on the amount of acceptable streams (**R3**) as well as to accept multiple wanted streams from different transmitters (**R4**). It further allows for multiple streams between the same transmitter-receiver pair, while for MUD-MAC, all MUD branches except one are solely used for interference cancelation. In case of moderate node density, these branches remain unused, while for FDSM-MAC, they can be exploited for transmitting multiple wanted data streams in parallel.

7.3.2. Transmit Power Adaptation

Transmitting multiple parallel data streams requires the overall transmit power per node P_{tot} to be distributed among the streams. In the absence of CSIT, the best strategy is to distribute the transmit power equally among the streams.
Distributing the power among multiple streams inherently decreases the transmission range of the data transmission compared to the range of a single antenna transmission with full power. This influences:

- routing decisions, since the one-hop, two-hop, and multi-hop neighbors of transmitting nodes are accordingly reduced, and
- decisions on the power during the control message phase, since the range of the control messages should match the range of the data transmission.

Routing Decisions

For routing decisions, two nodes are connected if they are in static communication range, i. e., if the receive power level is above a certain communication sensitivity. How the distribution of transmit power among multiple streams influences the average one-hop, two-hop, and multi-hop neighbors is shown in Fig. 7.2. There, 50 nodes are distributed randomly to a square area with varying edge length. In the left part, all nodes transmit with one antenna at full power, in the right part, nodes distribute the power equally among four antennas.
For each node, the shortest path to each other node is measured. This is performed 40 times for each edge length and for each antenna configuration. Subsequently, the average percentage of one-hop neighbors, two-hop neighbors, and multi-hop neighbors, i. e., neighbors that are farer away than two hops, is evaluated. Also, the average percentage of nodes that cannot be reached by a node (No connection) is evaluated.
If all nodes transmit with a single antenna at full power, the average percentage of nodes that cannot be reached by a certain node is negligible. For scenarios with an edge length of up to 100 m, the network is fully connected, i. e., each node can reach each other node. The percentage of one-hop neighbors decreases smoothly for increasing edge lengths.
If all nodes transmit with four antennas and distribute the power equally, except for an edge length of 50 m, the network is never fully connected. The average percentage of nodes that cannot be reached by a certain node gets significant for increasing scenario edge lengths. For large scenario edge lengths even the majority of nodes cannot be reached by a node. The percentages of one-hop neighbors decreases strongly for increasing edge lengths.

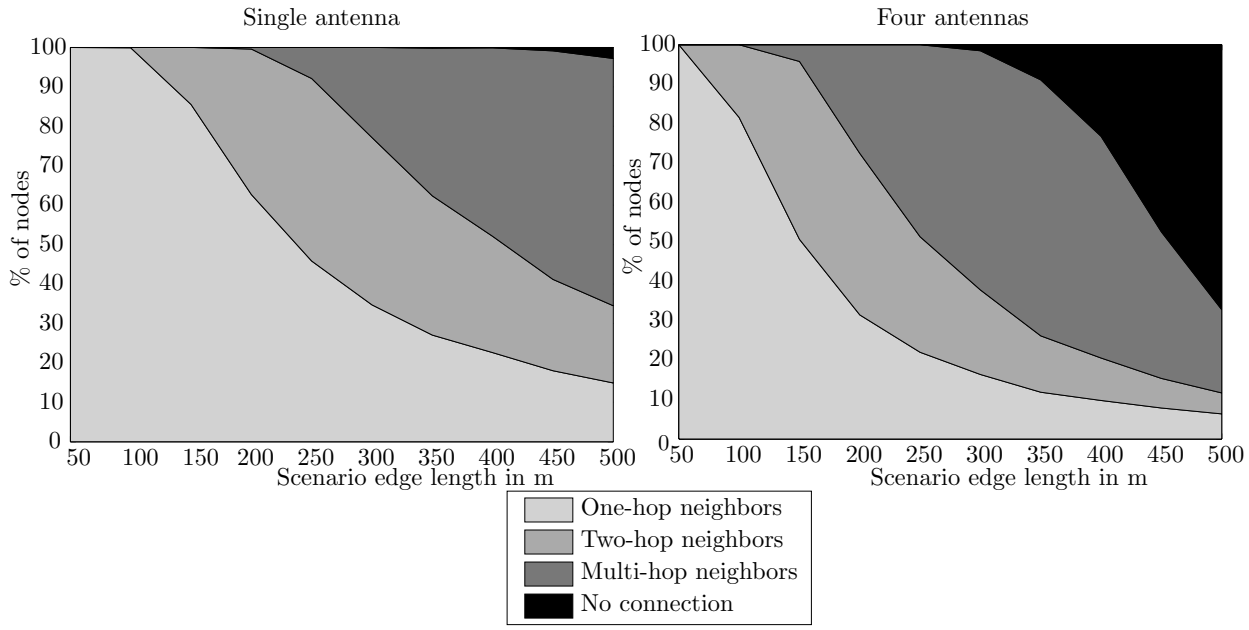

Figure 7.2.: Average percentage of one-hop, two-hop, and multi-hop nodes and nodes out of communication range over different edge length of the squared area. Left: Single antenna with full power. Right: Power equally distributed among four antennas.

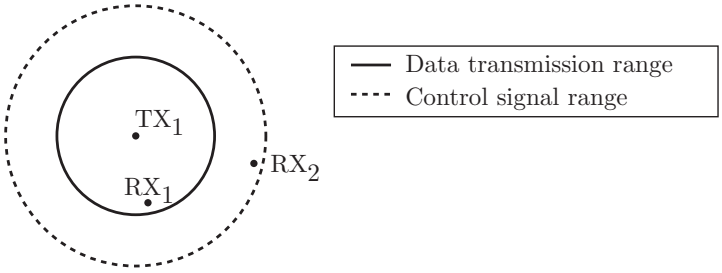

Figure 7.3.: Different transmission ranges of control messages with one antenna at full power and data transmission with one antenna and equal per antenna power distribution among all antennas.

This means, if the routing protocol decides on the possible partners of a node depending on a certain receive power requirement, the reduced power per stream has to be taken into account, resulting in a reduced set of one-hop neighbors compared with the case of one antenna transmission for increasing scenario sizes.
If the FDSM-MAC protocol is compared with other protocols like the CIE-MAC protocol, the comparison is restricted to scenarios with edge length of up to 50 m. Otherwise, the underlying connectivity in the system is not the same for the comparison schemes.

Control Message Power

Even if by an appropriate routing it is assured that a node is in communication range of its potential partner, for a shrinking data transmission range, the control message range should be adopted accordingly. Otherwise, a potential transmitter reserves an area that is larger than its actual transmission range, thus reducing the possible spatial reuse to a certain extent.
In the example of Fig. 7.3, TX_1 reaches not only its associated partner RX_1 with the control message that is transmitted with full power, but also an unintended receiver, namely RX_2. In case control and data packets are transmitted in different time slots, RX_2 is not harmed directly by the increased control message range, since during the data transmission phase, this range is reduced.
RX_2 is, however, not aware during the control message slot that the announced transmission would not harm its data reception. Thus, it reserves resources, e. g., a detection branch in case of MUD-MAC, to avoid interference by the announced transmission. This reduces the possible spatial reuse, since due to the resources reserved unnecessarily, the receiver might be constrained later on to block another newly starting transmission. From this example it follows that the control message range of a potential transmitter announcing a planned transmission should preferably equal its data transmission range.
This issue requires specific considerations if heterogeneously equipped nodes exist (**R6**). Since the overall transmit power per node P_{tot} is distributed among all antennas equally,

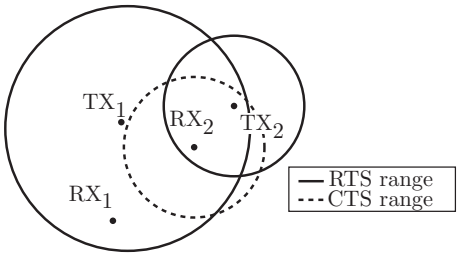

Figure 7.4.: Different transmission ranges due to varying transmit powers per stream.

the transmit power per stream for a node k is the overall transmit power divided by the individual number of transmit antennas M_k. Thus, each node has an individual transmission range of its control messages.
From power control based MAC protocol design it is well-known [KML04, CS07] that individual transmission ranges introduce *unfairness* and *packet collisions* in the system. This is explained by Fig. 7.4.
Assuming that the nodes in the scenario apply the well-known IEEE 802.11 protocol with RTS/CTS, but somehow combined with additional power adaptation. Further, the transmitter and the receiver of a transmission apply the same transmit power during the control signaling phase. Thus, the transmission range for TX_2 and RX_2 is significantly lower than for TX_1 and RX_1.

Unfairness: Whenever TX_1 starts a new transmission, TX_2 abstains from transmitting, since it overhears the RTS message. But if TX_2 starts to signal for a new transmission attempt, this is not noticed by TX_1 due to the reduced transmit power of TX_2. This introduces unfairness regarding the medium access of TX_1 and TX_2 into the system.

Packet Collisions: The CTS message of RX_2 cannot resolve the expected packet collision, since due to a reduced transmit power at RX_2, TX_1 is again not informed of the ongoing transmission. Thus, in case TX_1 starts transmitting while the transmission from TX_2 to RX_2 is ongoing, the packets collide at RX_2.

Both aspects have to be considered for the design of the FDSM-MAC control message part. The unfairness in the medium access due to the different transmit power levels causes weakly equipped transmitters to succeed during the minislots preceding an ANN message with a higher probability than transmitters with a high number of antennas. This higher success probability can be seen as a *prioritization* of weakly equipped transmitters. In case of the FDSM-MAC protocol it might help to balance an effect occurring during the medium access that otherwise penalizes these weakly equipped transmitters. The effect is related to a higher number of transmitter activities if the transmitters are equipped with many antennas compared with the number of activities if transmitters are weakly equipped.
In Fig. 7.5 the actions during the contention phase of several consecutive blocks of a single antenna transmitter are set in contrast to the actions of a multiple antenna transmitter. A block in Fig. 7.5 consists of a contention phase, followed by a data phase. The following

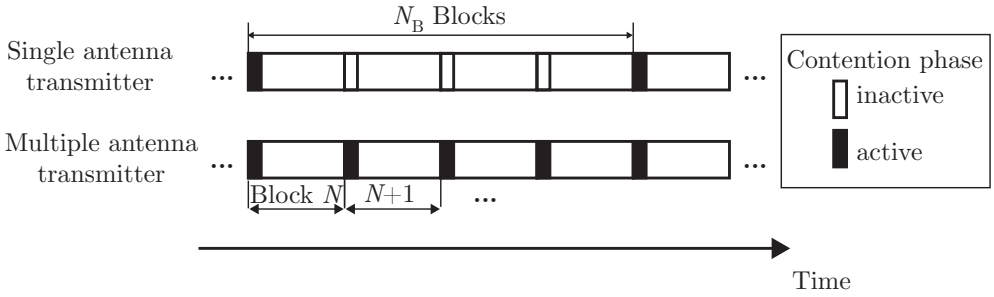

Figure 7.5.: transmitter actions during the contention phase of consecutive blocks for a single antenna transmitter and a multiple antenna transmitter.

acknowledgement phase is omitted for simplicity. In case the single antenna transmitter is successful once, it stays inactive during the course of the next $N_B - 1$ blocks, while the multiple antenna transmitter competes even in case of a success again for medium access with another antenna during the following block. Thus, the effect that leads to a prioritization of weakly equipped nodes is alleviated by the increased transmitter activities of transmitters with a high number of antennas.
The possibility of *packet collisions* requires, however, that the transmission range of a potential transmitter and an objecting receiver is aligned. Thus, for FDSM-MAC, a receiver raises an objection to an announced transmission with the same transmit power level as the announcing transmitter. It can determine this power level by the information about the transmitters' number of antennas, which is included in the ANN message for the FDSM-MAC protocol.
Related to the individual antenna equipment, also the transmission ranges of a transmitter and its associated receiver vary. Thus, a receiver acknowledges the successful reception of all N_B blocks also with the transmit power level applied by the transmitter for the ANN message.

7.3.3. Per Stream Backoff

If nodes transmit only a single stream at a time, they back off for a certain time interval, e. g., if they loose during a contention for channel access, or after they finished packet transmissions successfully. This behavior that is commonly used in, e. g., IEEE 802.11, is referred to as *per node backoff*. Applying this per node backoff in MAC protocol designs that support parallel transmissions of multiple streams results in unnecessarily interrupted packet transmissions. This is explained in Fig. 7.6.
The figure shows multiple consecutive blocks of a transmission with a time-slot-synchronous protocol design, but the same conclusions hold for MAC-layer-asynchronous protocol designs. In the upper row of Fig. 7.6, a single stream transmission is shown. After two consecutive blocks, the transmission is finished, and the successful transmitter goes into backoff. Assuming that the backoff lasts for one block, in the consecutive block, no transmission takes place.

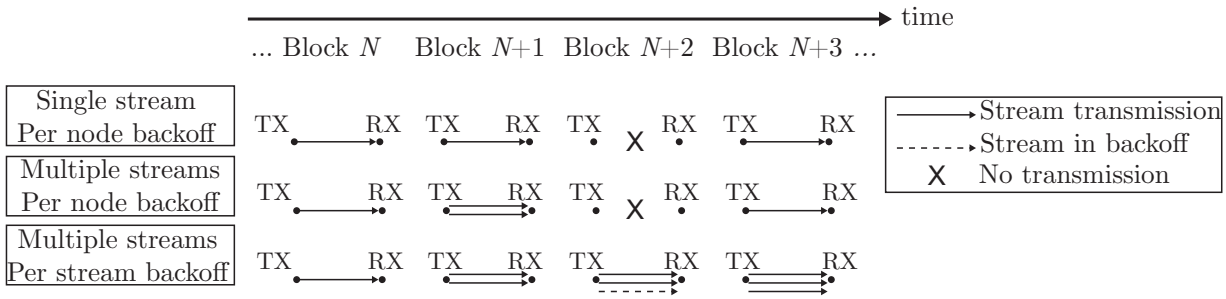

Figure 7.6.: Single antenna transmission with per node backoff. Per stream versus per node backoff for multiple antenna transmission.

Afterwards, a new single stream transmission starts.
In the middle row of Fig. 7.6, a multiple stream transmission with per node backoff is shown. In the first block, one single stream transmission is started. In the next block, an additional stream transmission is started, resulting in two parallel transmissions. In the third block, the newly starting transmission is unsuccessful, e. g., blocked by an objecting receiver. Thus, the unsuccessful transmitter goes into backoff, thereby unnecessarily interrupting the two ongoing streams as well.
This example shows that for parallel transmission of multiple streams, more advanced backoff strategies are required. A solution is shown in the lower row of Fig. 7.6. There, again, two streams are started consecutively in the first two blocks. Also, a third stream to be started is blocked. This time, however, not the whole node goes into backoff, but only the unsuccessful stream, resulting in a *per stream backoff*. This backoff is operated separately for each stream. For time-slot-synchronous MAC protocol designs, nodes can only start new transmissions at predefined points in time, namely if a new contention phase starts. Thus, the backoff duration per stream should be a multiple of the time slotted frame structure that is repeated consecutively. In case of the FDSM-MAC protocol, the per stream backoff should be a multiple of the block duration t_{BL}[1]. This is contrary to the backoff strategy in MUD-MAC that applies an exponential backoff similar to IEEE 802.11.
As a second requirement, to avoid congestion, the per stream backoff duration should increase in case the number of parallel contending transmissions increases. The number of parallel transmissions in the FDSM-MAC protocol depends on the average traffic generated per node as well as on the total number of transmit antennas in the network. We consider the total number of transmit antennas in the network for the backoff duration T_{Backoff} as follows

$$T_{\mathrm{Backoff}} = \sum_{i=1}^{M_{\max}} \left\lfloor \frac{i \cdot K_i}{K} \right\rfloor t_{\mathrm{BL}}. \tag{7.1}$$

$M_{\max}$ is the maximum number of antennas per node, and K_i is the number of nodes with i

[1]We introduced t_{BL} in Sec. 4.3.2 as the duration of one block of the MUD-MAC protocol. For the FDSM-MAC protocol, the duration is accordingly adapted.

antennas out of the K nodes transmitting. The information about the antenna equipment can be estimated at each node locally, i. e., by overhearing neighboring information. Another option is to obtain it globally during the exchange of routing messages, since the information on the antenna equipment is not time variant.
Eqn. 7.1 is one exemplary method how to relate an increasing total number of antennas to an increasing backoff duration. Still, multiple other methods are in principle possible. Also, the example in Eqn. 7.1 does not consider the average traffic generated per node. The generated traffic can vary strongly within a short period of time and is thus difficult to estimate. More advanced backoff strategies thus increase the backoff duration depending on the amount of consecutive collisions experienced by a node. Although at the moment not integrated into the per-stream backoff, taking the contention history into account is expected to improve the overall system performance clearly. Deriving more advanced terms for the backoff duration is, however, out of scope of this work.

7.4. Performance Approximation

Evaluating the performance of the LASTMUD receiver by means of bit level simulations requires a significantly high implementation effort. To reduce this implementation effort, we apply a physical layer approximation for the receiver performance.
The approach in [LTCZ07] models the SINR per stream for MIMO BLAST receivers, thus including also the V-BLAST receiver. The authors propose analytical expressions for the SINR for each detected stream. They model residual interference by previously detected streams as well as the influence of not yet detected streams on the cancelation process. Moreover, they also take errors that are introduced by streams which cannot be estimated by the receiver into account. This can, e. g., happen due to a receivers' limited channel estimation capabilities.
We adapt the model in [LTCZ07] to the LASTMUD receiver, i. e., additionally to the MIMO-MUD receiver, spread spectrum communication is included. Moreover, in contrast to the original model that assumes equal powers for all streams, we include variable transmit power levels for the streams of different nodes. This is required, since for heterogeneously equipped nodes, the transmit power per stream varies, as explained in Sec. 7.3.3.
In case there are M_{tot} streams arriving at the receiver and receiver r has enough degrees of freedom, it can detect all M_{tot} streams iteratively. During the i-th iteration of the detection process, already all streams with a lower detection order, i. e., streams with detection order 1 to $i-1$, are canceled. These streams are summarized in the set of already detected streams $\mathcal{S}_D$. They influence the detection process of the i-th iteration only in case of detection errors. The authors of [LTCZ07] propose, besides other models, a Gaussian model for this detection error. There, the residual interference $\sigma_e^2(j)$ from an already detected stream j depends on the SINR during the detection of stream j.
The streams with higher detection order than iteration i, namely order $i+1$ to M_{tot}, are not canceled yet. They build the set of undetected streams $\mathcal{S}_U$. In case the receiver has enough degrees of freedom and the space-code cross-correlation matrix has full rank, these streams' interference influence is canceled completely by the weighting vector of the i-th iteration,

$\boldsymbol{w}_r(i)$. Otherwise some residual interference remains, which depends on the individual transmit power levels of these streams. The transmit power available for a certain stream s is called $P^{(s)}$ in the remainder of the work.
The authors of [LTCZ07] further assume that a receiver can only estimate a limited number of channels to transmitters and thus suffers also from interference caused by transmitters that exceed this limited number.
For the FDSM-MAC protocol, this assumption is not appropriate, since the receiver estimates the channels one after the other by the preceding control message exchange. Still, such interference influences have to be modeled, since, if control packet collisions occur, or a control message is corrupted, the resulting interference situation is the same as the one with limited channel estimation capabilities. We refer to the channel from unknown transmitters to a receiver r as $\bar{\boldsymbol{H}}_r$ in the following. $\bar{\boldsymbol{H}}_r$ is of size $M_\mathrm{r} \times M_\mathrm{UK}$, where M_UK is the total number of UnKnown (UK) transmit antennas. Note that in case unknown transmit antennas exist, the detectable number of antennas reduces to $M_\mathrm{tot} - M_\mathrm{UK}$.
According to [LTCZ07], the interference power $\sigma^2_\mathrm{UK}(i)$ at the i-th iteration of the detection process at receiver r can be calculated as

$$\sigma^2_\mathrm{UK}(i) = ||\boldsymbol{w}_r^T(i)\boldsymbol{H}_r^H\bar{\boldsymbol{H}}_r\bar{\boldsymbol{\Sigma}}_\mathrm{UK}[\boldsymbol{H}_r^H\bar{\boldsymbol{H}}_r]^H||^2, \tag{7.2}$$

where $\bar{\boldsymbol{\Sigma}}_\mathrm{UK}$ is a diagonal matrix that contains the per stream powers of the unknown transmit antennas. The individual entries vary for heterogeneously equipped nodes.
The SINR $\gamma_{r,s}(i)$ of a stream s that is detected at the i-th stage of the iteration process at a receiver r is thus calculated as

$$\gamma_{r,s}(i) = \frac{P^{(s)}|\boldsymbol{w}_r^T(i)\boldsymbol{R}_{r.,\mathrm{TA}_s}|^2}{\sigma^2_\mathrm{n} + \sigma^2_\mathrm{UK}(i) + \sum\limits_{j\in\mathcal{S}_D}|\boldsymbol{w}_r^T(i)\boldsymbol{R}_{r.,\mathrm{TA}_j}|^2\sigma_e^2(j) + \sum\limits_{j\in\mathcal{S}_U}|\boldsymbol{w}_r^T(i)\boldsymbol{R}_{r.,\mathrm{TA}_j}|^2P^{(j)}}. \tag{7.3}$$

$\boldsymbol{R}_{r.,a}$ reflects the a-th column of $\boldsymbol{R}_r$, and TA_s is the the transmit antenna index for a stream s, cf. Sec. 7.2. Possible enhancement of the pure noise term by the zero forcing approach is not taken into consideration here. Since a relatively high SNR is required during the preceding control message exchange to decode the control message and to subsequently start the data transmission, the noise term is several magnitudes lower than the receive signal power. Thus, this simplification is not expected to influence the performance much.

7.5. Simulation Results

In the following, we present simulation results for the FDSM-MAC protocol in the $50\,\mathrm{m} \times 50\,\mathrm{m}$ scenario. To see how separating the nodes by pseudo-random codes of different code length influences the performance, we apply Gold codes [Gol67] of spreading length $S_\mathrm{N} = 1$ (no spreading), $S_\mathrm{N} = 7$, and $S_\mathrm{N} = 31$. Note that the number of distinct code sequences increases depending on the spreading code length. The influence of heterogeneously equipped nodes is investigated by equipping subgroups of the 50 nodes differently with 1, 2, 3, or 4 antennas. The simulated heterogeneous node constellations are listed in Tab. 7.1. Similar

Table 7.1.: Heterogeneous node constellations (HNC)s.

number of antennas	1	2	3	4	$\sum$
HNC-1	0	0	0	50	50
HNC-2	12	13	12	13	50
HNC-3	15	0	0	35	50

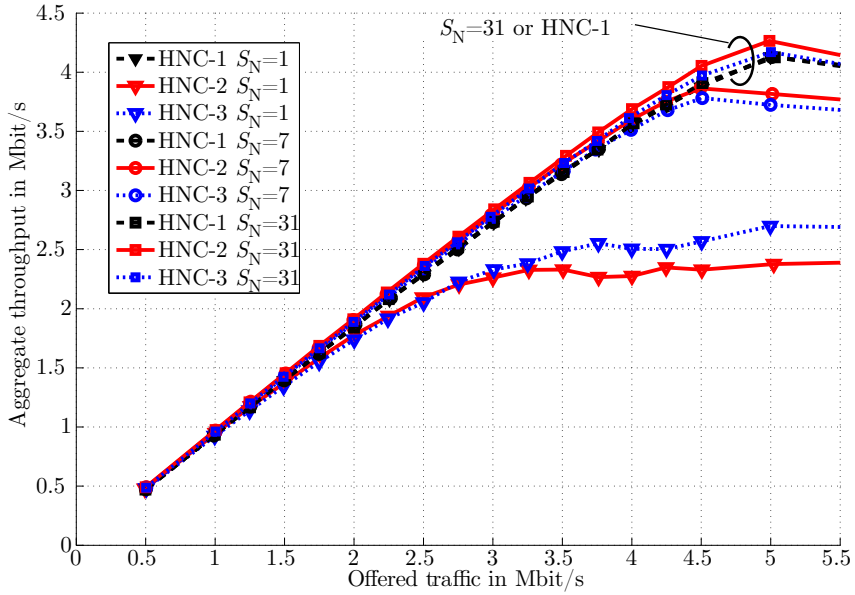

Figure 7.7.: Aggregate throughput versus offered traffic for different heterogeneous node constellations and different spreading code length S_N for the FDSM-MAC protocol.

to CIE-MAC, in the FDSM-MAC protocol due to the severe contention in the 50 m × 50 m scenario, a potential transmitter starts contending only with a probability of 25 %. We choose a nodes' potential sinks as described in Sec. 2.2.4. In contrast to the simulations presented in the Chapters 3–6, where each node chooses one other node as a sink, for the FDSM-MAC protocol a node chooses four sinks that it serves during the simulations. The packets for the different nodes are inserted into the single traffic queue of a transmitter according to their time of origin.

7.5.1. Aggregate Throughput and Influence of Spreading Codes

We compare the performance of FDSM-MAC for different spreading code lengths S_N and different HNCs. The results are shown in Fig. 7.7. All curves for HNC-1 (black dashed line), regardless of the actual spreading code length, are practically identical. The markers for HNC-1 with $S_N = 1$ and $S_N = 7$ are hidden by the markers for $S_N = 31$. Similar, all curves with spreading code length $S_N = 31$ (rectangular marker) show almost the same trend.

Here, a slight deviation can be observed. The curve for HNC-1 shows the lowest throughput, followed by the curve for HNC-3. The best results are achieved by HNC-2. HNC-2 is the node configuration with the lowest aggregate number of antennas in the system, namely 126. For HNC-3, the aggregate number of antennas is higher, namely 155, and the highest aggregate number of antennas, namely 200, is offered by HNC-1. An increased aggregate number of antennas results in a higher contention. This results in the slightly reduced throughput. A more detailed explanation for this effect is shown in Sec. 8.2.
Still, all curves for HNC-1 as well as for $S_{\mathrm{N}} = 31$ show a very similar trend. This means that if all nodes are sufficiently equipped with a large number of antennas, a pure V-BLAST type receiver without an additional separation of nodes by pseudo-random codes is sufficient. Also, in case a spreading code of noticeable length is applied, the antenna equipment of the nodes is irrelevant for the performance. Since the overall number of degrees of freedom at a receiver depends on both, spreading code length as well as antenna configuration, and thus a significantly high degree in one of the parameters balances deficiencies in the other parameter, this behavior could be expected.
If the nodes are heterogeneously equipped, even spreading codes with moderate spreading code length influence the performance remarkably. The curves for HNC-2 (red solid line) and HNC-3 (blue dotted line) differ significantly if no separation of nodes by spreading codes is applied (triangular marker) and if the spreading code length is set to a moderate length of $S_{\mathrm{N}} = 7$ (circular marker). For $S_{\mathrm{N}} = 7$, HNC-2 and HNC-3 show almost the same performance than the curves for HNC-1, since the differences in the trend of the curves get only significant if already a large number of packets is lost.
High losses compared with HNC-1 arise for both, HNC-2 as well as HNC-3 if no additional separation of nodes by spreading codes is applied (triangular marker). This shows clearly that if heterogeneously equipped nodes exist in the network, CDMA with even a moderate spreading code length can improve the overall system performance significantly compared to a pure V-BLAST type receiver. Deficiencies with respect to a weakly equipped nodes' degrees of freedom can be balanced by additional separating nodes by pseudo-random codes with moderate spreading code length.

7.5.2. Fairness

To investigate the fairness achieved by FDSM-MAC, we compare in Fig. 7.8 the cdf of the aggregate throughput per node for an offered traffic of 2.5 Mbit/s for all HNCs without separating nodes additionally by codes. The same relation but with a moderate spreading code length of $S_{\mathrm{N}} = 7$ is shown in Fig. 7.9. If the streams are separated solely by the spatial signatures, the throughput per node increases significantly for HNC-1 compared to the other HNCs. But the trend of the curves for all HNCs shows no breaks like a similar trend for HNC-2 for the CIE-MAC protocol (cf. Fig. 6.9). This indicates that the FDSM-MAC treats heterogeneously equipped nodes with a different number of antennas equally. If a moderate spreading code of length $S_{\mathrm{N}} = 7$ is applied additionally, the curves for all HNCs are similar. This was expected, since separating streams additionally by spreading codes balances potential shortcomings of weakly equipped node by additional degrees of freedom.

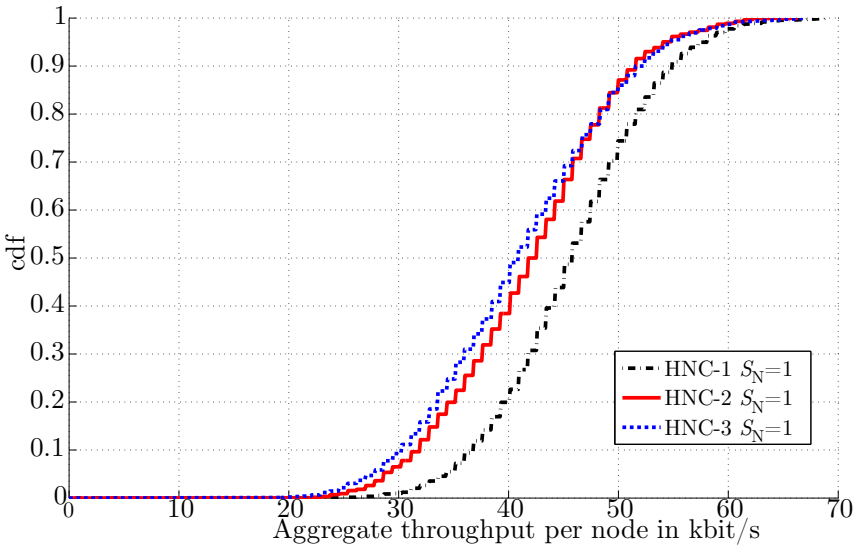

Figure 7.8.: Cdf of the throughput per node for an offered traffic of 2.5 Mbit/s for different HNCs. No additional separation of nodes by code sequences is applied.

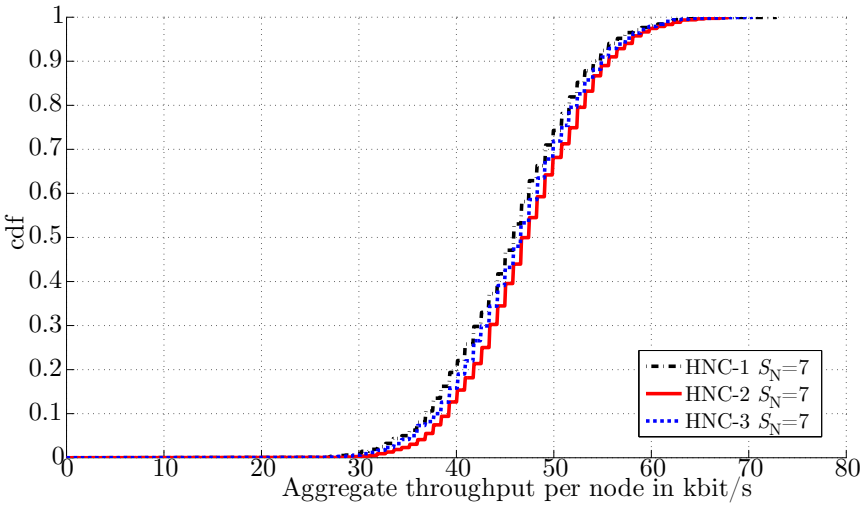

Figure 7.9.: Cdf of the throughput per node for an offered traffic of 2.5 Mbit/s for different HNCs. A moderate spreading code length of $S_N = 7$ is applied.

7.6. Summary and Further Work

Combining spatial multiplexing at the transmitters with an appropriate receiver design allows to exploit MIMO gains without requiring channel state information at the transmitters. The additional control message overhead can thereby be reduced significantly. The underlying physical layer strategy, however, requires an appropriate MAC protocol design that takes the specific challenges for multiple stream transmission into account. The considerations regarding multiple streams have to be adapted further if the nodes in the scenario are heterogeneously equipped.

We reviewed existing spatial multiplexing based cross-layer designs. From this review, we derived as one contribution important requirements that a new cross-layer design with a combination of spatial multiplexing and multiuser detection as the physical layer strategy should fulfill. As another contribution, we identified major challenges that arise for multiple streams transmission regarding routing decisions, power adaptation of control and data packets, and backoff strategies. We further presented solutions for these challenges that specifically take the requirements of heterogeneously equipped nodes into account.

We described the physical layer reception strategy that we chose for our proposed FDSM-MAC protocol, namely a LAyered Space Time MultiUser Detector (LASTMUD). To evaluate its performance, we adapted an appropriate physical layer approximation model for BLAST receivers to additionally include the influences of spread spectrum communication. The model was further adapted to support individual transmit powers per stream. This is required if nodes are heterogeneously equipped.

As a last contribution, we evaluated the performance of the FDSM-MAC protocol by simulations with a sufficiently detailed channel model. The FDSM-MAC protocol was shown to operate for different heterogeneous node constellations and performed well for moderate spreading code lengths and even if operated without separating streams by spreading codes. It also showed a fair behavior by treating nodes with different number of antennas equally. The backoff per stream instead of per node that we proposed is able to avoid unnecessary interruptions of successfully ongoing transmissions. The duration of the backoff is, however, at the moment only a function of the contending nodes in the system, considering their respective antenna equipment. Further work is required to include an adaptive backoff strategy that, similar to the per node backoff in IEEE 802.11, increases the backoff duration if a node experiences packet collisions repeatedly.

8. Comparison of CIE-MAC with FDSM-MAC

In Chapter 6, we presented the CIE-MAC protocol that exploits multiple antennas at the transmitters and receivers by beamforming combined with spatial nulling. An essentially different approach to exploit the multiple antennas is adopted by the FDSM-MAC protocol that we proposed in Chapter 7. It applies spatial multiplexing combined with multiuser detection as the physical layer strategy. Both schemes have in common that they expect the nodes in the network to be equipped with multiple antennas. But they differ significantly not only regarding their underlying physical layer strategy, but also regarding certain protocol aspects.

In this chapter, we compare the CIE-MAC protocol with the FDSM-MAC protocol. In contrast to the simulative comparison between power control and MUD based cross-layer designs in Chapter 3, we do in this chapter not target to identify the most favorable protocol by a simulative comparison. The outcome of a simulative comparison is namely strongly influenced by the modeling of the spatial antenna correlation. We modeled this antenna correlation according to a certain spatial channel model that reflects a specific environment, as explained in Sec. 5.2.4. Depending on the investigated environment, the spatial antenna correlation varies. In case the antennas at a node are fully correlated, spatial multiplexing fails to separate the different streams. In a similar way, beamforming is not sufficient if the antennas at a node are completely uncorrelated. Thus, for other environments than the investigated scenario, the outcome of a simulative comparison might differ.

The goal of this chapter is rather to examine influences of the specific physical layer strategies on the cross-layer design performance that hold for variable simulation environments. Further, protocol aspects that show to be in general advantageous or negative with respect to the cross-layer design performance should be identified.

The chapter is structured as follows. In Sec. 8.1 we compare the control message overhead of both protocols. Sec. 8.2 shows a detailed simulative comparison of both schemes. Related to the outcome of Sec. 8.2, in Sec. 8.3 some principal observations regarding the underlying physical layer strategies as well as regarding principal protocol aspects are presented. Sec. 8.4 finally summarizes this chapter.

8.1. Control Message Overhead

We compare the control overhead of the CIE-MAC protocol with the control overhead of the FDSM-MAC protocol. Only control messages that precede a data transmission are considered. The overhead from the subsequent acknowledgement is neglected, since it is the same for both schemes.

8.1.1. PHY and MAC Header

All control messages of the FDSM-MAC protocol and the CIE-MAC protocol are generated on the MAC layer. Before they are transferred to the physical layer, a MAC layer header is added to the control messages. In a similar way, the physical layer adds a physical header before transmitting a control message over the physical medium. These headers are the same for both cross-layer designs. To model the overhead from these headers, we adjust the respective headers of the IEEE 802.11 protocol for the RTS and CTS message to the specific properties of a time-slot-synchronous protocol design.

PHY Header

We include all information bits that are contained in the physical layer header of the IEEE 802.11 protocol for the definition of the modulation scheme, error correction, and future services into the physical header for the FDSM-MAC protocol and the CIE-MAC protocol. Since IEEE 802.11 is a MAC-layer-asynchronous protocol design that requires synchronization information preceding each control message, while FDSM-MAC and CIE-MAC are time-slot-synchronous, we neglect all bits for synchronization. Further, information that specifies transmission durations is not considered, since in time-slot-synchronous protocol designs the transmission duration is fixed by the predefined frame structure. The resulting physical layer overhead per message equals 32 bits.

MAC Header

We consider all bits of the MAC header of IEEE 802.11 for frame control and error correction purposes. The resulting MAC header overhead per control packet equals 48 bits. We further, in contrast to IEEE 802.11 that addresses a globally unique address space with 64 bits long addresses, address a non global address space with 8 bits long addresses. Thus, per node ID the MAC layer overhead is increased by 8 bits.

8.1.2. CIE-MAC Control Overhead

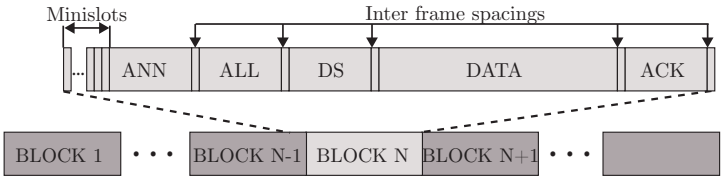

Figure 8.1.: Block structure of the CIE-MAC protocol.

The control message part of the CIE-MAC protocol that precedes a data transmission consists of an ANN message, an ALL message, and a DS message, see Fig. 8.1. As described in Sec. 6.4.1 each of these messages is split into a channel estimation phase where the channel to all antennas is estimated, and the actual control information exchange operated with a

Table 8.1.: Control message overhead of the CIE-MAC protocol.

	ANN in bits	ALL in bits	DS in bits
PHY Header	32	32	32
MAC Header	48	48	48
Channel Estimation	8	8	8
Complex Weights	64	64	64
Node ID	16	8	8
Sum per message	168	160	160
Sum	488		

single antenna. During the channel estimation phase known training symbols are transmitted successively from each antenna. By analyzing the attenuation and phase shift of the training symbols, all nodes that overhear the symbols can estimate the channel to the transmitting node.
According to [HH03] the optimal number of training symbols contained in a training interval to estimate a channel to a certain node equals this nodes' number of antennas. Thus, in case of heterogeneously equipped nodes, the duration of the channel estimation phase varies depending on the antenna configuration. In time-slot-synchronous protocol designs the training period can, however, not be adapted dynamically during runtime. Thus, it is set such that it allows for the estimation of up to $M_{\max}$ antennas per node. Nodes are thus restricted to this maximum number of antennas. For all simulations, $M_{\max}$ is set to four. For QPSK with 2 bits per symbol as the modulation scheme for the data transmission, the training phase is set accordingly to contain 8 bits.
Similar to the channel estimation phase that depends on a nodes' individual antenna configuration, also the overhead to transmit a complex-valued weight varies with the number of antennas. The duration is set to support a maximum of $M_{\max}$ antennas as well. The weights are transmitted as digitalized values and are quantized with 8 bits. This results in an overhead of 16 bits per complex value. A weight contains a maximum of $M_{\max}$ complex values, resulting in $M_{\max} \cdot 16$ bits $= 64$ bits. Further, the ANN message contains the ID of the transmitting node as well as the ID of the intended receiver. The ALL message contain the ID of the message addressee or an error ID. The DS message contains the ID of the message addressee.
The resulting control message overhead of the CIE-MAC protocol is shown in Tab. 8.1.

8.1.3. FDSM-MAC Control Overhead

The control message part of the FDSM-MAC protocol that precedes a data transmission consists of an ANN and an OBJ message, see Fig. 8.2. During the ANN message, the channel to the announcing transmitter is estimated. It is, in contrast to CIE-MAC, solely estimated to a single antenna, since in the FDSM-MAC protocol the transmitter applies

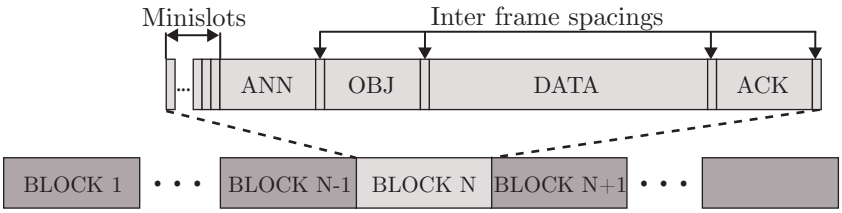

Figure 8.2.: One block of the FDSM-MAC protocol.

Table 8.2.: Control message overhead of the FDSM-MAC protocol.

	ANN in bits	OBJ in bits
PHY Header	32	32
MAC Header	48	48
Channel Estimation	2	0
Number of Antennas	2	0
Node ID	16	8
Sum per message	100	88
Sum	188	

spatial multiplexing and thus contents with each antenna separately. The resulting training phase is set to contain 2 bits. The ANN message includes the ID of the transmitter and the ID of the intended receiver. A transmitters' individual spreading sequence is generated by means of its ID and thus overhead with respect to the spreading code is not considered. The ANN message further contains 2 bits that quantify the transmitters' number of antennas. The OBJ message contains the ID of the message addressee. The resulting overhead for the FDSM-MAC protocol is shown in Tab. 8.2.

8.2. Simulation Results

In the following, we show a simulative comparison of the CIE-MAC protocol and the FDSM-MAC protocol. The simulation environment and the simulation settings are the same as in Sec. 7.5. Since CIE-MAC is a single band protocol and thus requires only 1 MHz of bandwidth, we do not incorporate CDMA to separate streams for the FDSM-MAC protocol ($S_{\mathrm{N}} = 1$). We simulate different heterogenous node constellations as specified in Tab. 6.2.

8.2.1. Aggregate Throughput

We investigate the aggregate throughput and the corresponding *lost packet percentage* for all HNCs. The lost packet percentage relates the amount of lost packets to the amount of

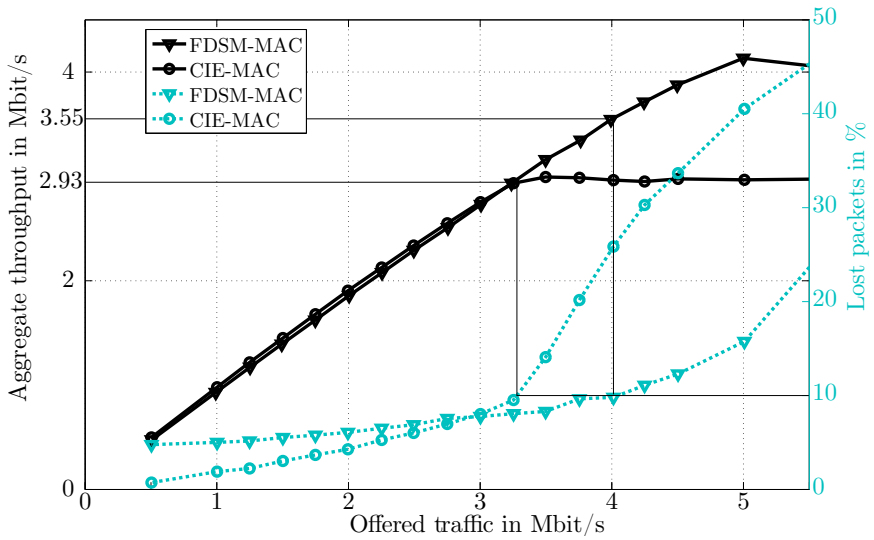

Figure 8.3.: Aggregate throughput (left axis) and corresponding lost packet percentage (right axis) versus offered traffic for HNC-1 for the CIE-MAC protocol and the FDSM-MAC protocol.

created packets. The term lost packets includes packets that are lost due to *control message errors*, packets *received corrupted*, and packets that are *dropped* since the maximum tolerable packet delay $\Delta_{\max} = 1.0\,\mathrm{s}$ for these packets is reached. An in detail inspection of the different packet loss criterions is shown in Sec. 8.2.2.

The aggregate throughput and the corresponding lost packet percentage versus the offered traffic are plotted in Fig. 8.3 for HNC-1. For moderate offered traffic loads, the FDSM-MAC protocol (triangular markers) and the CIE-MAC protocol (circular markers) perform similar in terms of aggregate throughput. For high offered traffic loads, the FDSM-MAC protocol outperforms CIE-MAC. The improvements are, however, obtained for offered traffic loads that are so high that already a non-negligible number of packets is lost. Thus, we mark the point where already 10 % of the packets are lost as a reference for both schemes.

In Fig. 8.4 and Fig. 8.5 the corresponding curves for HNC-2 and HNC-3 are shown. It can be observed that for HNC-2, the improvements of FDSM-MAC compared to CIE-MAC in the area where not more than 10 % of the packets are lost get marginal, and even slightly negative in case of HNC-3. This is reasoned by the different behavior of both protocols with respect to the per node fairness. In the FDSM-MAC protocol, better equipped nodes have to abstain from transmitting in order to protect the ongoing receptions of weakly equipped receivers. In the CIE-MAC protocol, weakly equipped nodes have to abstain from transmitting or receiving, in case they have not enough degrees of freedom to null neighboring transmissions. This unfair behavior of the CIE-MAC protocol improves the aggregate throughput for heterogeneously equipped nodes.

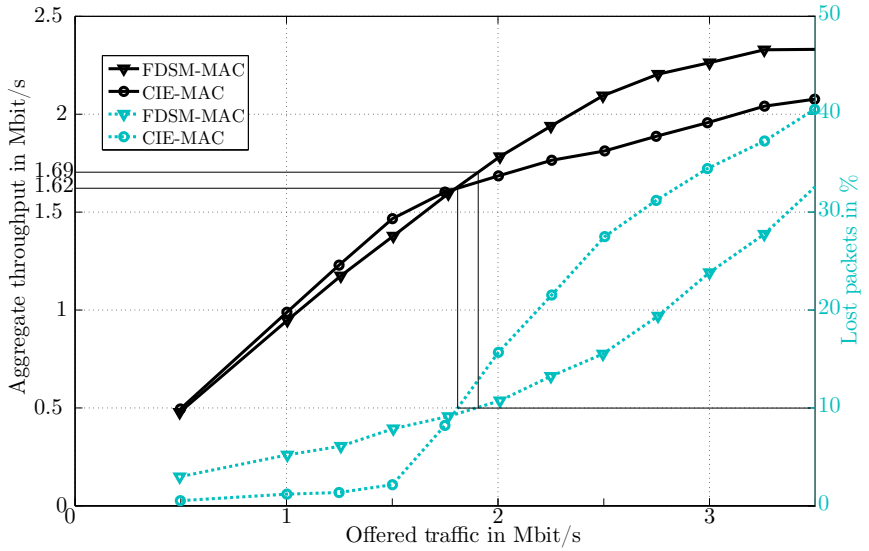

Figure 8.4.: Aggregate throughput (left axis) and corresponding lost packet percentage (right axis) versus offered traffic for HNC-2 for the CIE-MAC protocol and the FDSM-MAC protocol.

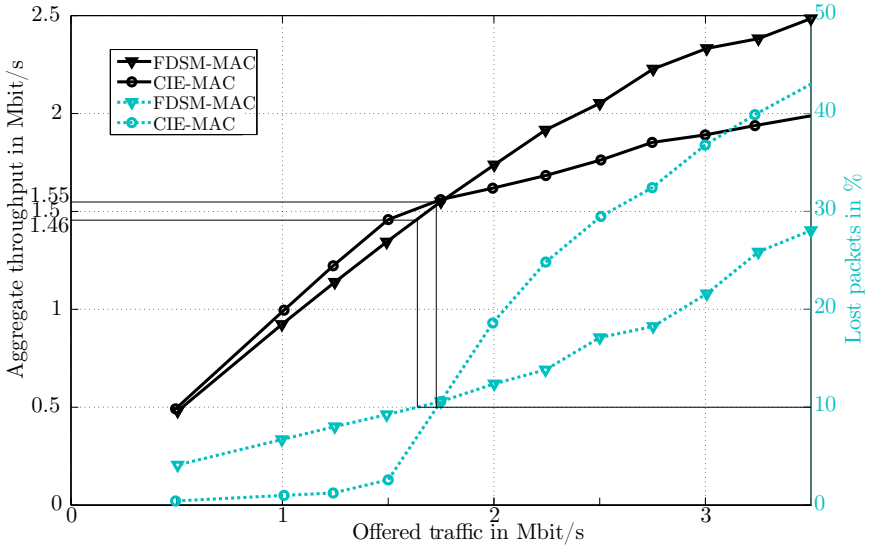

Figure 8.5.: Aggregate throughput (left axis) and corresponding lost packet percentage (right axis) versus offered traffic for HNC-3 for the CIE-MAC protocol and the FDSM-MAC protocol.

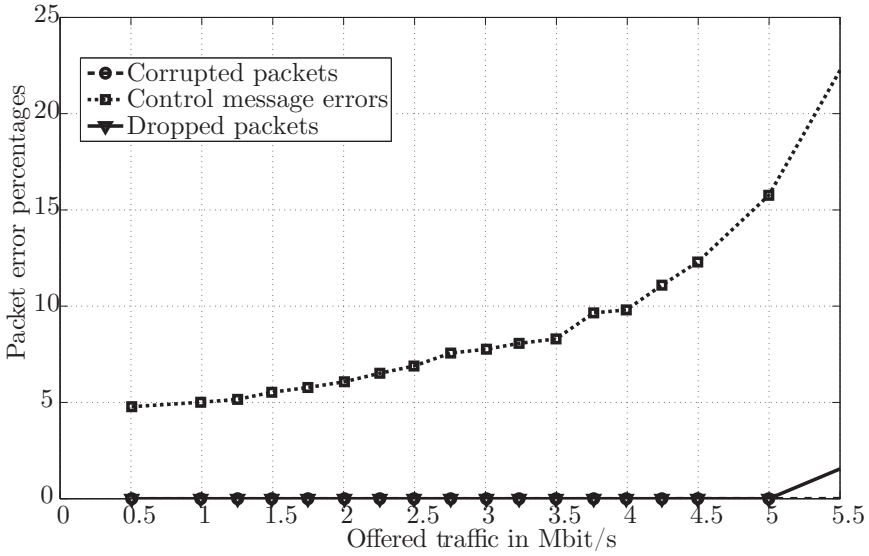

Figure 8.6.: Different packet error ratio percentages versus offered traffic for HNC-1 for the FDSM-MAC protocol.

8.2.2. Packet Failure Statistics

For a further explanation of the results for HNC-1 in Fig. 8.3, we investigate the different types of packet failures that lead to the overall packet loss rates in more detail. The corresponding curves for packets that are lost due to control message errors, packets received corrupted, and packets that are dropped, are shown in Fig. 8.6 for the FDSM-MAC protocol and in Fig. 8.7 for the CIE-MAC protocol. Although the results in aggregate throughput for FDSM-MAC and CIE-MAC are similar for moderate traffic loads, the corresponding curves for the different types of packet failures vary strongly.

Control Message Errors

For FDSM-MAC, the majority of packets is lost due to control message errors. Two effects account for control message errors, namely:

1. ANN collisions at the intended receiver due to multiple simultaneously sent ANN messages, and

2. corrupted ANN messages at the intended receiver.

ANN collisions: FDSM-MAC avoids that multiple potential senders transmit their ANN messages simultaneously by using minislots that precede the ANN message (cf. Sec. 3.2.2). Since the transmitters content for channel access with every antenna separately, resulting in a strongly increased contention compared to MUD-MAC, a potential transmitter additionally starts contending only with a probability of 25 %.

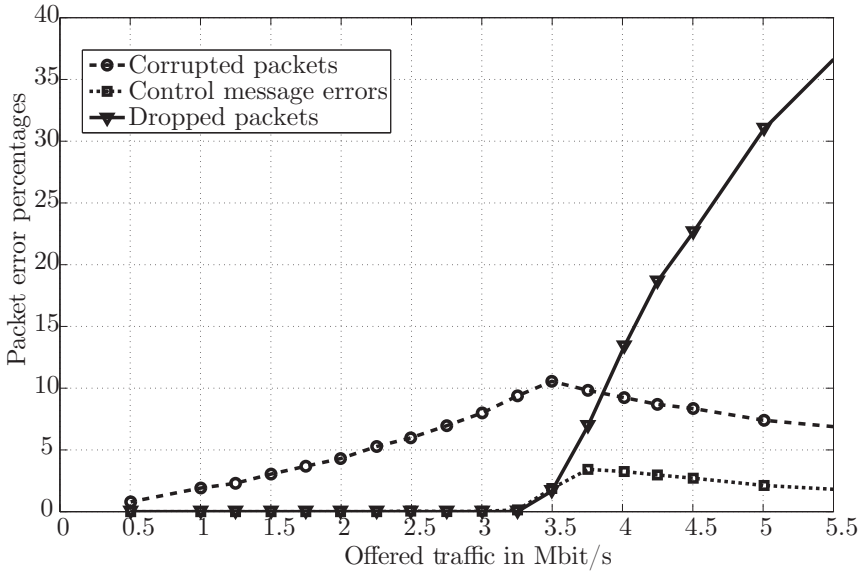

Figure 8.7.: Different packet error ratio percentages versus offered traffic for HNC-1 for the CIE-MAC protocol.

These methods, however, only reduce, but not completely avoid that multiple ANN messages collide. The higher the traffic load, the higher is also the probability that at least two nodes randomly choose the same minislot and, in case no other node transmits in a previous slot, transmit their ANN messages simultaneously. This results in colliding ANN messages at the associated partner.
For the extreme case that all 50 nodes plan to start a transmission simultaneously, after flipping a coin with a win probability of 25 %, on average 12.5 nodes are left. For 12 nodes, the probability p_{col} that in the first of ten minislots the signals of at least two nodes collide can be calculated by subtracting the probabilities that no node or only one node chooses that slot as

$$p_{\text{col}} = 1 - \text{B}(0|0.1, 12) - \text{B}(1|0.1, 12) \approx 34\%, \tag{8.1}$$

where B() is the Binomial distribution. For 13 nodes, p_{col} is increased to $\approx 38\%$.
Note that if nodes were equipped with a single antenna, the number of nodes simultaneously contending would always be significantly lower than the overall number of nodes in the network. If a node experienced a packet collision, it would go into backoff. If nodes are equipped with a high number of antennas and apply a per stream backoff, for very high traffic loads it can happen that all nodes content simultaneously, since in case they are not successful, only one of their streams backs off.
Another reason for ANN collisions is that the minislots require that potential transmitters are in mutual sensing range. For the simulated transmit power and receiver communication sensitivity, for a pure distance related power attenuation, the mutual sensing range is about 232 m. Assuming that the overall transmit power is distributed equally to four antennas, it

is reduced to 145 m. Thus, all nodes in the 50 m × 50 m scenario are in mutual sensing range. In fading environments, the signal can experience strong attenuation in the magnitude of multiple of 10 dB, even including a complete extinction of the signal. Thus, the nodes are in general only with a certain probability in mutual sensing range.
Both effects deteriorate with an increasing aggregate number of antennas in the system and thus lead to a slightly reduced aggregate throughput (cf. Fig. 7.7) as well as a slightly reduced throughput per node (cf. Fig. 7.9) for HNCs with a high aggregate number of antennas.

Corrupted ANN messages: The fading influences also the decoding process at a potential receiver. Even in case a fading margin (cf. Sec. 2.2.4) is taken into account, a certain outage probability remains.

Both effects occur likewise for FDSM-MAC and CIE-MAC. The probability for ANN collisions is, on the one hand, increased for FDSM-MAC compared to CIE-MAC, since a transmitter contends for channel access, even if it already transmits a packet successfully (cf. Sec. 7.3.2); on the other hand, it is reduced, since the transmission range of the ANN signal is reduced by the reduced per stream power.
The major difference between the two schemes lies, however, not in the probabilities by which these effects occur, but in the consequences following these effects. They differ significantly for both protocols. For FDSM-MAC, a potential transmitter is not aware that its associated partner did not receive the ANN message correctly, since the control message exchange does not involve a positive reply by the associated partner. Thus, in case no other node objects, the transmitter transmits data although its associated partner is not ready for the reception, since the preceding ANN message was lost. These unsuccessful packet transmissions count in the packet error statistics. For CIE-MAC, the transmitter expects the potential partner to reply with an ALL message after it transmitted an ANN message; otherwise it backs off. Thus, the control message errors do not lead to packet losses.

Corrupted Packet Reception

By comparing the trends of the corrupted packet percentages of FDSM-MAC in Fig. 8.6 and CIE-MAC in Fig. 8.7, it can be observed that for FDSM-MAC, except for very high traffic loads, no packets are received corrupted, while for CIE-MAC, the curve increases to about 10 % and starts decreasing for increasing control message errors.
The trends of the corrupted packet percentages reflect the different sensitivities of the protocols to control message losses that take place between a potential transmitter or receiver and **neighboring nodes other than its communication partner**.
In case of FDSM-MAC, only receivers need to overhear the ANN messages of neighboring transmissions. In case they are involved in an ongoing data reception and cannot decode an ANN message, they estimate the additional interference by the corrupted ANN message. If this interference is high, they object to the announced transmission. Only if a node is not an active receiver while it misses an ANN message and it gets active as a receiver in one of the N_{B} following blocks after the corrupted ANN message, the data reception of this node is

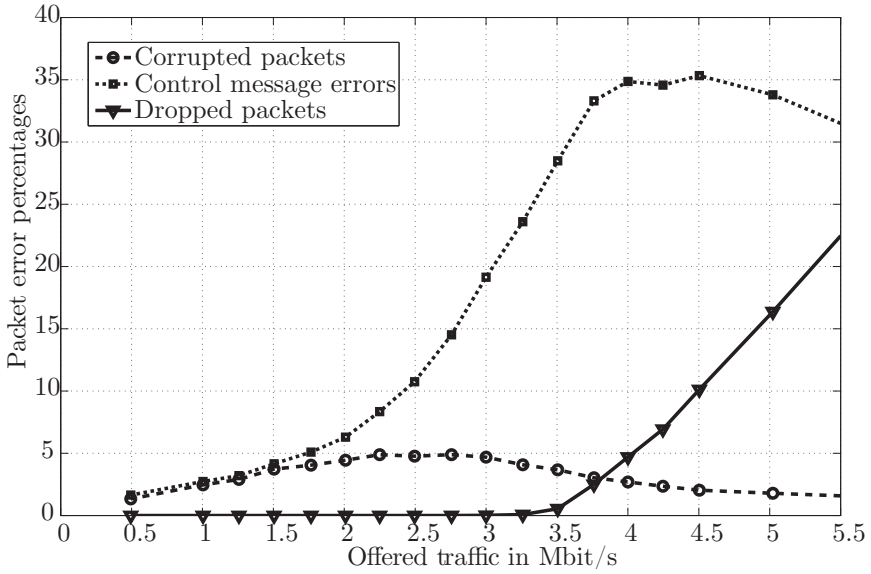

Figure 8.8.: Different packet error ratio percentages versus offered traffic for HNC-2 for the FDSM-MAC protocol.

influenced. In this case, this nodes' reception is disturbed by interference that is referred to as interference from unknown antennas σ^2_{UK} in Eqn. 7.3. The range of this interference is, however, strongly reduced for HNC-1 since the power at a potential interferer is distributed among four antennas. Thus, packet corruptions due to interference from unknown antennas are very unlikely to happen.

That packet corruptions indeed happen if the interfering ranges of potential interferers are not strongly reduced is shown by the curves corresponding to HNC-2, depicted in Fig. 8.8. There, up to 5 % of the packets are corrupted. Note that the percentage of control message collisions stagnates at a value that fits to the percentages evaluated by Eqn. 8.1 for 12 and 13 nodes, respectively. The corresponding curves for HNC-2 for the CIE-MAC protocol as well as for HNC-3 can be found in Appendix A.

In contrast to FDSM-MAC, for the CIE-MAC protocol, potential receivers as well as potential transmitters require knowledge of the ongoing transmissions in their vicinity. In case a transmitter misses the ALL message of a preceding transmission, and it announces a new transmission that would harm the existing one, the interfered receiver objects, thus avoiding packet corruptions.

In case a potential receiver missed a preceding DS message, it calculates its weight without taking the interference from this transmission into account. In this case, packet corruptions are very likely to happen. Since the full transmit power is applied during data transmission, the probability of packet corruptions is increased compared with FDSM-MAC.

Note that for both schemes, packet corruptions due to pure fading influences are expected to happen rarely, since in case the channel between a transmitter and its potential partner experiences a deep fade, already the preceding control message exchange aborts the planned

transmission.

Dropped Packets

The trends of the dropped packet percentages vary strongly for both protocols for the following reason. For FDSM-MAC, after control message errors, packets are transmitted although the partner is not ready, and thus counted as packets lost by control message errors. For the CIE-MAC protocol, in case of control message errors, such packets are not transmitted at all. The data transmission slot following a failed control message exchange can, however, not be utilized by CIE-MAC either. Thus, such packets stay in the transmitters' queue and count as dropped packets if their maximum tolerable delay is reached.
Still, especially for high traffic loads, an improvement in the dropped packet percentages and thus in the aggregate throughput can be observed for FDSM-MAC compared with CIE-MAC. CIE-MAC requires that transmitters as well as receivers null ongoing transmissions in their vicinity. This causes transmitters that have not enough degrees of freedom to abstain from transmitting for high traffic loads. For FDSM-MAC, limitations arise only on the receiver side, leading to an improved performance for very high traffic loads compared with CIE-MAC.

8.3. Conclusions with Respect to Cross-Layer Designs

We compared two cross-layer designs that vary not only with respect to their physical layer strategy, but also with respect to certain aspects of the MAC protocol design. Summarizing the results in Sec. 8.2 and including also some results from Chapter 6 and Chapter 7, some general observations can be made. These observations reflect principal properties of the underlying physical layer strategy as well as aspects of an appropriate protocol design.

8.3.1. Observations Regarding Physical Layer Strategy

Regarding beamforming combined with spatial nulling in ad hoc networks, we point out the following advantages and disadvantages:

+ it improves the communication range in case more than one degree of freedom is applied to serve the associated partner (Fig. 6.6),

+ for the same number of nodes and the same number of antennas per node, the transmit contention of beamforming is moderate compared with spatial multiplexing,

- it requires a huge protocol overhead since the spatial information has to be distributed in the network (cf. Sec. 8.1),

- even in the absence of additional channel estimation errors it is sensitive to control packet failures, since the interferences of uninformed nodes sum up at the receivers (Fig. 8.7), and

- it is restricted to one stream from or to each node at a time.

For spatial multiplexing combined with multiuser detection at the receiver we state that:

+ it supports multiple simultaneous streams from or to different nodes,

+ it requires almost no additional protocol overhead since no additional spatial information has to be distributed in the network (cf. Sec. 8.1),

- it suffers from a reduced connectivity compared to beamforming due to the transmit power allocation among multiple antennas (cf. Fig. 7.2),

- for the same number of nodes and the same number of antennas per node, the transmit contention of spatial multiplexing is increased strongly compared to beamforming.

8.3.2. Observations Regarding Protocol Aspects

In fading environments even by including an additional fading margin packet losses occur:

- between a transmitter and its intended receiver,
- between a transmitter and unintended nodes in its vicinity,
- between a receiver and unintended nodes in its vicinity.

These points require consideration for the protocol design in ad hoc networks:

- the first point necessitates a positive reply by the intended receiver during the control message exchange, since otherwise packets are transmitted although the receiver is not ready (cf. Fig. 8.6 and Fig. 8.8),
- the second and the third point require a receiver objection capability that allows active receivers to protect their receptions against interference that resulted from control message failures.

In case the underlying physical layer strategy allows for multiples streams at each transmitting node:

- the increased contention has to be considered by an improved contention resolution.
- A per stream backoff avoids unnecessary interruptions of ongoing transmissions. This backoff has, however, to be adaptive to the traffic load in the system since otherwise the contention becomes severe.
- The distribution of the transmission power among multiple streams requires that:
  - control and data transmission ranges have to be adapted accordingly,
  - the reduced transmission range has to be considered for routing decisions.

8.4. Summary and Further Work

In this chapter, we compared the FDSM-MAC protocol with the CIE-MAC protocol. The goal of this comparison was to obtain some insights into both, general properties of the different physical layer strategies as well as the MAC protocol aspects of the cross-layer designs.
We compared the two protocols regarding their required control message overhead. Further, a simulative comparison for different heterogeneously equipped node constellations in terms of aggregate throughput was performed. The results were related to the lost packet percentages. The statistics of the lost packet percentages were investigated subsequently in more detail and specific effects were explained in-depth, including also some theoretical considerations. The comparison not only allowed to get insight into the assets and drawbacks of the specific cross-layer designs, but also allowed to see some principle advantages and disadvantages of spatial multiplexing and beamforming based cross-layer designs in wireless ad hoc networks. Further, some advantages and shortcomings of the respective MAC protocol designs were identified.
Restricting the cross-layer designs to either spatial multiplexing or beamforming as the physical layer strategy limits the possibilities to exploit the degrees of freedom that are offered by multiple antennas. The applicability of each strategy depends strongly on the antenna correlation. Future research can go into the direction of a combined beamforming and spatial multiplexing approach. This helps to overcome the sensitivity of the individual methods to specific antenna correlation properties, since both methods complement one another. The MAC protocol design of the combined beamforming and spatial multiplexing approach should consider the principal aspects of an appropriate protocol design that we, as an outcome of the comparison, identified in this chapter.

9. Conclusions

This work contributed to the research of joint PHY-MAC cross-layer designs by thoroughly investigating classes of cross-layer designs that avoid multiple access interference by means of different physical layer strategies. The first part of the work investigated cross-layer designs that propose power control as a method to suppress MAI at the transmitters and cross-layer designs that cancel MAI with multiuser detection at the receivers.

The first contribution was an in-depth comparison of both classes of cross-layer designs. By comparing two reference schemes, one for each class, it could be shown that the applicability of power control based cross-layer designs is limited to scenarios with medium MAI. Due to some general properties of power control based medium access, this class of cross-layer designs fails to resolve severe interference situations. The class of cross-layer designs that cancels MAI with multiuser detection at the receivers is, however, capable to handle such severe interference situations. The reference scheme for this class could even obtain a good spatial reuse. We could further show that these achievements do not originate from an one-sided support of favorable nodes that disadvantages other nodes. The reference scheme rather obtained the gains by a fair treatment of all nodes in the network. Further work is required to complement the simulative comparison by considerations with respect to energy efficiency as well as with respect to the computational complexity of both classes of cross-layer designs.

As another contribution, we developed an adaptive, fully distributed contention resolution algorithm for time-slot-synchronous protocol designs. It improves the aggregate throughput of a network with heterogeneously equipped nodes in case of overload situations. In these networks, fairness in the sense that each node achieves the same performance fails to consider the different access prerequisites of heterogeneously equipped nodes. We defined fairness in such scenarios as a trade-off between, on the one hand, allowing better equipped nodes to exploit their advanced equipment and, on the other hand, avoid a complete starving of weakly equipped nodes. The proposed algorithm increases the aggregate throughput of the system for very high traffic loads, but simultaneously avoids a complete blocking of weakly equipped nodes.

The second part of the work investigated PHY-MAC cross-layer designs that apply different multiple antenna signal processing technologies on the physical layer. We contributed to this field of research with a new cross-layer design that applies beamforming combined with spatial nulling to avoid multiple access interference in ad hoc networks. The CIE-MAC protocol overcomes challenges known from directional transmission, is fully applicable in fading environments, and specifically considers networks where nodes are heterogeneously equipped. By investigating the statistics of different control messages, we could show the necessity of a receiver objection capability. This receiver objection is required since the underlying physical layer strategy is sensitive to control message failures like channel estimation errors. Further

work could aim at improving the fairness of the CIE-MAC protocol. A possible solution to this challenge would probably shift the responsibility to avoid MAI from a weakly equipped node to better equipped nodes. This might also further improve the spatial reuse in the network.
As a fourth contribution, we developed a new joint PHY-MAC cross-layer design that exploits multiple antennas at the transmitters and receivers by spatial multiplexing combined with multiuser detection as the physical layer strategy. The FDSM-MAC protocol fulfills requirements that we, from a review of existing spatial multiplexing based cross-layer designs, identified to be essential. We contributed to the research in this field by elaborating major challenges for multiple stream transmissions regarding routing decisions, power adaptation of control messages and data transmission, and backoff strategies. Further research could improve the proposed per stream backoff to adjust to variable traffic loads.
The fifth contribution was a comparison of the CIE-MAC protocol with the FDSM-MAC protocol. It offered insights into principal aspects of both, the different underlying physical layer strategies as well as appropriate MAC protocol solutions. Future research could combine both physical layer strategies to achieve a broader field of application. The insights obtained by the comparison can help to improve the protocol design for a combined spatial-multiplexing and beamforming based cross-layer solution.

A. Packet Error Ratio Percentages

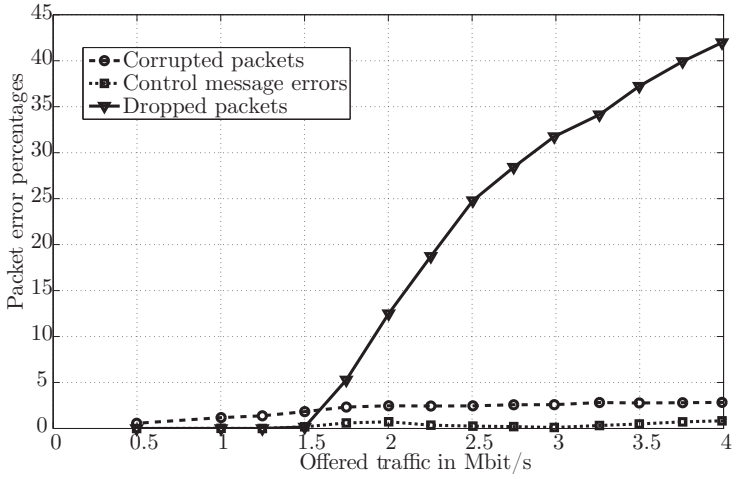

Figure A.1.: Different packet error ratio percentages versus offered traffic for HNC-2 for the CIE-MAC protocol.

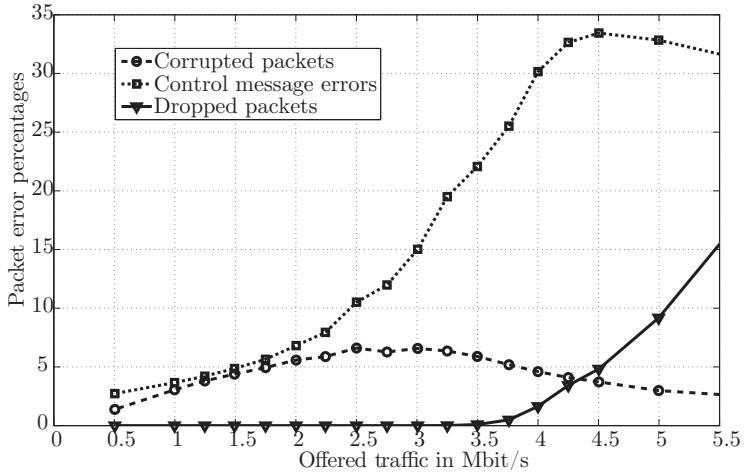

Figure A.2.: Different packet error ratio percentages versus offered traffic for HNC-3 for the FDSM-MAC protocol.

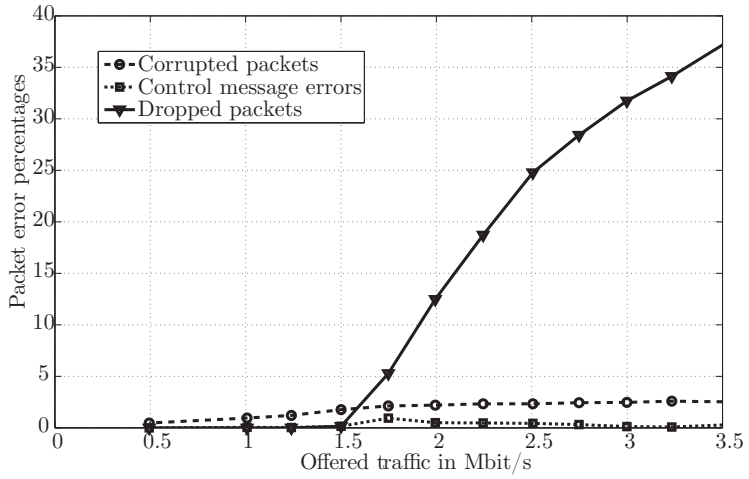

Figure A.3.: Different packet error ratio percentages versus offered traffic for HNC-3 for the CIE-MAC protocol.

B. List of Symbols, Mathematical Notation, and Abbreviations

List of Symbols

A_{PL}	Path loss attenuation
B	Bandwidth
B_{c}	Coherence bandwidth
BWB	Upper backoff window bound of IEEE 802.11
BWB_{init}	Initial value of upper backoff window bound of IEEE 802.11
CC	Contention cycle
CC_{Het}	Contention cycle for heterogeneously equipped nodes
CC_{Hom}	Contention cycle for homogeneously equipped nodes
CW	Contention window
$\boldsymbol{d}$	Receiving vector
$d_{\mathrm{TX,RX}}$	Distance between sender and receiver
d_0	Reference distance
$\boldsymbol{D}$	Receiving matrix
DI	Delay index
DI_{init}	Initial delay index
DI_{max}	Maximum delay index
DI_{min}	Minimum delay index
f_{d}	Doppler spread
$f_{x_{\mathrm{I}}}(x_{\mathrm{I}})$	PDF of x_{I}
$f_{x_{\mathrm{Q}}}(x_{\mathrm{Q}})$	PDF of x_{Q}
$f_{x_{\mathrm{I}},x_{\mathrm{Q}}}(x_{\mathrm{I}}, x_{\mathrm{Q}})$	Joint distribution of x_{I} and x_{Q}
F_J	Jain's fairness index
$g_k(w)$	Fraction of overall medium access
G_{B}	Directional antenna gain
G_{r}	Omnidirectional antenna gain at the receiver
G_{t}	Omnidirectional antenna gain at the transmitter
G_0	Omnidirectional antenna gain
$h_{i,j}$	Complex channel gain between antenna i and antenna j
$\boldsymbol{h}_{k,d}$	Effective channel between desired partner d and node k
$\boldsymbol{h}_{k,i}$	Effective channel between node i and node k
$\boldsymbol{h}_r^{(j)}$	Channel gain from all transmit antennas to the j-th receive antenna of a receiving node r
$\boldsymbol{H}$	Channel matrix
$\boldsymbol{H}_{\mathrm{eff}_k}$	Matrix of node k containing all effective channel vectors

$\boldsymbol{H}_{\text{iid}}$	Channel matrix with i.i.d entries
$\boldsymbol{H}_{i,k}$	Channel matrix between node i and node k
$\boldsymbol{H}_{\text{Im}}$	Imaginary parts of $\boldsymbol{H}_{\text{iid}}$
$\boldsymbol{H}_r$	Channel matrix from all transmit antennas to receiver r
$\bar{\boldsymbol{H}}_r$	Channel from unknown transmitters to a receiver r
$\boldsymbol{H}_{\text{Re}}$	Real parts of $\boldsymbol{H}_{\text{iid}}$
J_0	Bessel function of the first kind and 0-th order
K	Number of nodes
K-factor	Rician K-factor
K_i	Number of nodes equipped with i antennas
K_{N}	Number of nodes to be nulled
$\mathcal{K}_{\mathcal{N}}$	Set of nodes to be nulled
$K_{N_{\text{br}_s}}$	Number of nodes with N_{br_s} branches
$L_{k,i}$	Contention level of node k during frame i
$\boldsymbol{m}$	Precoding vector
$\boldsymbol{M}$	Precoding matrix
M_k	Number of antennas of node k
M_{max}	Maximum number of antennas per node
M_{r}	Number of receive antennas
M_{t}	Number of transmit antennas
M_{tot}	Overall number of active transmit antennas
M_{UK}	Total number of unknown antennas
$\boldsymbol{n}$	Noise vector
$\boldsymbol{n}_r^{(j)}$	Noise vector of the j-th receive antenna of receiver r
n_{TX_i}	Number of channels accesses of transmitter TX_i during a contention window
N	Index of a block
N_{B}	Number of blocks
N_{br}	Number of multiuser detection branches
$N_{\text{br}_{\text{max}}}$	Maximum number of multiuser detection branches
N_{CW}	Number of frames per contention window
N_{fair}	Number of fair channel accesses in OACR
$N_{k,r}$	Number of successfully transmitted packets of node k in run r
N_{P}	Packet size in bits
N_{R}	Number of runs
N_{T}	Number of transmissions
N_0	Noise power spectral density
p_{col}	Collision probability
p_{tot}	Overall transmit power per node
p_{win}	Win probability during contention phase of PBOA
P_{r}	Receive power
$P^{(s)}$	Transmit power of stream s
P_{t}	Transmit power
$\boldsymbol{R}_r$	Space-code cross-correlation matrix at receiver r

$\boldsymbol{R}_{r.,a}$	a-th column of $\boldsymbol{R}_r$
$\boldsymbol{R}_{\mathrm{RX}}$	Receive correlation matrix
$\boldsymbol{R}_{\mathrm{TX}}$	Transmit correlation matrix
RX	Receiver
$\boldsymbol{s}_k$	Spreading sequence of node k
s_{r}	Number of received streams
s_{t}	Number of transmitted streams
$s_{Th_{\mathrm{pN}}}$	Standard deviation of throughput per node
$\boldsymbol{S}$	Spreading matrix
$\mathcal{S}_D$	Set of already detected streams
S_{N}	Length of spreading sequence
$\mathcal{S}_U$	Set of undetected streams
t_{BL}	Block duration
t_{slot}	Fixed slot duration for backoff calculation of IEEE 802.11
$\mathcal{T}$	Set of transmitters
TA_s	Transmit antenna index of stream s
T_{Backoff}	Per stream backoff duration
T_{c}	Coherence time
Th	Aggregate throughput
$\overline{Th}$	Mean aggregate throughput
$Th_{k,r}$	Throughput for node k at run r
Th_{pN}	Throughput per node
$\overline{Th}_{\mathrm{pN}}$	Mean of throughput per node
Th_r	Aggregate throughput of run r
T_{sim}	Simulation time
TX	Transmitter
u_k	Number of parallel transmitted streams of node k
$\boldsymbol{U}$	Matrix containing singular vectors
UI	Utility index
UI_{init}	Initial utility index
UI_{max}	Maximum utility index
UI_{min}	Minimum utility index
v_{m}	Velocity of mobile node
$\boldsymbol{V}$	Matrix containing singular vectors
w	Sliding window
$\boldsymbol{w}_k$	Beamforming weight of node k
$\boldsymbol{w}_r(i)$	Beamforming weight of receiver r during i-th iteration
$\boldsymbol{x}$	Vector of transmitted symbols
x_{I}	In-phase component of received signal
x_{Q}	Quadrature component of received signal
$\boldsymbol{y}$	Vector of received symbols
$\tilde{\boldsymbol{y}}$	Vector of received symbols
$\hat{\boldsymbol{y}}$	Vector of received symbols

$\boldsymbol{y}_r^{(j)}$	Spread received signal at antenna j of receiver r
α	Path loss coefficient
$\gamma_{r,s}(i)$	SINR of stream s in the i-th stage of iteration at receiver r
δ	weighting constant
$\Delta_{\max}$	Maximum packet delay
$\Delta_{\mathrm{p}_{k,i}}$	Delay for packet i of node k
$\overline{\Delta}_{\mathrm{p}_{k,r}}$	Mean packet delay of node k
λ	Wavelength
$\mu_{\frac{1}{2}}(\overline{\Delta}_{\mathrm{p}_{k,r}})$	Median of mean packet delays per node
ρ	Correlation coefficient
σ^2	Variance
$\sigma_e^2(j)$	Residual interference from already detected stream j
σ_{n}^2	Noise variance
$\sigma_{\mathrm{UK}}^2(i)$	Interference power from unknown antennas at the i-th iteration of the detection process
$\boldsymbol{\Sigma}$	Diagonal matrix containing singular values
$\bar{\boldsymbol{\Sigma}}_{\mathrm{UK}}$	Diagonal matrix that contains the powers applied per stream at unknown transmit antennas

Mathematical Notation

$\boldsymbol{A}^H$	Hermitian transpose operator of $\boldsymbol{A}$
$\boldsymbol{A}^+$	Moore-Penrose pseudoinverse of $\boldsymbol{A}$
B()	Binomial distribution
diag($\boldsymbol{a}$)	Generation of a matrix that contains the entries of $\boldsymbol{a}$ on the main diagonal and zeros otherwise
$\boldsymbol{A}^{1/2}$	Square root of $\boldsymbol{A}$ that satisfies $\boldsymbol{A}^{1/2} \cdot \left(\boldsymbol{A}^{1/2}\right)^H = \boldsymbol{A}$
$\mathbb{E}\{\}$	Expected value
TR($\boldsymbol{A}$)	Trace of $\boldsymbol{A}$
$\min\{a, b\}$	Minimum of a and b
%	Modulo operator
nint (a)	Nearest integer to a
$O()$	Computational complexity

Abbreviations

ACK	Acknowledgement
ANN	Announcement
ALL	Allowance
ATPMAC	Adaptive Transmission Power controlled MAC
BEB	Binary Exponential Backoff
BER	Bit Error Rate

BPSK	Binary Phase Shift Keying
cdf	Cumulative Distribution Function
CDMA	Code Division Multiple Access
CIE	Channel Information Exchange
COMPOW	COMmon POWer
CSI	Channel State Information
CSIR	Channel State Information at Receiver
CSIT	Channel State Information at Transmitter
CSMA-CA	Carrier Sense Multiple Access Collision Avoidance
CTS	Clear To Send
DATA	Data transmission
DCF	Distributed Coordination Function
DoA	Direction of Arrival
DoD	Direction of Departure
DPC/ALP	Distributed Power Control algorithm with Active Link Protection
DS	Data Send
FDSM	Fully Distributed Spatial Multiplexing
FER	Frame Error Rate
FIFO	First In First Out
GPS	Global Positioning System
GSM	Global System for Communication
HNC	Heterogeneous Node Constellation
ID	IDentifier
IDMA	Interleave Division Multiple Access
ISO	International Organization for Standardization
LASTMUD	LAyered Space Time MultiUser Detector
LLC	Logical Link Control
MAC	Medium Access Control
MAI	Multiple Access Interference
MIMO	Multiple Input Multiple Output
MMSE	Minimum Mean Square Error
MUD	MultiUser Detection
NAV	Network Allocation Vector
OACR	Overload Adaptive Contention Resolution
OBJ	Objection
OSI	Open Systems Interconnection
PBOA	Progressive BackOff Algorithm
pdf	Probability Density Function
PER	Packet Error Rate
PHY	Physical layer
PIC	Parallel Interference Cancelation
UMTS	Universal Mobile Telecommunication System
QoS	Quality of Service

QPSK	Quadrature Phase Shift Keying
RMS	Root Mean Square
RTS	Request To Send
SIC	Successive Interference Cancelation
SINR	Signal to Interference and Noise Ratio
SIR	Signal to Interference Ratio
SNR	Signal to Noise Ratio
SVD	Singular Value Decomposition
TDMA	Time Division Multiple Access
V-BLAST	Vertical-Bell Laboratories Layered Space-Time

Bibliography

Publications by the Author

[KCH+10] U. Korger, Y. Chen, C. Hartmann, K. Kusume, and J. Widmer. A Fair and Adaptive Contention Resolution Algorithm for Time-Slotted MAC Protocol Designs. In *Proc. IEEE International Symposium on Personal, Indoor and Mobile Radio Communications (PIMRC 2010)*, Istanbul, Turkey, September 2010.

[KGGH08a] U. Korger, G. Del Galdo, A. Grosch, and M. Haardt. Channel Representative Interference Cancellation (CRIC) for MIMO Multi-Hop Systems in the Manhattan Scenario. In *Proc. IEEE Int. Conf. Acoust., Speech and Signal Processing (ICASSP 2008)*, Las Vegas, USA, April 2008.

[KGGH08b] U. Korger, G. Del Galdo, A. Grosch, and M. Haardt. Quality of Service oriented spatial processing in the Manhattan grid. In *Proc. International ITG/IEEE Workshop on Smart Antennas (WSA 2008)*, Darmstadt, Germany, February 2008.

[KH11] U. Korger and C. Hartmann. Spatial Multiplexing for Heterogeneously Equipped Nodes in Wireless Ad Hoc Networks. In *Proc. the 73rd IEEE Vehicular Technology Conference (VTC Spring 2011)*, Budapest, Hungary, May 2011.

[KHKW10a] U. Korger, C. Hartmann, K. Kusume, and J. Widmer. Power Control versus Multiuser Detection based Cross-Layer Design in Ad Hoc Networks. In *Proc. IEEE International Symposium on Personal, Indoor and Mobile Radio Communications (PIMRC 2010)*, Istanbul, Turkey, September 2010.

[KHKW10b] U. Korger, C. Hartmann, K. Kusume, and J. Widmer. Quality of Service Oriented Analysis of Cross-Layer Design in Wireless Ad Hoc Networks. In *Proc. 3rd International Workshop on Multiple Access Communications (MACOM 2010)*, Barcelona, Spain, September 2010.

[KHKW11] U. Korger, C. Hartmann, K. Kusume, and J. Widmer. Quality of Service Implications of Power Control and Multiuser Detection based Cross-Layer Design. *EURASIP Journal on Wireless Communications and Networking - Special Issue on Multiple Access Communications in Future-Generation Wireless Networks*, 2011, 2011.

[KWH+10] U. Korger, M. Wocheslander, C. Hartmann, K. Kusume, and J. Widmer. Beamforming for Heterogeneously Equipped Nodes in Wireless Ad Hoc Networks. In *IFIP Wireless Days 2010*, Venice, Italy, October 2010.

Other References

[And05] J. G. Andrews. Interference Cancellation for Cellular Systems: A Contemporary Overview. *IEEE Wireless Communications*, 12(2):19–29, April 2005.

[BCC+07] E. Biglieri, R. Calderbank, A. Constantinides, A. Goldsmith, A. Paulraj, and H. V. Poor. *MIMO wireless communications*. Cambridge University Press, 2007.

[BCP00] N. Bambos, S. C. Chen, and G. J. Pottie. Channel Access Algorithms with Active Link Protection for Wireless Communication Networks with Power Control. *IEEE/ACM Trans. on Networking*, 8(5):583–597, October 2000.

[BDSZ94] V. Bharghavan, A. Demers, S. Shenker, and L. X. Zhang. MACAW: A Media Access Protocol for Wireless LAN's. *ACM SIGCOMM Computer Communication Review*, 24(4):212–225, October 1994.

[BHHT01] S. Bandyopadhyay, K. Hasuike, S. Horisawa, and S. Tawara. An Adaptive MAC Protocol for Wireless Ad Hoc Community Network (WACNet) Using Electronically Steerable Passive Array Radiator Antenna. In *Proc. IEEE Global Telecommunications Conference (GLOBECOM)*, San Antonio, USA, November 2001.

[Big05] E. Biglieri. *Coding for Wireless Channels*. Springer US, 2005.

[BJ11] O. Bazan and M. Jaseemuddin. A Survey On MAC Protocols for Wireless Adhoc Networks with Beamforming Antennas. *IEEE Communications Surveys & Tutorials*, PP:1–24, 2011.

[Chi07] K. W. Chin. SpotMAC: A Pencil-Beam MAC for Wireless Mesh Networks. In *Proc. IEEE International Conference on Computer Communications and Networks (ICCCN)*, Honolulu, Hawaii, August 2007.

[CISN05] L. U. Choi, M. T. Ivrlac, E. Steinbach, and J. A. Nossek. Bottom-up Approach to Cross-layer Design for Video Transmission over Wireless Channels. In *Proc. IEEE 2005 Spring Semiannual Vehicular Technology Conference*, Stockholm, Sweden, May 2005.

[CLZ06] P. Casari, M. Levorato, and M. Zorzi. DSMA: an Access Method for MIMO Ad Hoc Networks Based on Distributed Scheduling. In *Proc. ACM/IEEE International Wireless Communications and Mobile Computing Conference (IWCMC '06)*, Vancouver, Canada, July 2006.

[CLZ08] P. Casari, M. Levorato, and M. Zorzi. MAC/PHY Cross-Layer Design of MIMO Ad Hoc Networks with Layered Multiuser Detection. *IEEE Trans. on Wireless Communications*, 7(11):4596–4607, November 2008.

[CM05] C. Comaniciu and N. B. Mandayam. *Wireless Networks: Multiuser Detection in Cross-Layer Design*. Springer US, 2005.

[CPN08] S.-H. Choi, D. E. Perry, and S. M. Nettles. A Software Architecture for Cross-Layer Wireless Network Adaptations. In *Proc. Seventh Working IEEE/IFIP Conference on Software Architecture (WICSA 2008)*, Vancouver,Canada, March 2008.

[CS07] M. Cui and V. R. Syrotiuk. Fair Variable Transmission Power Control. In *Proc. IEEE Global Communications Conference (GLOBCOM 2007)*, Washington, USA, November 2007.

[CT91] T. Cover and J. Thomas. *Elements of Information Theory*. John Wiley & Sons, 1991.

[CW10] S. Chu and X. Wang. Opportunistic and Cooperative Spatial Multiplexing in MIMO Ad Hoc Networks. *IEEE Transactions On Networking*, 18(5):1610–1623, October 2010.

[CYRV06] R. R. Choudhury, X. Yang, R. Ramanathan, and N. H. Vaidya. On Designing MAC Protocols for Wireless Networks Using Directional Antennas. *IEEE Trans. Mobile Computing*, 5(5):477–491, May 2006.

[DHHZ95] A. Duel-Hallen, J. Holtzman, and Z. Zvonar. Multiuser Detection for CDMA Systems. *IEEE Personal Communications*, 2:46–58, April 1995.

[DNW04] H. Dai, K. W. Ng, and M. Y. Wu. An overview of MAC protocols with directional antennas in wireless ad hoc networks. In *Proc. 2nd International Conference on Wireless and Mobile Communications (ICWMC 2006)*, Bucharest, Romania, July 2004.

[DVB01] Anurag Dugar, Nitin Vaidya, and Paramvir Bahl. Priority and Fair Scheduling in a Wireless LAN. In *IEEE MILCOM*, October 2001.

[ECS+07] Y. Eisenberg, K. Conner, M. Sherman, J. Niedzwiecki, and R. Brothers. MUD Enabled Media Access Control for High Capacity, Low-Latency Spread Spectrum Communications. In *Proc. IEEE Military Communications Conference (MILCOM '07)*, Orlando, USA, October 2007.

[EE04] T. ElBatt and A. Ephremides. Joint Scheduling and Power Control for Wireless Ad Hoc Networks. *IEEE Trans. on Wireless Communications*, 3(1):74–85, January 2004.

[ESK+04] V. Erceg, L. Schumacher, P. Kyritsi, et al. TGn Indoor MIMO WLAN Channel Models. Technical report, IEEE 802 11-03/940r2, January 2004.

[FDA09] K. Fakih, J. F. Diouris, and G. Andrieux. Beamforming in Ad Hoc Networks: MAC Design and Performance Modeling. *EURASIP Journal on Wireless Communications and Networking*, 2009, 2009.

[FGA08] F. Foukalas, V. Gazis, and N. Alonistioti. Cross-Layer Design Proposals for Wireless mobile Networks: A Survey and Taxonomy. *IEEE Communications Surveys & Tutorials*, 10(1):70–85, 2008.

[Gol67] R. Gold. Optimal binary sequences for spread spectrum multiplexing (corresp.). *IEEE Transactions on Information Theory*, 13(4):619–621, October 1967.

[Gol06] A. Goldsmith. *Wireless Communications*. Cambridge University Press, 2006.

[HH03] B. Hassibi and B. Hochwald. How much training is needed in multiple antenna wireless links ? *IEEE Trans. Inform. Theory*, 49(4):951–963, April 2003.

[HL07] I. W. H. Ho and S. C. Liew. Impact of Power Control on Performance of IEEE 802.11 Wireless Networks. *IEEE Trans. on Mobile Computing*, 6(11):1245–1258, November 2007.

[ITU94] ITU-T Recommendation X.200 (1994) — ISO/IEC 7498-1 (1994), Information technology - Open Systems Interconnection - Basic reference model: The basic model, 1994.

[Jan03] T. Janevski. *Traffic Analysis and Design of Wireless IP Networks*. Artech House Inc., 2003.

[JCH84] R. Jain, D. Chiu, and W. Hawe. A Quantitative Measure of Fairness and Discrimination for Resource Allocation in Shared Computer Systems. Technical Report TR-301, Digital Equipment Corporation, September 1984.

[JE94] W. C. Jakes and D. C. Cox (Editors). *Microwave Mobile Communications*. Wiley-IEEE Press, 1994.

[KBK02] V. Kühn, R. Böhnke, and K. Kammeyer. Multi-user detection in multicarrier-CDMA systems. *e & i Elektrotechnik und Informationstechnik*, 119(11):395–402, November 2002.

[KK05] V. Kawadia and P. R. Kumar. Principles and Protocols for Power Control in Wireless Ad Hoc Networks. *IEEE Journal on Selected Areas in Communications*, 23(1):76–88, January 2005.

[KML04] M. Krunz, A. Muqattash, and S.-J. Lee. Transmission Power Control in Wireless Ad Hoc Networks: Challenges, Solutions, and Open Issues. *IEEE Network*, 18(5):8–14, September/October 2004.

[KVM+09] K. Kusume, R. Vilzmann, A. Müller, C. Hartmann, and G. Bauch. Medium Access in Spread Spectrum Ad Hoc Networks with Multiuser Detection. *EURASIP Journal on Advances in Signal Processing - Special Issue on Cross-Layer Design for the Physical, MAC, and Link Layer in Wireless Systems*, 2009, 2009.

[LGF09] P. Li, X. Geng, and Y. Fang. An Adaptive Power Controlled MAC Protocol for Wireless Ad Hoc Networks. *IEEE Transactions On Wireless Communications*, 8(1):226–233, January 2009.

[LKL03] X.-H. Lin, Y.-K. Kwok, and V. K. N. Lau. A New Power Control Approach for IEEE 802.11 Ad Hoc Networks. In *Proc. IEEE Int. Symposium on Personal, Indoor and Mobile Radio Communications (PIMRC '03)*, volume 2, pages 1761–1765, Beijing, China, September 2003.

[LR97] J. D. Laster and J. H. Reed. Interference Rejection in Digital Wireless Communications. *IEEE Signal Processing Magazine*, 14(3):37–62, May 1997.

[LTCZ07] M. Levorato, S. Tomasin, P. Casari, and M. Zorzi. Physical Layer Approximations for Cross-Layer Performance Analysis in MIMO-BLAST Ad Hoc Networks. *IEEE Trans. on Wireless Communications*, 6(12):4390–4400, December 2007.

[LTZ08] M. Levorato, S. Tomasin, and M. Zorzi. Cooperative Spatial Multiplexing for Ad Hoc Networks with Hybrid ARQ: System Design and Performance Analysis. *IEEE Trans. Communications*, 56(9):1545–1555, September 2008.

[MBH01] J. P. Monks, V. Bharghavan, and W. W. Hwu. A power controlled multiple access protocol for wireless packet networks. In *Proc. of INFOCOM*, Anchorage, USA, April 2001.

[MK03] A. Muqattash and M. M. Krunz. CDMA-based MAC Protocol for Wireless Ad Hoc Networks. In *Proc. ACM Int. Symposium on Mobile Ad Hoc Networking and Computing (MobiHoc '03)*, Annapolis, USA, Jun. 2003.

[MK04] A. Muqattash and M. M. Krunz. A Distributed Transmission Power Control Protocol for Mobile Ad Hoc Networks. *IEE Transactions On Mobile Computing*, 3(2):113–128, April–June 2004.

[MK05] A. Muqattash and M. Krunz. POWMAC: A Single-Channel Power-Control Protocol for Throughput Enhancement in Wireless Ad Hoc Networks. *IEEE Journal on Selected Areas in Communications*, 23(5):1067–1084, May 2005.

[Mol05] A. F. Molisch. *Wireless Communications*. John Wiley & Sons, 2005.

[MRV07] J. C. Mundarath, P. Ramanathan, and B. D. Van Veen. A cross layer scheme for adaptive antenna array based wireless ad hoc networks in multipath environments. *Wireless Networks*, 13(5):597–615, October 2007.

[NAP04] H. T. Nguyen, J. B. Andersen, and G. F. Pedersen. A stochastic model of spatio-temporally correlated narrowband MIMO channel based on indoor measurement. In *15th IEEE International symposium on Personal, Indoor and Mobile Communications*, Barcelona, Spain, September 2004.

[NKGB00] T. Nandagopal, T.-E. Kim, X. Gao, and V. Bharghavan. Achieving MAC layer fairness in wireless packet networks. In *Proc. ACM International Conference on Mobile Computing and Networking (MobiCom '00)*, Boston, USA, August 2000.

[NLJ05] P. C. Ng, S. C. Liew, and L. B. Jiang. Achieving Scalable Performance in Large-Scale IEEE 802.11 Wireless Networks. In *Proc. IEEE Wireless Communications and Networking Conference (WCNC '05)*, New Orleans, USA, March 2005.

[NP06] S. H. R. Naqvi and L. M. Patnaik. A Distributed Channel Access Protocol for Ad Hoc Networks with Feedback Power Control. *IEEE Transactions on Mobile Computing*, 5(10):1448–1459, October 2006.

[OCB05] M. Ozcelik, N. Czink, and E. Bonek. What makes a good MIMO channel model? In *Proc. IEEE Vehicular Technology Conference (VTC Spring 2005)*, Stockholm, Sweden, May/June 2005.

[PNG03] A. Paulraj, R. Nabar, and D. Gore. *Introduction to Space-Time Wireless Communications*. Cambridge University Press, 2003.

[Pro89] J. G. Proakis. *Digital Communications*. McGraw-Hill Book Company, 1989.

[Rap02] T. S. Rappaport. *Wireless Communications, Principles and Practice*. Prentice-Hall, Inc., second edition, 2002.

[SM05] V. Srivastava and M. Motani. Cross-Layer Design: A Survey and the Road Ahead. *IEEE Communications Magazine*, 43(12):112–119, December 2005.

[SML03] S. Sfar, R. D. Murch, and K. B. Letaief. Layered Space-Time Multiuser Detection Over Wireless Uplink Systems. *IEEE Trans. on Wireless Communications*, 2(4):653–668, July 2003.

[SPM02] L. Schumacher, K. I. Pedersen, and P. E. Mogensen. From Antenna Spacings To Theoretical Capacities - Guidelines For Simulating MIMO Systems. In *13th IEEE International symposium on Personal, Indoor and Mobile Communications (PIMRC 2002)*, Lisbon, Portugal, September 2002.

[SSIC04] K. Sundaresan, R. Sivakumar, M. A. Ingram, and T.-Y. Chang. A Fair Medium Access Control Protocol for Ad-hoc Networks with MIMO Links. In *Proc. IEEE International Conference on Computer Communications (INFOCOM)*, Hong Kong, China, March 2004.

[SV04] J. So and N. Vaidya. MTSF: A timing synchronization protocol to support synchronous operations in multihop wireless networks. Technical report, University of Illinois, Urbana-Champaign, Oct. 2004.

[SW02] A. Springer and R. Weigel. *UMTS: The Physical Layer of the Universal Mobile Telecommunications System*. Springer, 2002.

[TAB10] A. Tyrrell, G. Auer, and C. Bettstetter. Emergent Slot Synchronization in Wireless Networks. *IEEE Transactions on Mobile Computing*, 9(5):719–732, May 2010.

[TG06] S. Toumpis and A. J. Goldsmith. New Media Access Protocols for Wireless Ad Hoc Networks Based on Cross-Layer Principles. *IEEE Trans. on Wireless Communications*, 5(8):2228–2241, August 2006.

[TNV04] Lang Tong, Vidyut Naware, and Parvathinathan Venkitasubramaniam. Signal Processing in Random Access. *IEEE Signal Processing Magazine*, 21(5):29–39, September 2004.

[VBH06] R. Vilzmann, C. Bettstetter, and C. Hartmann. Beammac: A new paradigm for medium access in wireless networks. *International Journal of Electronics and Communications (AEÜ)*, 60(1):3–7, January 2006.

[Ver98] S. Verdu. *Multiuser Detection*. Cambridge University Press, New York, NY, 1998.

[Vil09] R. Vilzmann. *Wireless Multi-Hoc Networks with Beamforming Antennas and Multiuser Detection*. PhD thesis, Technische Universität München, 2009.

[WFGA98] P. W. Wolniansky, G. J. Foschini, G. D. Golden, and R. A.Valenzuela. V-BLAST: an architecture for realizing very high data rates over the rich-scattering wireless channel. In *Proc. IEEE ISSSE*, Pisa, Italy, September 1998.

[WLA97] IEEE Std 802.11-1997 Information Technology- Telecommunications And Information Exchange Between Systems-Local And Metropolitan Area Networks-specific Requirements-Part 11: Wireless LAN Medium Access Control (MAC) And Physical Layer (PHY) Specifications, November 1997.

[XS01] S. Xu and T. Saadawi. Does the IEEE 802.11 MAC protocol work well in multihop wireless ad hoc networks? *IEEE Communications Magazine*, 39(6):130–137, June 2001.

[ZDGK09] J. Zhang, Z. Dziong, F. Gagnon, and M. Kadoch. Multiuser Detection Based MAC Design for Ad Hoc Networks. *IEEE Transactions On Wireless Communications*, 8(4):1836–1846, April 2009.

[Zim80] H. Zimmermann. OSI Reference Model - The ISO Model of Architecture for Open Systems Interconnection. *IEEE Transactions on Communications*, 28:425–432, April 1980.

[ZL07] D. Zhou and T. H. Lai. An Accurate and Scalable Clock Synchronization Protocol for IEEE 802.11-Based Multihop Ad Hoc Networks. *IEEE Transactions on Parallel and Distributed Systems*, 18(12):1797–1808, December 2007.

[ZZA+06] M. Zorzi, J. Zeidler, A. Anderson, B. Rao, J. Proakis, A. L. Swindlehurst, M. Jensen, and S. Krishnamurthy. Cross-Layer Issues in MAC Protocol Design for MIMO Ad Hoc Networks. *IEEE Wireless Communications*, 13(4):62–76, August 2006.